

UNITED STATES  
DEPARTMENT OF THE INTERIOR  
GEOLOGICAL SURVEY

National Center for Earthquake Research  
345 Middlefield Road  
Menlo Park, California 94025

Correlations between seismic wave velocities and physical  
properties of near-surface geologic materials in the  
southern San Francisco Bay region, California

by

Thomas E. Fumal

Open-File Report 78-1067

1978

This report is preliminary and has  
not been edited or reviewed for  
conformity with Geological Survey  
standards and nomenclature.

Any use of trade names and trademarks in this publication is for  
descriptive purposes only and does not constitute endorsement  
by the Geological Survey.

## ABSTRACT

To identify geologic units with distinctly different seismic responses for the purposes of seismic zonation, compressional and shear wave velocities have been measured in boreholes at 59 sites in the San Francisco Bay region in a wide range of near-surface (0-30m) geologic materials. Several physical parameters, which can be readily determined in the field, were found to correlate with the shear wave velocities and were used to define seismically distinct groups. For the unconsolidated to semiconsolidated sediments, texture, standard penetration resistance and depth were used to define eight seismically distinct groups. For the bedrock materials, fracture spacing and hardness were used to differentiate ten distinct categories.

The correlations obtained between shear wave velocity and the physical parameters were used to regroup the map units defined for the San Francisco Bay region into seismically distinct units. The map units for the younger unconsolidated sediments can be really differentiated seismically. In contrast, the older semiconsolidated sedimentary deposits and bedrock units, which have experienced significant variations in post-depositional changes, show wider and overlapping velocity ranges. The map units for the sedimentary deposits have been regrouped into eight seismically distinct geotechnical units. The bedrock map units have been broadly regrouped into five distinct categories.

Compressional wave velocities were not found to be well correlated with the physical parameters dependent on the soil or rock

structure. For materials above the water table, the wide velocity variations found for each geotechnical group can be attributed to differences in degree of saturation.

The strong correlations observed between shear wave velocity and other readily determine physical properties suggest that geologic maps which incorporate these parameters are most useful for seismic zonation.

## ACKNOWLEDGMENTS

The work was done while the author was employed at the U. S. Geological Survey, Branch of Ground Motion and Faulting.

The author wishes to express his appreciation to Professor Albert T. Smith and Roger D. Borchardt of the U. S. Geological Survey for providing direction throughout the study and critically reviewing the thesis. In addition, thanks are gratefully extended to John C. Tinsely, William B. Joyner and Ray C. Wilson, also of U.S.G.S. for kindly providing their time for reviewing the thesis.

Many of the author's colleagues in the U. S. Geological Survey assisted in the study. The seismic wave velocity measurements were carried out by James F. Gibbs, assisted by Edward F. Roth and the author. Michael J. Bennett provided assistance and laboratory space for making the density measurements. I especially wish to thank Kenneth R. Lajoie for many helpful discussions of the geology of the San Francisco Bay region and Richard E. Warrick for discussions of techniques of measuring seismic wave velocities.

## TABLE OF CONTENTS

Chapter		Page
	Abstract . . . . .	ii
	Acknowledgments . . . . .	iv
I	Introduction . . . . .	1
II	General Geology of the Southern San Francisco Bay Region . . . . .	5
III	Experimental Method . . . . .	9
	Selection of Sites . . . . .	9
	Field Procedures . . . . .	9
	Drilling and Sampling . . . . .	9
	Recording Procedures . . . . .	10
	Reduction of Geologic Data . . . . .	13
	Description of Samples . . . . .	13
	Geologic Log . . . . .	14
	Density Measurements . . . . .	14
	Reduction of Seismic Data . . . . .	18
	Identification of Shear Wave Onset . . . . .	18
	Travel Times . . . . .	18
	Interval Velocities . . . . .	20
IV	Discussion of Results . . . . .	25
	Shear Wave Velocities in the Sedimentary Deposits	25
	Correlations between S-Wave Velocity and	25
	Physical Properties . . . . .	25
	Texture . . . . .	25
	Standard Penetration Resistance . . . . .	31
	Long-Term Water Levels . . . . .	35
	Short-Term Water Levels . . . . .	39
	Relative Density . . . . .	41
	Depth . . . . .	43
	Summary . . . . .	52
	Shear Wave Velocities for Sedimentary Map Units .	55
	Holocene and Late Pleistocene Alluvium . . . .	58
	Velocity Characteristics . . . . .	58
	Distribution and Physical Properties . . . .	58
	Bay Mud . . . . .	63
	Dune Sand . . . . .	63
	Artificial Fill . . . . .	65
	Merced Formation . . . . .	65
	Colma Formation . . . . .	65
	Santa Clara Formation . . . . .	66
	Purisima Formation . . . . .	66
	Comparisons with Results for the Los Angeles Area	67
	Summary . . . . .	68

## IV (Continued)

Shear Wave Velocities in Bedrock Materials . . . . .	73
Correlations between S-Wave Velocity and Physical Properties . . . . .	73
Weathering . . . . .	73
Hardness . . . . .	76
Fracture Spacing . . . . .	80
Shear Wave Velocity for Bedrock Map Units . . . . .	82
Summary . . . . .	84
P-Wave Velocities for Sedimentary Deposits and Bedrock Materials . . . . .	89
Factors Affecting P-Wave Velocity . . . . .	89
Effective Stress and Void Ratio . . . . .	89
Interstitial Fluids . . . . .	94
Summary . . . . .	96
Elastic Moduli . . . . .	101
Shear and Bulk Moduli . . . . .	101
Poisson's Ratio . . . . .	101
Summary . . . . .	105
Bibliography . . . . .	108

## LIST OF ILLUSTRATIONS

Figure		Page
1	Field Apparatus for Seismic Wave Velocity Measurements	12
2	Explanation for Geologic Logs . . . . .	15
3	Example of Geologic Log . . . . .	17
4	Example of Record Section . . . . .	19
5	Example of Record of Energy Generated by Hammer Impacts . .	21
6	Example of Travel Time Curve . . . . .	22
7	Sedimentary Deposits Differentiated According to Physical Properties . . . . .	27
8	Grain Size Classification of Sands . . . . .	30
9	Variation of Shear Wave Velocity with Standard Penetration Resistance . . . . .	32
10	Scatter Diagram for Shear Moduli and N-values from 220 Sites in Japan . . . . .	33
11	Distribution of Soil Colors in Cohesive Sediments . . . . .	37
12	Distribution of Soil Colors in Sandy Sediments . . . . .	38
13	Relative Degree of Saturation in Cohesive Sediments . . . . .	40
14	Relative Degree of Saturation in Sands . . . . .	42
15	Comparison with Data Compiled by Hamilton . . . . .	45
16	Variation of S-wave velocity with void ratio . . . . .	50
17	Distribution of Sands for which S-Wave Velocity Measured <u>in situ</u> is approximately equal to the Calculated Velocity versus those for which the <u>in situ</u> Velocity is Signifi- cantly greater than the Calculated Velocity . . . . .	51
18	Classification Scheme for Differentiating Sedimentary Deposits . . . . .	53
19	Shear Wave Velocities in Sedimentary Geologic Units . . . . .	56
20	Schematic Cross Section of Alluvial Fan-Bay Complex . . . . .	60
21	Geologic Logs of Sites on Holocene and Late Pleistocene Sedimentary Deposits . . . . .	62

Figure		Page
22	Schematic Cross Section Showing Distribution of Depositional Environments, Textural Groupings and S-Wave Velocity Ranges . . . . .	64
23	Comparison with Data by Campbell and Duke . . . . .	69
24	Seismically Distinct Geotechnical Units for Sedimentary Deposits . . . . .	71
25	Relative Degree of Weathering in Bedrock Materials . . . . .	75
26	Variation of the Difference between Shear Wave Velocity with Moderate Weathering . . . . .	77
27	Bedrock Materials Differentiated According to Physical Properties . . . . .	78
28	Relative Hardness in Bedrock Materials . . . . .	81
29	Relative Fracture Spacing in Bedrock Materials . . . . .	83
30	Bedrock Materials Grouped According to Geologic Unit . . . . .	85
31	Compressional Wave Velocities in Sedimentary Deposits . . . . .	90
32	Compressional Wave Velocities in Bedrock Materials . . . . .	92
33	Compressional Wave Velocities in Seismically Distinct Geotechnical Units for Sedimentary Deposits . . . . .	97
34	Compressional Wave Velocities in Seismically Distinct Bedrock Geologic Units . . . . .	99
35	Variation of Shear Modulus with Shear Wave Velocity and Bulk Modulus with P-Wave Velocity . . . . .	103
36	Variation of Poisson's Ratio with Shear Wave Velocity . . . . .	104

## LIST OF TABLES

Table		Page
1	Shear Wave Velocity in Sedimentary Deposits . . . . .	28
2	Measured and Calculated Properties of Sand Samples . .	49
3	Shear Wave Velocities in Sedimentary Geologic Map Units	57
4	Shear Wave Velocities in Seismically Distinct Geotechnical Units of Sedimentary Deposits . . . . .	72
5	Shear Wave Velocities in Bedrock Materials . . . . .	79
6	Shear Wave Velocities in Bedrock Geologic Units . . . .	86
7	Shear Wave Velocities in Bedrock Geotechnical Units . .	87
8	P-Wave Velocities in Sedimentary Physical Property Units	91
9	P-Wave Velocities in Bedrock Physical Property Units	93
10	P-Wave Velocities in Sedimentary Geotechnical Units . .	98
11	P-Wave Velocities in Bedrock Geologic Units . . . . .	100

## I. INTRODUCTION

Observations of the geographical distribution of damage due to earthquake ground shaking often show a clear correspondence between intensity and local geologic conditions. Damage in valleys underlain by thick deposits of unconsolidated sediments is frequently much greater than that at nearby locations on bedrock. For example, investigations after the 1906 San Francisco earthquake showed that apparent intensities were violent on recent estuarine mud, strong to very strong on other thick sedimentary deposits, and generally weak on thin sedimentary deposits and bedrock areas (Wood, 1908).

Consequently, the desire to predict ground response to earthquake motions, both for building design and seismic microzonation purposes, has generated considerable effort aimed at clarifying the relationship between ground motion and local geology. For the southern San Francisco Bay region, several important data sets have been developed which bear on this problem. In addition to the intensity data for the 1906 earthquake, the 1957 San Francisco earthquake was recorded by strong-motion instruments at several sites. This provided an opportunity for comparisons between site geology and instrumental records of earthquake ground motion (Seed and Idriss, 1969). Ground motion generated by nuclear explosions at the Nevada Test Site has been recorded at 99 sites throughout the southern S. F. Bay region. These data show consistent correlations between the characteristics of surface ground motions, geologic map unit and the intensity data from the 1906 earthquake (Borcherdt, 1970; Gibbs and Borcherdt, 1974). In particular, it was found that

sedimentary deposits can significantly modify incoming motions by enhancing peak amplitudes at certain frequencies and increasing the duration of strong shaking. Furthermore, ground response was found to vary considerably within a given geologic map unit for the unconsolidated and semi-consolidated sedimentary deposits.

Recent theoretical studies by Vergnaud (1974) show some of the effects of small variations in the soil profile on ground response. He found that ground motion can be significantly modified by changing the rock depth in a shallow deposit, changing the thickness of a soft layer in a deeper deposit or by changing the rigidity of soft layers with a constant rock depth. Shear modulus (rigidity) is also the key parameter in specifying a soil deposit for calculating its seismic response characteristics (Joyner and Chen, 1975). These studies suggest that the usefulness of the nuclear explosion data might be greatly extended if the pertinent details of the local geology were known.

Towards this goal, a program to investigate the geologic and seismic properties of the near-surface geologic materials of the southern San Francisco Bay region has been undertaken by the U.S. Geological Survey. To date, data has been obtained at 59 sites in a spectrum of geologic materials ranging from hard granitic rock to soft, water-saturated bay mud. At each site selected a hole is drilled to a depth of 30 m to provide data on the stratigraphy of the site. Seismic travel times are measured in each borehole using a downhole technique to provide logs of compressional and shear wave velocities. The data gathered in these investigations have been previously published (Gibbs et al., 1975, 1976, 1977).

This report focuses on the correlations between the geologic properties and seismic velocities of the near-surface materials at the sites.

Its purpose is to analyze the data collected in order to:

- (1) identify those geologic properties of the materials studied which have a significant effect on the seismic wave velocities and which are readily determined in the field, and
- (2) specify the velocity characteristics of the geologic units mapped in the southern S. F. Bay region and to identify those which are seismically distinct.

Numerous laboratory studies have investigated the effect of various parameters on seismic wave velocities. For example, a comprehensive study by Hardin and Drenevich (1972) showed that the most important factors affecting shear modulus in soils were strain amplitude, effective mean principle stress, and the void ratio of the material. The degree of saturation, over-consolidation ratio, and time effects were additional important factors for cohesive soils. However, values for these material parameters can only be obtained through time consuming laboratory analysis and are not available on a regional scale. Thus, the results of laboratory parametric studies are not directly useful for microzonation purposes.

Studies relating in-situ measurements of seismic wave velocity with geologic properties are few in number and generally limited in scope. Kitsunezaki (1965) measured wave velocities in saturated granitic rocks at the site of a power plant in Japan. He found distinct P- and S-wave ranges for type of material classified according to degree of weathering. Campbell and Duke (1976) report near-surface compressional and shear wave velocities from seismic refraction surveys conducted at 63 sites on a

variety of geologic materials in the Los Angeles Basin and the San Fernando Valley. Unfortunately, they give no details as to the physical properties of these materials, limiting the use of this data for estimating velocities for geologic materials in other regions.

Emphasis in this report is on correlations with shear wave velocity in view of its importance in calculating seismic response. However, since some analyses also require a value of Poisson's ratio to be specified, compressional wave velocity data will be briefly discussed and values of elastic moduli calculated from the wave velocities presented.

Results of this study show that the younger unconsolidated sediments are readily differentiated seismically, while older semi-consolidated sedimentary deposits and bedrock units show wider velocity variations and greater degrees of overlap between units. This accords with the wide variety of physical properties found in the older deposits which have experienced significant variations in post-depositional changes. It was found that the most important factor affecting shear wave velocity in unconsolidated and semi-consolidated sedimentary materials was texture (relative grain size distribution). In addition, effects in fine-grained sediments could also be attributed to long-term water table effects as revealed by color. For the bedrock materials, the most important factor was found to be fracture spacing.

## II. GENERAL GEOLOGY OF THE SOUTHERN SAN FRANCISCO BAY REGION

The purpose of this section is to provide an overview of the regional geologic setting of the study area and to indicate the general character and distribution of the major geologic units. More detailed descriptions of the lithologies and engineering properties of the bedrock units in the Santa Cruz Mountains-San Francisco area can be found in reports by Ellen et al. (1972) and Schlocker (1974). Descriptions of the unconsolidated and semi-consolidated sedimentary deposits along with engineering data accompany recent maps of these deposits (Helley and Brabb, 1971; Helley et al., 1972; Lajoie et al., 1974; and Schlocker, 1974).

The San Francisco Bay region lies within the central portion of the Coast Ranges geomorphic province. As is typical of this province, the region consists of two sub-parallel northwest oriented mountain ranges, the Santa Cruz Mountains on the west and the Berkeley Hills to the east, separated by a narrow structural depression, the Santa Clara Valley. The drowned northern end of this valley comprises San Francisco Bay proper.

The major active faults which traverse the Bay Area are the San Andreas fault zone which transects the San Francisco peninsula and the Hayward fault which runs along the foot of the Berkeley Hills. In addition, there are numerous smaller faults which are parallel to or branch from these major faults.

These faults divide the region into three major structural blocks which have had distinct geologic histories. The Montara-Santa Cruz Moun-

tains block lies to the west of the San Andreas fault and the Pilarcitos fault, one of its main branches. This block is underlain by Cretaceous granitic rocks along with remnants of the older Sur Series metamorphic rocks. The granitic rocks are exposed in a large zone in the Montara Mountain area. Fresh to slightly weathered granitic rock is hard and fractured at close to wide spacing. (Terms used to describe rock hardness and fracture spacing are those of Ellen et al., 1972. See figure 2 of this report.) Over most of the area the physical properties of the granitic rock have been profoundly modified by deep weathering to grus, a soft granular material, to depths from 3 to greater than 30 meters. These rocks are overlain by a variety of upper Cretaceous and Tertiary marine sedimentary and volcanic rock units. The sedimentary rocks of Upper Cretaceous through Miocene age are generally hard to firm for fresh to moderately weathered material with sandstones having moderate to wide fracture spacings while shales and mudstones are closely fractured. Sandstones of the Purisima Formation of Pliocene age are generally softer than the older sandstones. Unconsolidated sedimentary deposits are found in relatively small areas on marine terraces and stream valleys. These deposits have physical properties similar to their counterparts in the Santa Clara Valley.

Rocks of the Franciscan Formation, from Jurassic to Cretaceous in age, are the oldest rocks exposed on the San Francisco block located between the San Andreas and Hayward faults. In this region the Franciscan consists of roughly equal amounts of sandstone and greenstone with large areas of sheared rocks and minor amounts of chert, conglomerate, limestone and metamorphic rocks. The sandstone and greenstone are generally hard to

firm but are more intensely fractured and more deeply weathered (to greater than 10 m) than many of the Mesozoic Tertiary rocks of the Santa Cruz Mountains. Areas mapped as sheared rock are composed of roughly equal amounts of shale and sandstone sheared to less than 1 cm and masses of fractured sandstone similar to those mapped as Franciscan sandstone. Chert, the only other Franciscan rock type sampled in this study is hard and closely fractured. In the Palo Alto area those rocks are overlain by a sequence of Tertiary marine sedimentary and volcanic rocks correlated with those of the Santa Cruz Mountains.

Tectonic movements since the late Pliocene have tilted or down-dropped the San Francisco block to form the Santa Clara Valley. This trough has been filled by a sequence of continental and marine sedimentary deposits. The oldest of these sediments are the marine sediments of the Merced Formation and the alluvial and lacustrine deposits of the upper Merced, the Santa Clara Formation and the Packwood Gravels. All of these deposits have since been highly deformed by faulting and folding. The Merced is exposed in a narrow belt east of the San Andreas fault from Daly City to Burlingame. It is composed largely of soft to firm sandstone, siltstone and claystone physically similar to that of the Purisima Formation. The Santa Clara Formation outcrops along the San Andreas fault from Crystal Springs Reservoir to Coal Mine Ridge and in the foothills south from Palo Alto. The Packwood Gravels make up the foothills on the east side of the Santa Clara Valley, south of Fremont. These units are predominantly poorly sorted, poorly to moderately well indurated conglomerate with interbeds of firm to soft sandstone. Sedimentary deposits of late Pleistocene and Holocene age are widely distributed throughout

the southern Bay region. In the northern part of the area these deposits are largely well-sorted sandy sediments deposited in estuarine, coastal and eolian environments. Sediments of the flat lands of Santa Clara Valley consist of gravel, sand, silt and clay deposited in a variety of predominantly alluvial environments. The late Pleistocene deposits tend to be more coarse-grained and more indurated than the younger deposits. Sediments underlying the San Francisco Bay are mostly clay, silt and sand and gravel deposited in estuarine alluvial and eolian environments. The youngest deposits in the bay are soft, normally consolidated clay and silty clay up to 40 m thick.

The Berkeley Hills block lies between the Hayward fault zone on the west and the Calaveras fault zone on the east. While rocks of the Franciscan assemblage are exposed within the Hayward fault zone and to the east of the Calaveras fault, the oldest rocks exposed on the Berkeley Hills block are the marine sedimentary rocks of the Great Valley Sequence of Jurassic and Cretaceous age. These are overlain by a variety of Tertiary marine sedimentary and Quaternary volcanic rock units. These rocks have physical properties similar to those of the Santa Cruz Mountains.

### III. EXPERIMENTAL METHOD

#### Selection of Sites

Locations of the 59 sites at which data was collected for this study are shown on the accompanying geologic map. Most sites were chosen in order to provide geologic and seismic data for comparison with ground motion as revealed by instrumental records from nuclear explosions (31 sites) or strong motion stations (14 sites) or by intensity data from the 1957 San Francisco earthquake (4 sites). Accessibility determined how many of the 99 nuclear explosion stations could be occupied for this study. An additional 13 sites were chosen in order to make a more complete sample of the range of such geologic properties as lithologic, stratigraphic and hydrologic conditions within each major geologic unit.

#### Field Procedures

##### Drilling and Sampling

At each site selected, a hole 12.4 cm in diameter was drilled to a depth of 30 m, using rotary-wash drilling equipment. The hole was then cased with poly-vinyl-chloride pipe. Casing assures an open hole and provides a secure surface for clamping the down hole instrument. Back-filling around the casing gives good coupling between the casing and the borehole walls.

Relatively few samples were taken in conjunction with drilling. Continuous sampling at the large number of sites needed would have been too costly and time consuming. In addition, it was thought that extensive recovery and laboratory testing of samples would not be needed in obtaining sufficiently detailed geologic data for making useful correla-

tions with seismic wave velocities.

The type and number of samples taken at each site was determined by the kind of material, the number of significant lithologic boundaries and variations in weathering. At most bedrock sites, samples were taken at depths of 3 m, 7.5 m and 30 m to obtain samples of deeply weathered, moderately weathered and fresh rock. Samples were generally taken in the sedimentary deposits at depths of 3 m, 10 m, 20 m and 30 m.

Standard penetration measurements, which yield a somewhat disturbed sample, were made in cohesive soils, loose sand and deeply weathered rock. Undisturbed samples were taken in denser sands, soils containing large amounts of hard rock fragments and firm rock using a Pitcher core barrel with a Shelby thin tube liner. Samples were recovered in hard rock using a core barrel with a diamond bit.

#### Recording Procedures

The downhole seismic survey method was used to determine in-situ compressional and shear wave velocities. In this technique, seismic wave velocities are calculated from measurements of travel times of body waves traveling vertically between a surface energy source and a bore-hole geophone. This method yields better average velocity data in horizontally layered materials than the surface refraction or inter-hole techniques due to the geometry of the seismic wave travel (Schwarz and Musser, 1972).

Shear waves were generated using the horizontal traction method introduced by Kobayashi (1959) and discussed by Warrick (1974). Use of this source overcomes the usual problems in identification of S-wave

arrivals due to interference by P-waves as it produces a high proportion of shear to P-wave energy. The polarity of the shear waves can be reversed by reversing the direction of energy impulse. The field apparatus for this study is shown in figure 1. A timber (244 x 30 x 18 cm) was placed 2.0 m from the hole on a leveled ground surface and securely coupled to the soil by parking the front wheels of a truck on top of it. The end of the timber was impacted horizontally with a 30 kg hammer rolling on bearings along a pipe extending through the timber. Two impacts were made, one in each direction. A three-component geophone (natural frequency 14 Hz), set within 9 cm of the center of the timber, and an inertia switch attached to the hammer are used to determine the origin time of the S-waves.

Compressional waves were generated by the vertical impact of a sledge hammer on a steel plate. A signal produced by an inertia switch fastened near the hammer head is recorded for determining the origin time of the impulse.

The seismic probe used in the first 12 drill holes (Gibbs et al., 1975) consists of three sensors--one vertical, two horizontal (Mark Products L-10, natural frequency 14 Hz). This instrument could not be oriented from the surface so that one horizontal sensor was in line and the other transverse. Later holes were logged using an instrument with a declinometer and an inflatable diaphragm (Oyo Corp.). Under most conditions, the sensors could be properly oriented, aiding in identifying the S-wave arrivals.

The signals generated by each of the three hammer impacts (one vertical, two reversed horizontal) are recorded separately on photographic

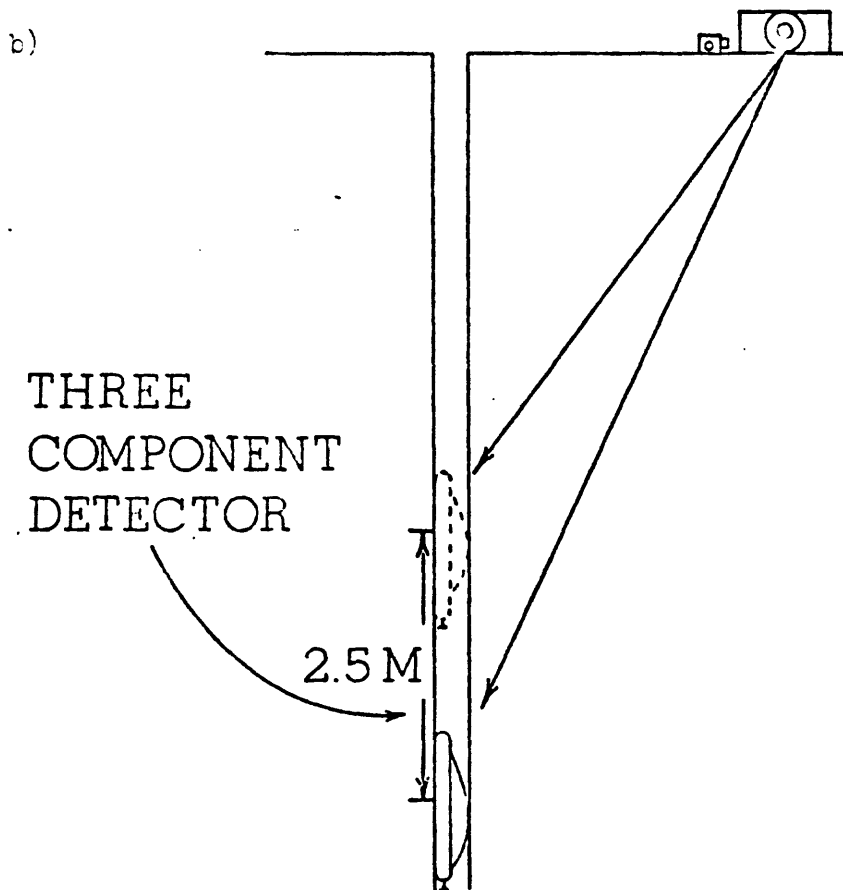
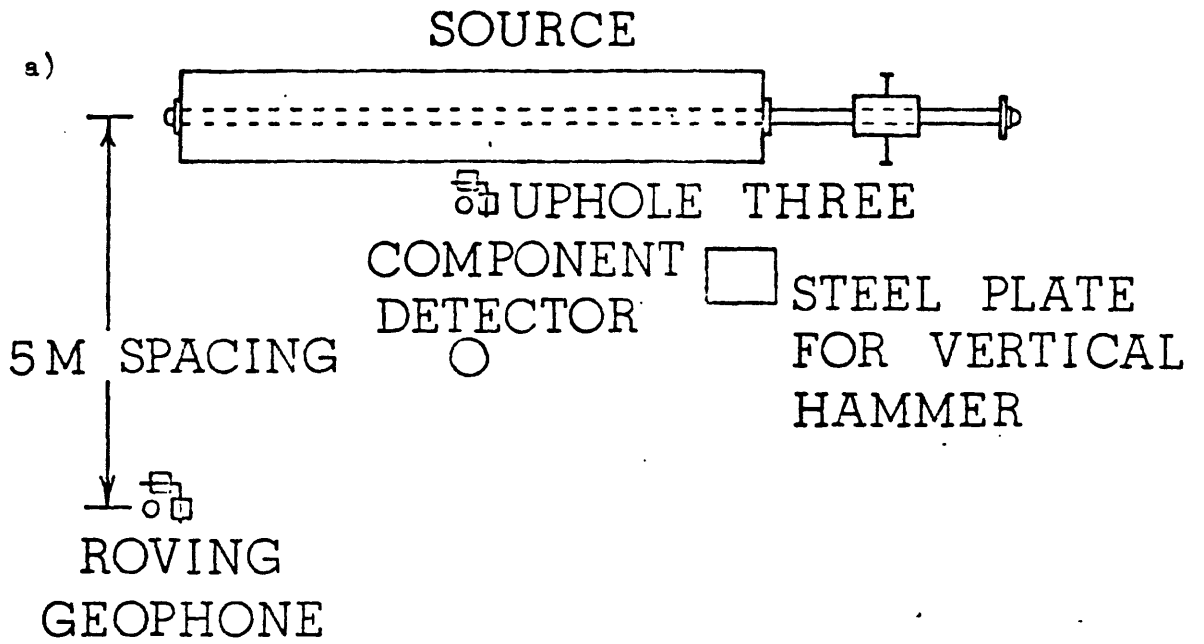


Figure 1. Field apparatus for seismic wave velocity measurements (a) plan view, (b) vertical section.

paper at intervals of 2.5 m up the hole. In sedimentary deposits, variations of this spacing were used depending on thickness of the individual layers.

### Reduction of Geologic Data

#### Description of Samples

Portions of each sample are examined and described in the laboratory. The terms for the descriptions are summarized in figure 2. Sample descriptions are presented in the left-hand column of the geologic logs (figure 3).

The soil samples are described using the field methods of the Soil Conservation Service and those specified for the Unified Soil Classification System. Descriptions include soil texture, color, amount and size of coarse grains, plasticity, wet and dry consistency and moisture conditions. Texture refers to the relative proportions of clay, silt, and sand particles less than 2 mm in diameter. Proportions of larger fragments are indicated by modifiers of textural class names. Determination is made in the field mainly by feeling the moist soil. The dominant color of the soil and prominent mottles are determined from the Munsell Soil Color Charts.

Descriptions of rock samples include rock name, weathering condition, color, grain size, hardness and fracture spacing. Classifications of rock hardness and fracture spacing are those used by Ellen et al. (1972) in describing bedrock units in San Mateo County. The weathering classification is modified from that used by Aetron-Blume-Atkinson (1965) in describing Tertiary sedimentary rocks in the foothills of the Santa Cruz Mountains.

### Geologic Log

Geologic logs are compiled for each hole using the field log and descriptions of samples (fig. 2). The field log is based on a continuous record of drill cuttings, reaction of the drill rig, preliminary on-site inspection of samples and inspection of nearby outcrops and road-cuts. Most information needed for describing relatively well-sorted soils and such properties of rock as lithology, color and hardness are readily obtained from cuttings. Inspection of samples and nearby outcrops is necessary to determine the nature of poorly-sorted materials and to determine fracture spacing. Reaction of the drill rig is also useful in determining degree of fracturing. The rate of penetration of the drill in rock is highest for very closely fractured and sheared material and drilling roughness generally is at a maximum in closely to moderately fractured rock. In-situ consistency of soil is determined largely from standard penetration measurements and rate of drill penetration.

### Density Measurements

Values for density are required to calculate elastic moduli from measurements of seismic velocity. Densities were measured for the diamond core samples and most of the penetration samples by weighing a small piece of the sample and obtaining its volume by the mercury displacement method. A different procedure is used for very friable materials such as grus or poorly-sorted materials which necessitated using a large sample. A section is cut from the Shelby tube containing the sample, its height and diameter measured and the sample extruded for weighing.

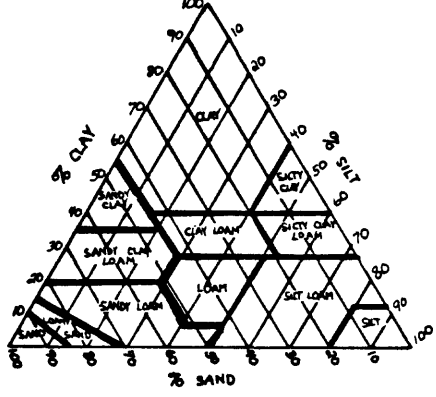
<p>ELEVATION: DATE :</p>	<p>LOCATION : LAT. LONG. 7 1/2' QUAD</p>	<p>HOLE NO: Brabb (1970) Brabb and Pampayan (1972) SITE : Helley and Brabb (1971) GEOLOGIC Helley et al. (1972) MAP UNIT: Lajoie et al. (1974) Robinson (1956)</p>																																											
<p><b>SAMPLE DESCRIPTION</b></p> <p><b>DRILLING:</b> Auger Rotary-wash (mud drilling fluid) Drilling rate (min./ft) 2</p> <p><b>SAMPLING:</b> Standard penetration sample taken inside a 1 1/2" I.D. split spoon driven 18" into the soil by a 140 lb. weight falling 30" at the top of the drill rod. Blow count for last 12" or, if penetration &lt; 12", for depth driven as noted. 36 California penetration sample taken inside a 2" I.D. split spoon driven into the soil by 425 lb. slip jars falling inside the boring. Ca. Shelby sample taken inside a 3" I.D. thin-walled tube mounted on end of drill rod and pushed into soil by drill rig. S Pitcher undisturbed sample taken inside a 3" I.D. Shelby tube mounted in a Pitcher core barrel. Rock core sample taken inside a NX (2 1/4") size core barrel with a diamond bit.</p> <p><b>DENSITY:</b> Results of laboratory tests</p>	<p><b>DRILLING</b> <b>BLOW</b> <b>SAMPLING</b></p>	<p><b>DESCRIPTION</b></p> <p><b>DESCRIPTION:</b> Texture: the relative proportions of clay, silt, and sand below 2mm. Proportions of larger particles are indicated by modifiers of textural class names. Determination is made in the field mainly by feeling the moist soil. (Soil Survey Staff, 1951)</p>  <p><b>Color:</b> Standard Munsell color names are given for the dominant color of the moist soil and for prominent mottles.</p> <p><b>Plasticity:</b> estimated from the strength of air dried sample and toughness of thread formed when soil is rolled at the plastic limit. (Sowers and Sowers, 1970)</p> <table border="1" data-bbox="854 1253 1367 1388"> <thead> <tr> <th>elasticity</th> <th>dry strength</th> <th>field test</th> </tr> </thead> <tbody> <tr> <td>non plastic</td> <td>v. low</td> <td>falls apart easily</td> </tr> <tr> <td>slightly</td> <td>slight</td> <td>easily crushed</td> </tr> <tr> <td>medium</td> <td>medium</td> <td>friable with difficulty</td> </tr> <tr> <td>highly</td> <td>high</td> <td>cannot crush with fingers</td> </tr> </tbody> </table> <p><b>Relative density of sand and consistency of clay is correlated with penetration resistance: (Terzaghi and Peck, 1948)</b></p> <table border="1" data-bbox="854 1471 1367 1647"> <thead> <tr> <th>blows/ft.</th> <th>relative density</th> <th>blows/ft.</th> <th>consistency</th> </tr> </thead> <tbody> <tr> <td>0-4</td> <td>v. loose</td> <td>&lt; 2</td> <td>v. soft</td> </tr> <tr> <td>4-10</td> <td>loose</td> <td>2-4</td> <td>soft</td> </tr> <tr> <td>10-30</td> <td>medium</td> <td>4-8</td> <td>medium</td> </tr> <tr> <td>30-50</td> <td>dense</td> <td>8-15</td> <td>stiff</td> </tr> <tr> <td>&gt;50</td> <td>v. dense</td> <td>15-30</td> <td>v. stiff</td> </tr> <tr> <td></td> <td></td> <td>&gt;30</td> <td>hard</td> </tr> </tbody> </table> <p>CL, MH, etc.: Unified Soil Classification Group Symbol (U.S. Army Corps of Engineers, 1960)</p>	elasticity	dry strength	field test	non plastic	v. low	falls apart easily	slightly	slight	easily crushed	medium	medium	friable with difficulty	highly	high	cannot crush with fingers	blows/ft.	relative density	blows/ft.	consistency	0-4	v. loose	< 2	v. soft	4-10	loose	2-4	soft	10-30	medium	4-8	medium	30-50	dense	8-15	stiff	>50	v. dense	15-30	v. stiff			>30	hard
elasticity	dry strength	field test																																											
non plastic	v. low	falls apart easily																																											
slightly	slight	easily crushed																																											
medium	medium	friable with difficulty																																											
highly	high	cannot crush with fingers																																											
blows/ft.	relative density	blows/ft.	consistency																																										
0-4	v. loose	< 2	v. soft																																										
4-10	loose	2-4	soft																																										
10-30	medium	4-8	medium																																										
30-50	dense	8-15	stiff																																										
>50	v. dense	15-30	v. stiff																																										
		>30	hard																																										

Figure 2. Explanation for geologic logs showing types of samples and terminology and methods for describing soil and rock materials.

ELEVATION: DATE :	LOCATION: LAT. LONG.  7 1/2' QUAD	HOLE NO : SITE: GEOLOGIC MAP UNIT:																		
SAMPLE DESCRIPTION	DESCRIPTION																			
	<p><i>Rock hardness : response to hand and geologic hammer: (Ellen et al., 1972)</i>  <i>hard - hammer bounces off with solid sound</i>  <i>firm - hammer dents with thud, pick point dents or penetrates slightly</i>  <i>soft - pick point penetrates</i>  <i>friable material can be crumbled into individual grains by hand.</i></p> <p><i>Fracture spacing: (Ellen et al., 1972)</i></p> <table border="1"> <thead> <tr> <th>cm</th> <th>in</th> <th>fracture spacing</th> </tr> </thead> <tbody> <tr> <td>0-1</td> <td>0-2</td> <td>v. close</td> </tr> <tr> <td>1-5</td> <td>2-2</td> <td>close</td> </tr> <tr> <td>5-30</td> <td>2-12</td> <td>moderate</td> </tr> <tr> <td>30-100</td> <td>12-36</td> <td>wide</td> </tr> <tr> <td>&gt;100</td> <td>&gt;36</td> <td>v. wide</td> </tr> </tbody> </table> <p><i>Weathering: (Aetron-Blume-Atkinson, 1965)</i>  <i>Fresh: no visible signs of weathering</i>  <i>Slight: no visible decomposition of minerals, slight discoloration</i>  <i>Moderate: slight decomposition of minerals and disintegration of rock, moderate discoloration</i>  <i>Deep: moderate decomposition of minerals, extensive disintegration of rock, deep and thorough discoloration</i>  <i>Decomposed: extensive decomposition of minerals and complete disintegration of rock but original structure is preserved</i></p>		cm	in	fracture spacing	0-1	0-2	v. close	1-5	2-2	close	5-30	2-12	moderate	30-100	12-36	wide	>100	>36	v. wide
cm	in	fracture spacing																		
0-1	0-2	v. close																		
1-5	2-2	close																		
5-30	2-12	moderate																		
30-100	12-36	wide																		
>100	>36	v. wide																		

Figure 2. Continued.

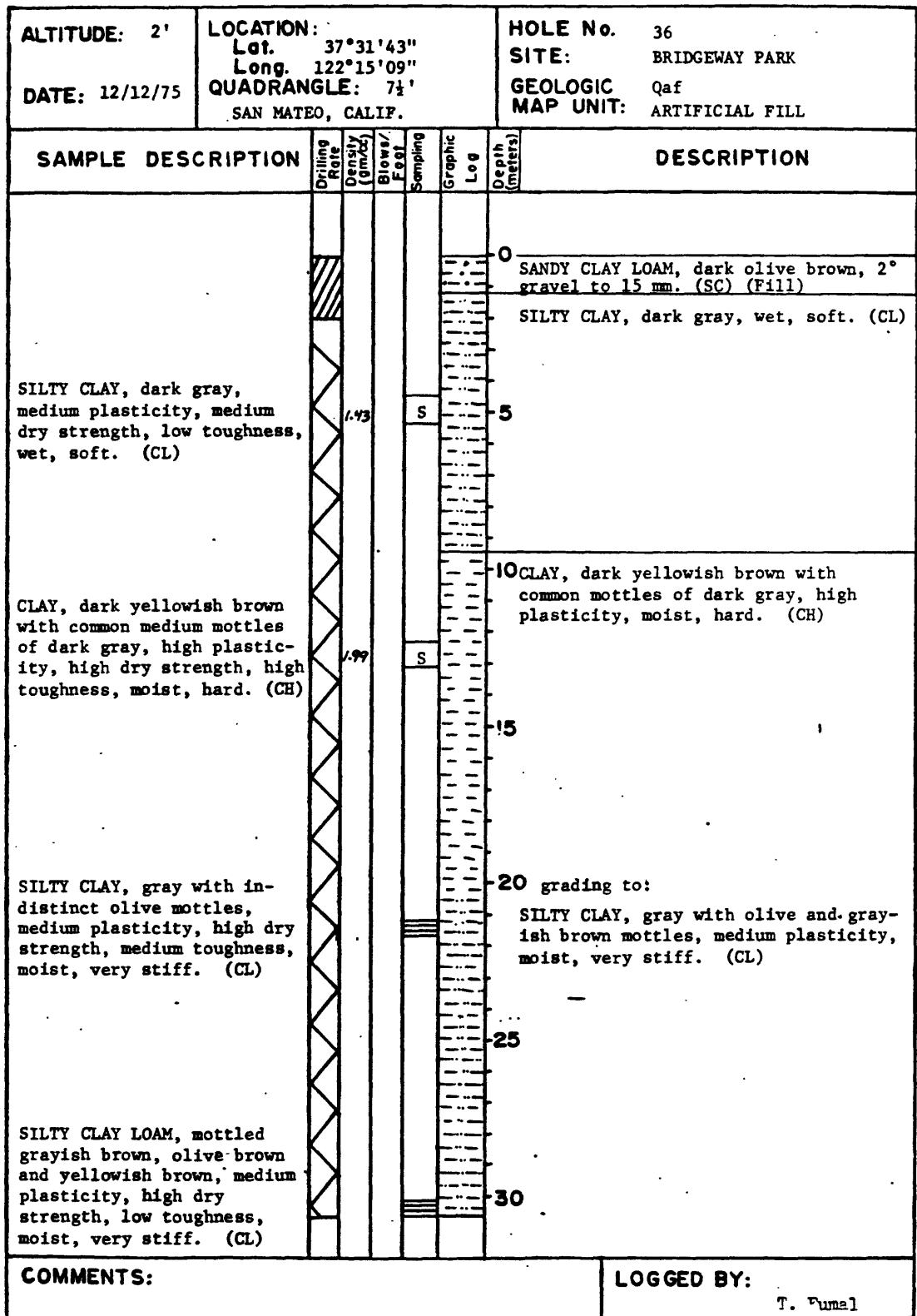


Figure 3. Sample geologic log.

While the accuracy of the density measurements is generally sufficient for calculation of elastic moduli, a number of the samples used to obtain densities were not entirely representative of the in-situ material. Materials that were sampled by penetration are somewhat disturbed and many had dried out before measurements could be made. Densities of hard rock obtained using intact rock fragments are maximum densities. Depending on the amount and openness of fractures, these densities could be higher than in-situ densities by approximately 0.1 - 0.2 gm/cc.

### Reduction of Seismic Data

#### Identification of Shear Wave Onset

To aid in the identification of the shear wave arrivals the signals recorded by the downhole sensor from each pair of horizontal hammer blows are superimposed and drafted on a common time base (fig. 4). The S-wave group is easily identified by the large amplitude and 180° phase reversal. The onset of the S-wave arrival is taken as the start of the first clear departure from coincidence in the group. Interpretation proceeds from the bottom record to the top using phase correlation at each depth. Phase correlation aids in interpreting seismograms containing significant P-wave energy or probable P to S converted waves. The onset of the S-wave is generally easier to identify in unconsolidated sediments than in bedrock.

#### Travel Times

A sample record is shown in figure 5. To determine the travel time for the S-wave the following times are measured with respect to the break

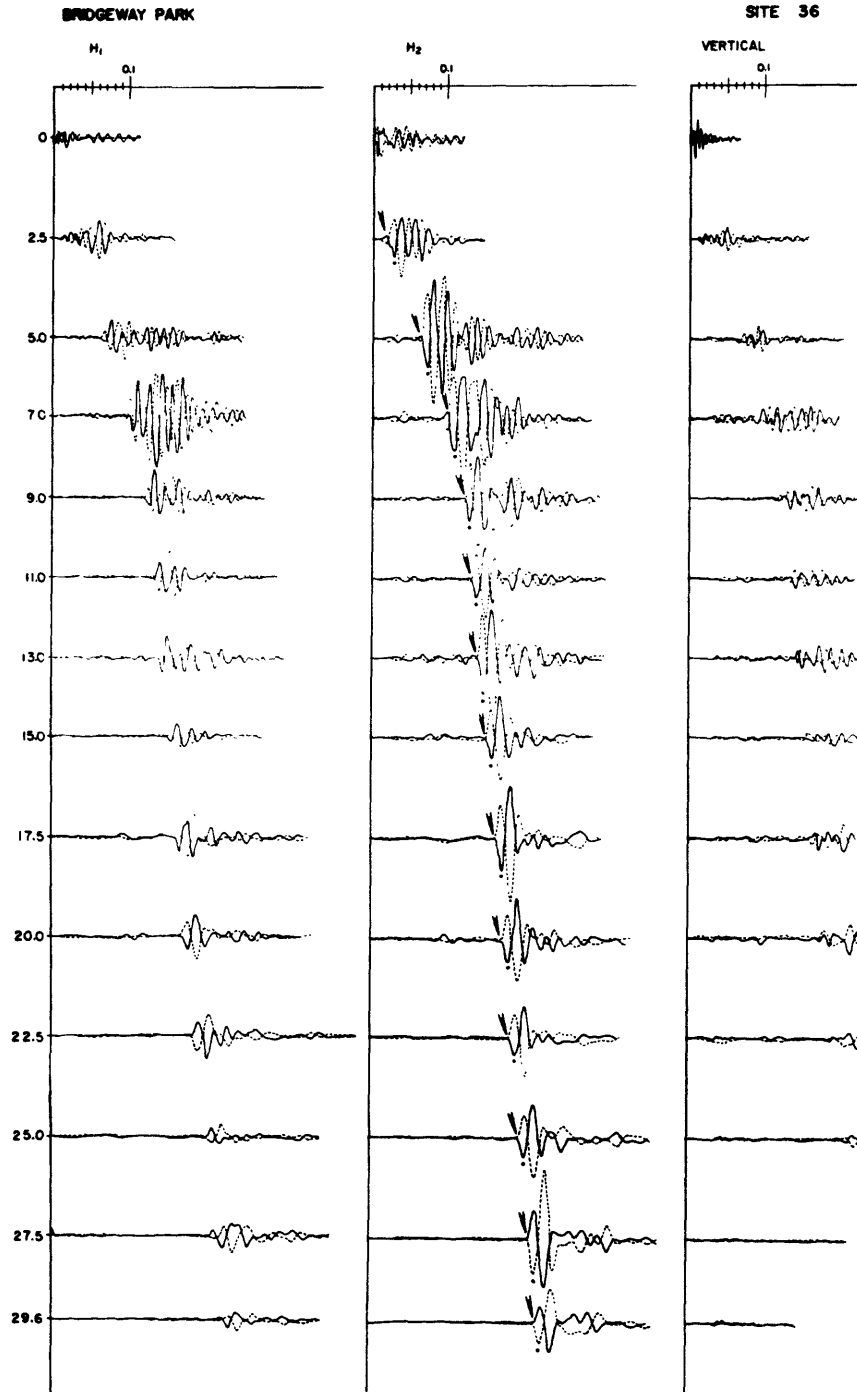


Figure 4. Example of record section. Arrows indicate first arrivals of S-wave energy.

in the signal from the hammer inertia switch ( $t_0$ ):

- 1)  $t_1$  = time of onset of S-wave on inline uphole sensor;
- 2)  $t_2$  = time of onset of S-wave on downhole sensors.

The time of onset of the S-wave on the inline uphole sensor is taken as the origin time of the S-wave pulse. Because of uncertainty in identifying this onset, an average value ( $t_A$ ) is determined for the set of values,  $t_1 - t_0$ , measured on each record. The travel time for the S-wave is given by

$$t_s = (t_2 - t_0) - t_A.$$

A corrected S-wave travel time ( $t_{sc}$ ), corresponding to the travel time for a vertical ray path is calculated using

$$t_{sc} = t_s + t_c$$

where  $t_c$  is a correction (cosine of angle of ray incidence) due to the distance the timber is offset from the center of the hole.

The travel times for the P-waves generated by the vertical hammer impact are determined in the same manner except that the origin time for the P-wave is given by the impact switch and no origin correction is necessary.

#### Interval Velocities and Elastic Moduli

Average velocities were calculated for depth intervals over which the velocity is approximately constant. To determine these depth intervals, the travel time data are plotted as a function of depth and compared with the geologic logs (fig. 6). Depth intervals for velocity calculations are determined on the basis of distinct changes in slope of the travel time plots and evidence for geologic boundaries. For those

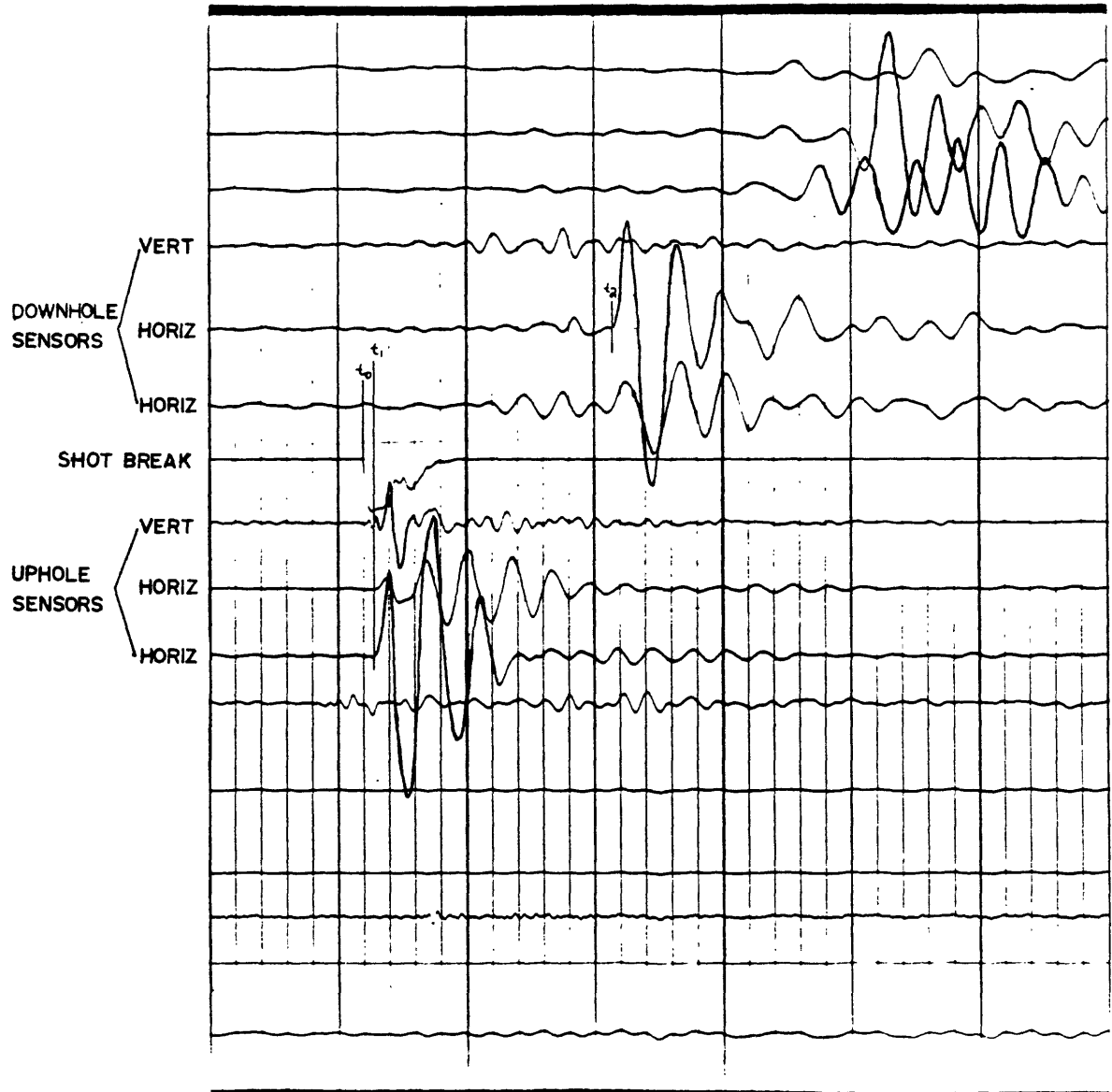


Figure 5. Example of record from downhole and uphole sensors of energy generated by impact of horizontal hammer. Times  $t_0$ ,  $t_1$ , and  $t_2$  used to calculate travel time of S-wave energy are indicated.

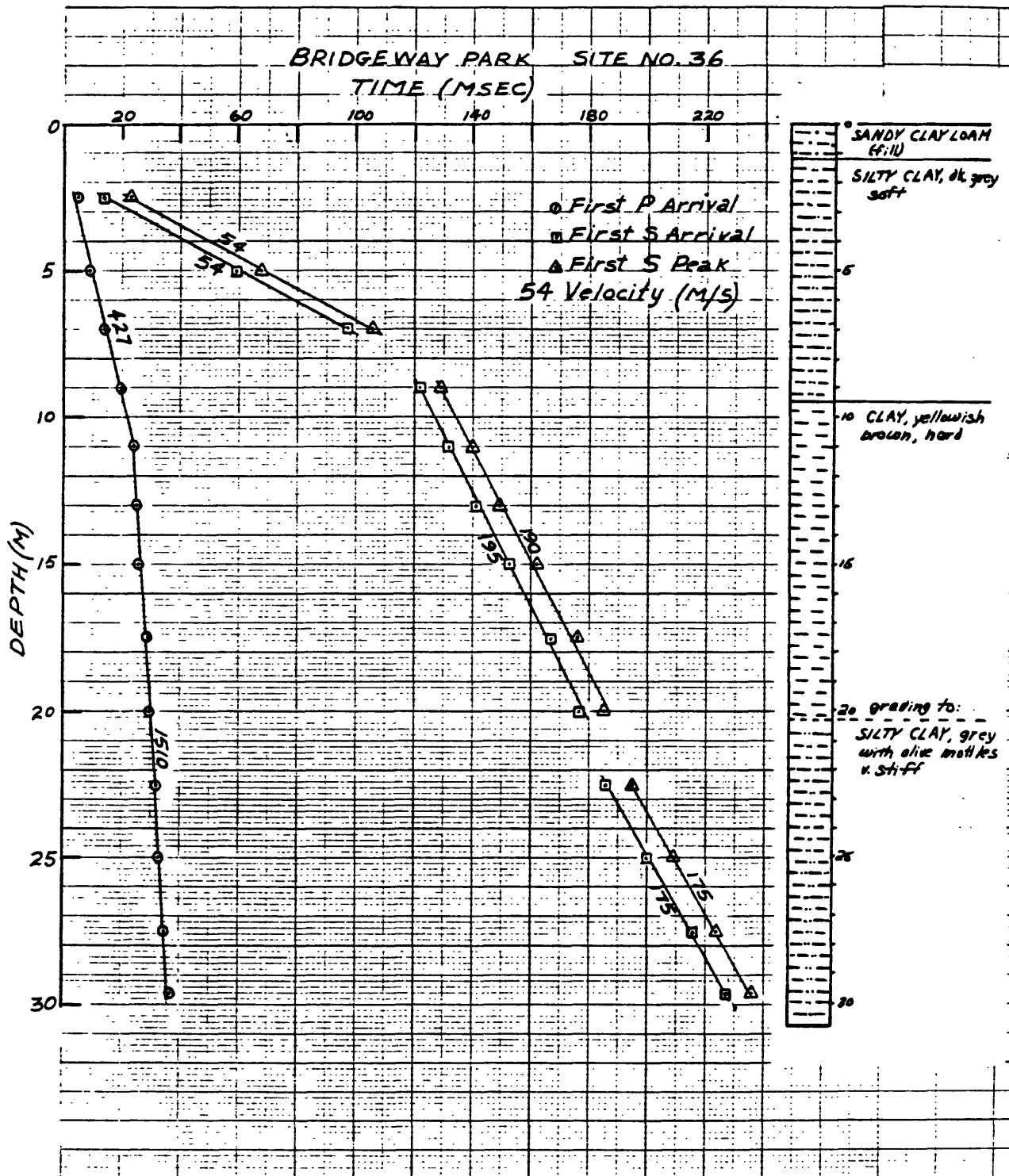


Figure 6. Example of travel time curves for P and S-waves along with simplified geologic log.

materials with S-velocities greater than 350 m/sec, the intervals were required to contain at least four travel time measurements. This avoids determining a velocity from a travel time difference due largely to measurement error. Velocities are calculated for the selected intervals from the slope of the linear regression line which best fits the travel time data in a least squares sense (Borcherdt and Healy, 1968).

For those depth intervals with measurements of density ( $\rho$ ), the shear modulus (G) and bulk modulus (k) are calculated using

$$G = \rho V_s^2$$

$$\text{and } k = \rho V_p^2 - \frac{4}{3} G.$$

Poisson's ratio ( $\sigma$ ) is calculated using

$$\sigma = \frac{\frac{V_p^2}{V_s^2} - 2}{2 \frac{V_p^2}{V_s^2} - 2}$$

The value of shear modulus for a given material is strongly dependent on the shearing strain amplitude (Hardin and Drenevich, 1972a). Computations using shear wave velocity (strain amplitude  $< 0.25 \times 10^{-4}\%$ ) give the maximum values of shear modulus. Estimations of shear moduli at earthquake strain levels can be derived from appropriate design curves (Hardin and Drenevich, 1972b).

#### IV. DISCUSSION OF RESULTS

Seismic wave velocities were measured at fifty-nine sites in a spectrum of near-surface geologic materials. Results of these measurements will be discussed first in terms of correlations between interval velocities and several other physical properties of the materials. As determinations of the physical properties were made using field methods, they are generally only relative evaluations of the average properties of the soil or rock mass. Standard penetration resistance, density, and seismic wave velocity were the only quantitative tests performed.

The primary physical properties which control velocities of seismic waves in soils are different from those in rock. Therefore, the geologic materials sampled in this study have been divided into two broad categories based on degree of induration: 1) unconsolidated to moderately consolidated sedimentary deposits and 2) bedrock. The first group is comprised of all deposits ranging in age from Holocene through Pliocene-Pleistocene including the Santa Clara Formation, the Merced Formation and the Purisima Formation. The single exception is the Stevens Creek site (STCR) which was drilled entirely in gravels of the Santa Clara Formation, which are moderately well-cemented and will therefore be considered with the bedrock units. The velocity characteristics of each of these two categories will be discussed separately.

For purposes of seismic zonation, geologic maps have been used as an important source of data (Lajoie and Helley, 1975). A discussion of the seismic characteristics of the geologic units used in mapping in the San Francisco Bay region follows each section on correlations between velocities and physical properties. Finally, a regrouping of the geologic

units based on the range of significant physical properties within them is proposed.

A. Shear Wave Velocities in the Sedimentary Deposits

Correlations between S-wave velocity and physical properties

Unconsolidated to moderately consolidated sedimentary deposits comprise the entire drilled sections at thirty-one sites and the upper parts of four others. The results of the measurements of the shear waves in these deposits are summarized in figure 7 showing average velocity over the depth intervals obtained from travel-time curves. Since these sediments are for the most part thickly bedded, the velocity intervals generally correspond to materials with relatively homogeneous physical properties. From two to five such velocity intervals were obtained at each site.

In figure 7, the sediments have been grouped on the basis of several primary physical properties and secondary soil indices which are related to those factors found to significantly affect shear wave velocity in laboratory studies and for which data are available. The most important of these parameters are soil texture, standard penetration resistance and depth below the surface. Mean, range, and standard deviation of the velocities in each group are shown in Table 1. Correlations between interval velocities and each of the geotechnical properties will be discussed in turn.

Texture

Petrographic factors which can significantly influence the engineering properties of sedimentary deposits include texture (relative grain-

size distribution), shape, mineralogical composition of the grains and chemical composition of the adsorbed layers of clay particles. Of these factors, texture appears to have the largest effect on shear wave velocity. This result is as expected, as the average particle size and sorting are very important in determining the void ratio of both cohesive and cohesionless soils (Meade, 1968). In general, the data in figure 7 show an increase in shear wave velocity with increasing grain size. The sediments can be divided into five categories based on grain size distribution:

<u>Textural Group</u>	<u>Soil Textural Classes Included</u> (from figure 2)
Clay and silty clay	Clay, silty clay, clay loam, silty clay loam
Sandy clay	Sandy clay, sandy clay loam
Silt loam	Silt, silt loam
Sand	Sand, loamy sand, sandy loam, loam, gravelly sand
Gravel	Greater than 15-20% coarse fragments

At several sites near San Francisco Bay, sections ranging from 4. to 16.5 meters in thickness were found to consist of interbedded silty clays and sandy gravels. Individual beds were too thin to allow determination of velocities for each distinct type of material so an average velocity over the entire interval was calculated. These interbedded sediments have been designated as an additional textural grouping.

Clays and silty clays show the most distinct velocity characteristics of the groupings. The main overlap is at very shallow depths (0 < 5 m) where velocities measured in Holocene dune sands were as low as any

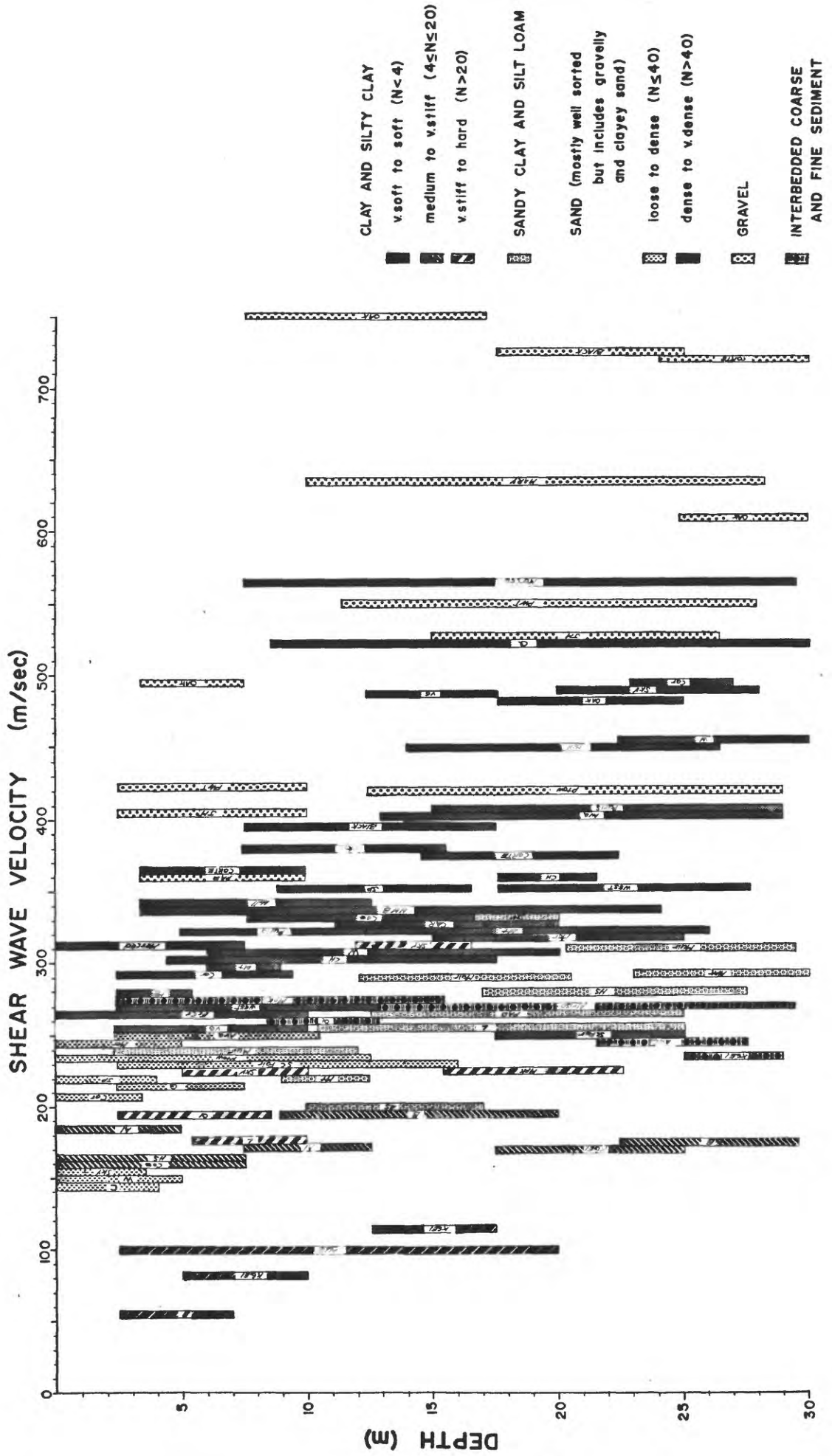


Figure 7. Shear wave velocity-depth intervals for unconsolidated to semiconsolidated sedimentary deposits differentiated according to physical properties.

TABLE 1

## SHEAR WAVE VELOCITIES IN SEDIMENTARY DEPOSITS

Physical Property Unit	Interval(m)	No.	Shear Wave Velocity (m/sec)		
			Mean	Standard Deviation	Range
<b>Silty Clay and Clay</b>					
v. soft to soft (N<4)					
near surface	2.5-12	3	80	19	54-101
at depth	12-20	2	108	17	101-114
Medium to v. stiff (4≤N≤20)					
	0-30	7	175	11	160-195
v. stiff to hard (N>20)					
near surface	2.5-12	3	200	22	175-229
at depth	12-22	2	270	43	226-312
<b>Sandy Clay and Silt Loam</b>					
near surface	2.5-12	3	222	14	203-238
at depth	12-30	7	290	15	255-329
<b>Sand</b>					
N≤40	0-16	10	206	36	150-249
N>40					
near surface	0-12	11	306	40	251-380
at depth	12-30	22	398	83	253-522
<b>Gravel</b>					
near surface	2.5-10	4	421	49	360-497
at depth	10-30	8	616	113	418-749
<b>Interbedded Sediment</b>					
	2.5-30	5	258	15	233-276

of the fine-grained sediments except the bay mud. Also, the silty clay sampled at the Skyline (SKY) site showed a velocity that was 100 m/sec higher than any other silty clay. This sediment, part of the Pliocene-Pleistocene Merced Formation, was the only silty clay older than late Pleistocene.

Although the silt loams are much better sorted than the sandy clays, they may have similar void ratios. They do have similar velocity ranges and so have been grouped together. At near-surface depths ( $D \leq 12$  m) the velocities for this group overlap with the lower end of the range for sands. At depth ( $D > 12$  m), the separation is much better except for the silt loam in the Merced Formation at the Skyline site. This sediment has a velocity which is 60 m/sec faster than any other silt loam and overlaps with velocities obtained for sands.

The interbedded silty clays and sandy gravels show a relatively narrow velocity range and an average velocity similar to that for sandy clays and silt loams.

The sand category can be subdivided into four groups based on average grain size and sorting:

<u>Sorting</u>	<u>Grain size (predominant size range in mm)</u>
Well-sorted	Very fine (.05 - .1)
Well-sorted	Fine to medium (.1 - .5)
Well-sorted	Coarse to very coarse (.5 - 2)
Poorly-sorted	

These groupings are shown in fig. 8. The only significant velocity distinction evident here is that the well-sorted, very fine-grained sands have lower velocities than other sands except for the Holocene fine- to

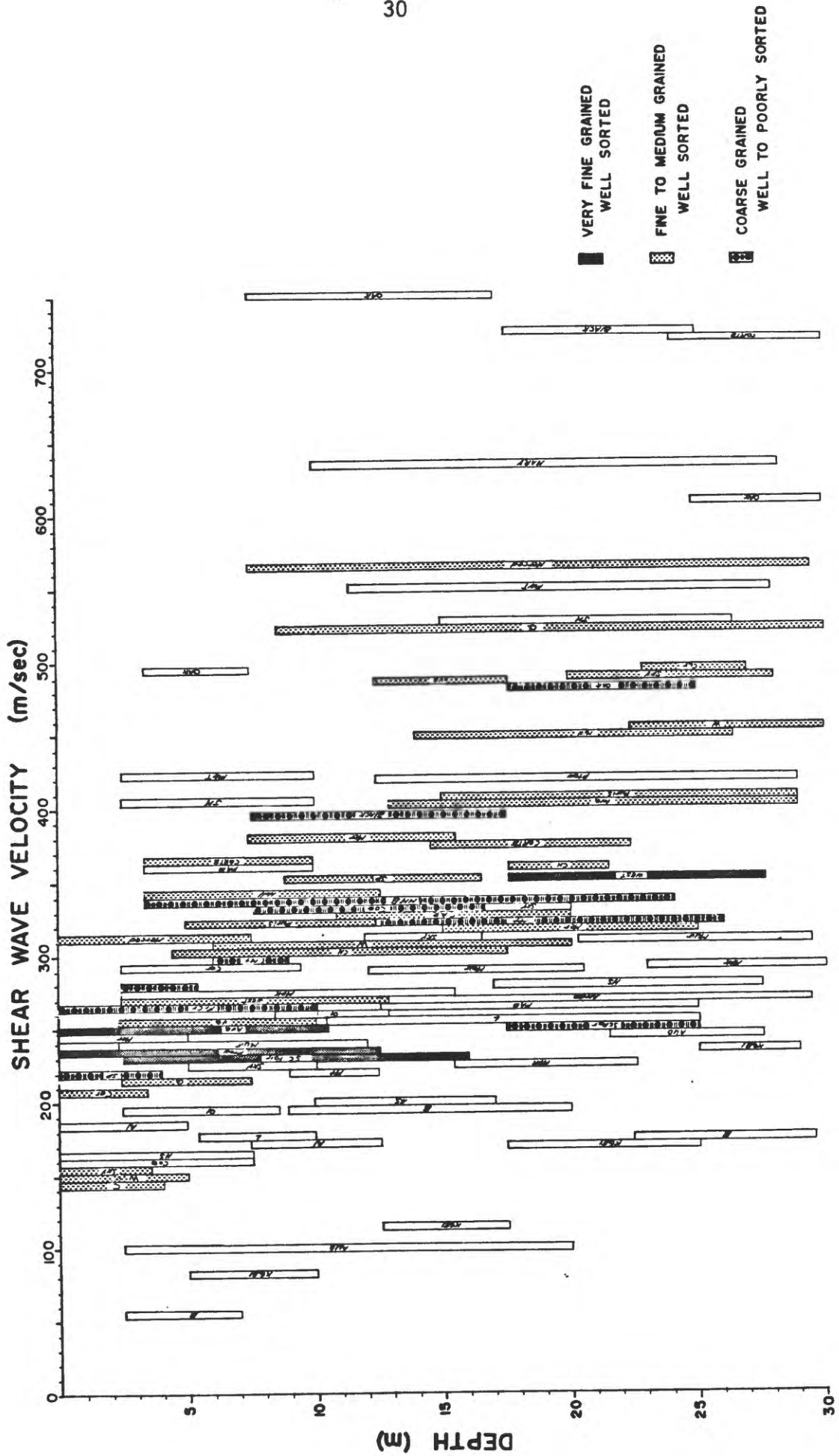


Figure 8. S-wave velocity-depth intervals showing grain size classification of sands.

medium-grained dune sands at the Windmill (W), Chain of Lakes (CH), and Quintara (Q) sites. Thus, although there is a large velocity variation in the sands, it appears that little of it is due directly to textural variations.

The gravelly sediments generally show higher velocities than any of the other sediments. The main exception is the Parkway Towers (PTOW) site where a velocity that is 140 m/sec slower than any other gravel was measured. This variation may be due in part to differences in sorting. Samples of the gravels at Joaquin Miller School (JM) and Pulgas Water Temple (PWT) were poorly sorted. While an undisturbed sample was not recovered at Parkway Towers, it appeared to be better sorted on the basis of drill cuttings and rapid loss of drilling fluid.

#### Standard Penetration Resistance

Standard penetration resistance tests were carried out in unconsolidated sedimentary materials according to the procedure detailed in figure 2. Results of these tests are shown in figure 9 with the resistance in blows per foot for a given sample plotted against the average velocity obtained for the depth interval containing that sample. The scatter in this data is very wide, even when divided into cohesive and cohesionless soil categories. This wide variation is similar to that obtained by other workers. For example, figure 10 shows a comparison of 220 measurements from a variety of soils underlying high-rise buildings in Japan (Ohasaki and Iwasaki, 1973) with those of this study. A significant part of the scatter may be due to the difference in sampling scale of the techniques for obtaining N-values and shear wave velocity. The N-value is recorded cumulatively over a 0.5 m interval and is very sensitive to

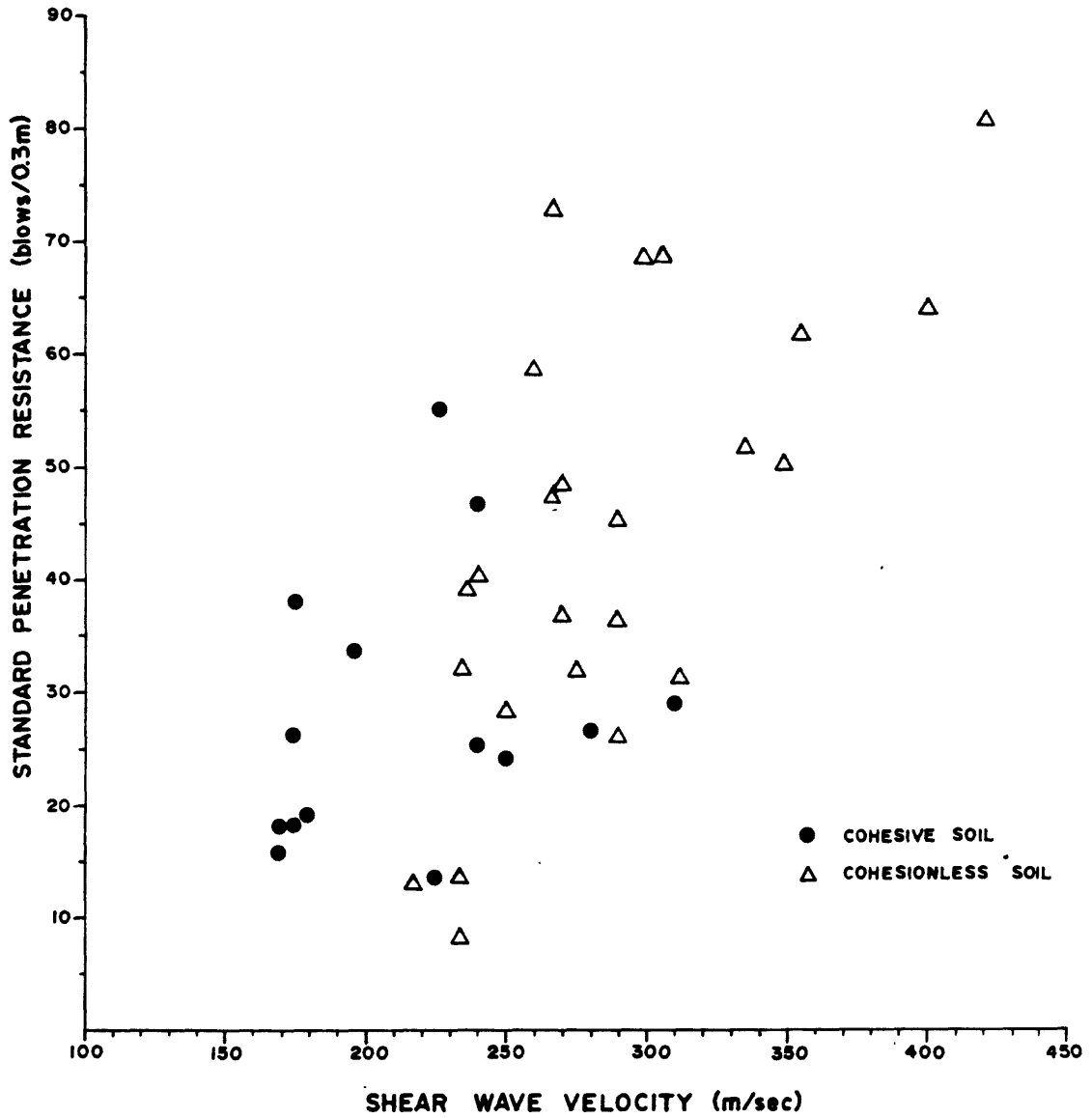


Figure 9. Variation of shear wave velocity with standard penetration resistance.

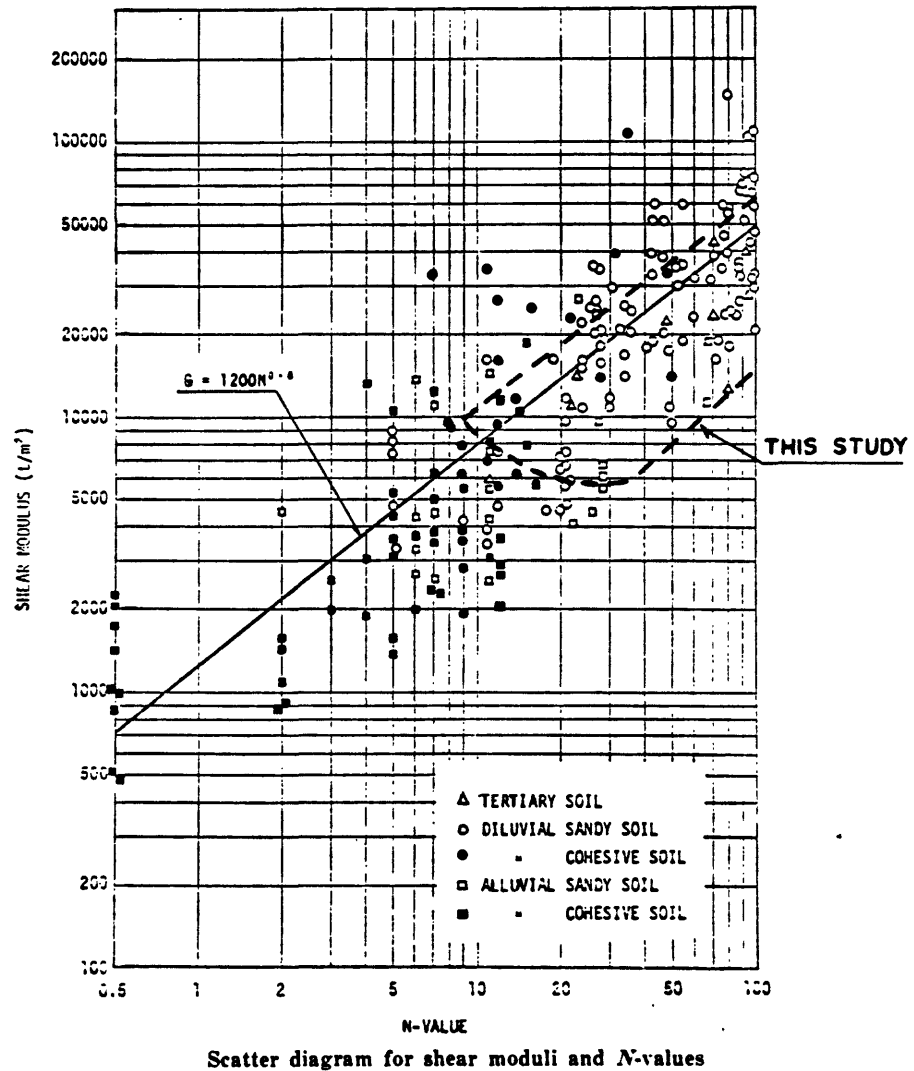


Figure 10. Scatter diagram for shear moduli and N-values from 220 sites in Japan (Ohasaki and Iwasaki, 1973). Data from the present study (Fig. 9) fall within the dashed line.

small inhomogeneities. The S-wave velocity, on the other hand, is an average value over 5 to as many as 22.5 meters. As an example, for very fine sand at Parkway Towers, blow counts of 7 and 32 were recorded in the 235 m/sec interval.

It appears that a useful correlation between standard penetration resistance and shear wave velocity cannot be formulated for the sedimentary materials as a whole. However, N-value has been correlated (Lambe and Whitman, 1969) with other index properties of soils which are affected by the same primary physical properties which influence shear wave velocity. These index properties can be used to explain some of the variation within the textural groupings and thus provide a basis for subdividing the broader categories.

For cohesive soils, N-value serves as an index to the consistency (relative firmness) and shear strength of a soil. The clays and silty clays have been subdivided into three groupings based on this relationship: v. soft to soft ( $N < 4$  blows/ft), medium to v. stiff ( $4 \leq N \leq 20$  blows/ft) and v. stiff to hard ( $N > 20$  blows/ft). The velocity differences between the v. soft to soft and the medium to v. stiff clays is very large while there is some overlap in velocities between the medium to v. stiff and v. stiff to hard categories (Table 1).

The consistency of a cohesive soil is affected by many factors, including soil structure, void ratio, cementation and overconsolidation due to loading or dessication. The magnitude of some of these effects can be estimated from the data in fig. 7. The large difference in velocities between the clays with  $N < 4$  and those with  $4 \leq N \leq 20$  is in part due to variation in soil structure (and hence void ratio) related to deposi-

tional environment. The clays with  $N < 4$  are estuarine muds and were probably deposited with a salt-flocculated structure, while the  $4 \leq N \leq 20$  clays are alluvial flood basin sediments and may have a more dispersed structure (Rosenquist, 1960). In a study of sedimentary deposits in the San Joaquin Valley, Meade (1968) found that shallow marine silts at depths of 240 m - 600 m had substantially higher void ratios (1 - 1.6) than overlying flood plain silts (.7 - 1).

#### Long-Term Water Levels

Several factors which act to increase consistency and shear wave velocity, such as cementation and overconsolidation, are related to the position of the water table before and after deposition. Flood basin clays are deposited in thin layers and are seasonally dessicated. They thus have the characteristics of highly overconsolidated soils even though they may have never been deeply buried (Terzaghi, 1955; Komornik et al., 1970). After deposition they may remain above the water table for extended periods of time and thus may be subjected to various weathering processes such as cementation.

The long-term water table effects may be indicated by the color of the sediment. In the southern San Francisco Bay area, soil color is primarily determined by the oxidation state of iron compounds and the content of organic matter. Ferric iron produces red and yellow colors while ferrous iron causes grey colors. Organic matter serves mainly to darken colors. Thus, many brown soils contain relatively large amounts of organic matter, as well as ferric iron oxides. Yellow colors, which are relatively unstable under moist conditions, indicate good drainage and aeration. Grey colors are associated with soils which have been

saturated during and since deposition. Poorly drained soils are usually mottled with various shades of grey, brown and yellow, especially in the zone of fluctuating water table. The proportion of grey generally increases with increasing wetness (Soil Survey Staff, 1951). Figure 11 shows the colors of the cohesive sediments divided into three color groupings: grey, mottled with shades of grey, brown and yellow, and shades of yellow and brown. Group boundaries obtained from standard penetration resistance are included for comparison. Groupings based on the two different indices agree quite well. The grey colors correspond to the  $N < 20$  clays and the yellowish brown and brown soils with the  $N > 20$  clays and silty clays and the sandy clays-silt loams (which have  $N > 25$ ).

A specific example of the magnitude of the effects of dessication may be found at Bridgeway Park (figure 6). The sediments from 9.5 to 31 meters were probably deposited in an alluvial flood basin prior to the formation of the Bay (10,000 - 6,000 years B.P.) and deposition of the overlying estuarine muds (Atwater et al., 1977). The section from 9.5 to 20 m, which is yellowish brown mottled with grey, is more strongly oxidized and has a shear wave velocity 25 m/sec higher than the lower part which is grey mottled with olive and greyish brown. The slightly higher clay content in the upper section may be due in part to the greater exposure to weathering processes.

Figure 12 shows a similar grouping on the basis of color for sandy sediments. Unlike the cohesive sediments, there is no useful correlation between color and S-wave velocity except for a tendency for yellowish brown sands to have higher velocities at depths greater than 10 m. This

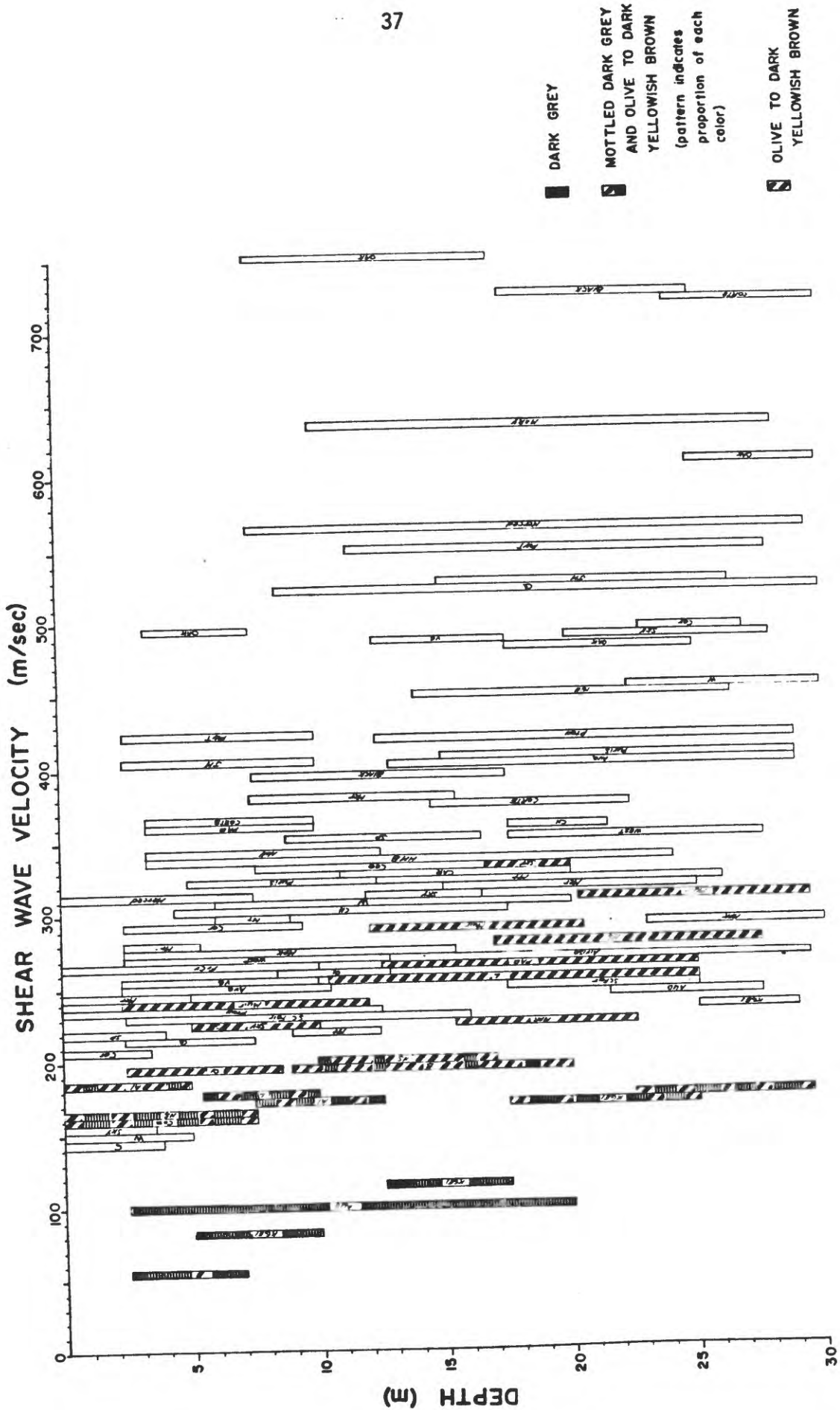


Figure 11. Distribution of soil colors in cohesive sediments. Boundaries of standard penetration resistance groups are indicated.

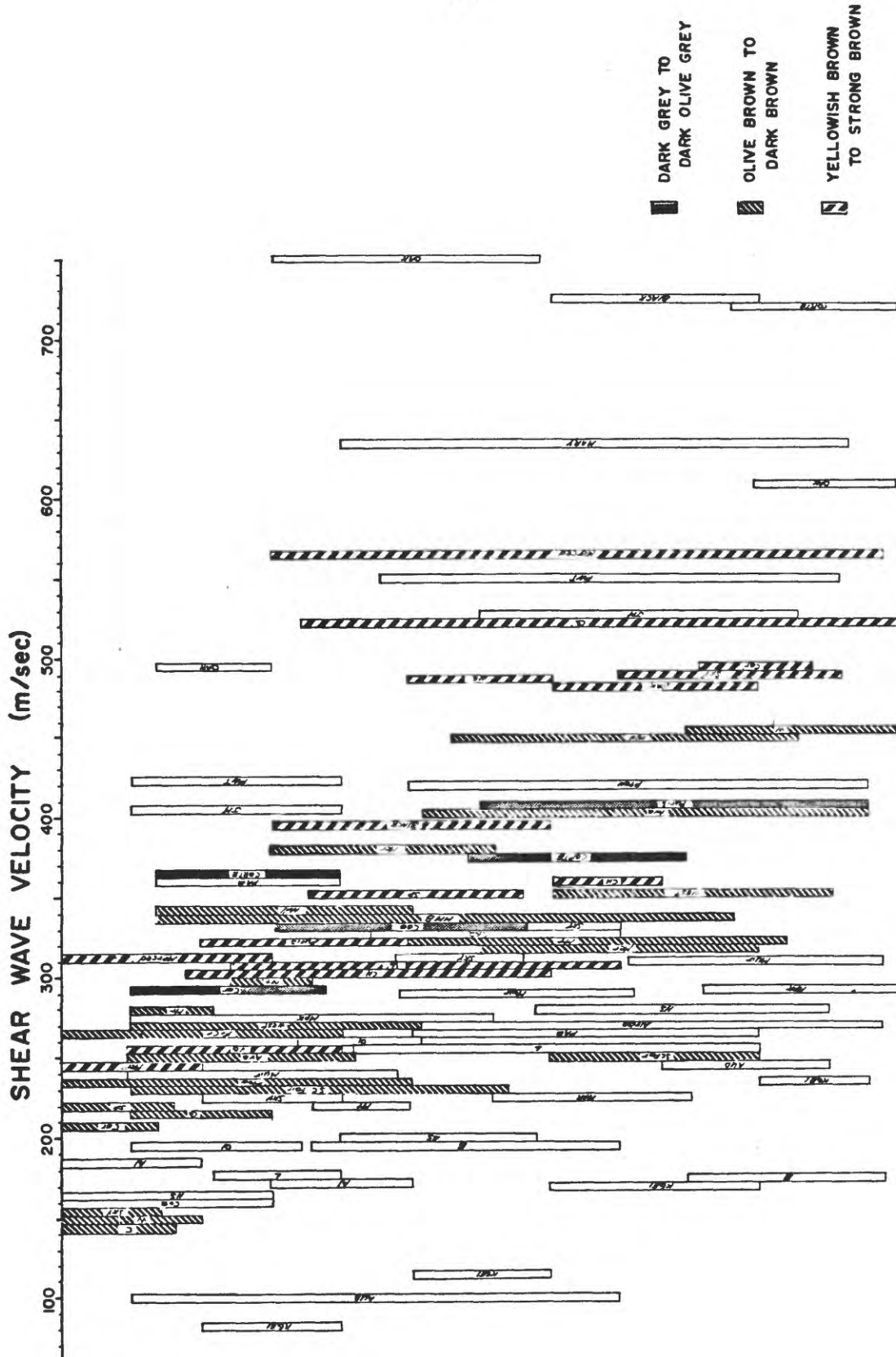


Figure 12. Soil color for sand sediments.

URATED  
ATURATED

nts.

lack of correlation is to be expected as sands are little affected by wetting and drying.

#### Short-Term Water Levels

For comparison, presently water-saturated and unsaturated cohesive sediments (as indicated by present water table levels) are shown in figure 13. The level of the water table is taken as the depth at which the P-wave velocity increased to approximately 1500 m/sec. In the case of the bay muds (clays with  $N < 4$ ) P-wave velocities ranged from 450 to 1100 m/sec. As water tables at the times of drilling and velocity logging were within 2 m of the ground surface, these sediments were taken to be water-saturated over the intervals for which S-wave velocities are reported.

In contrast to the long-term water table effects, the short-term water levels shown in figure 13 do not provide a useful correlation with S-wave velocity. Although there is a general tendency for the unsaturated sediments to have higher velocities at a given depth, this trend can be attributed to other factors. The silty clays at the Skyline site (SKY) are Pliocene-Pleistocene in age--an order of magnitude older than the other cohesive sediments sampled. The sediments at the Muir School site (MUIR) are sandy clays and could be expected to have relatively higher velocities on that basis. At this site the S-wave velocity appears to increase slightly (291 to 309 m/sec) going from unsaturated to saturated sandy clay. Thus for the data presented in figure 13, it is not possible to determine whether the higher velocities are the result of the sediments being presently unsaturated or due to other factors such as texture and time-dependent effects.

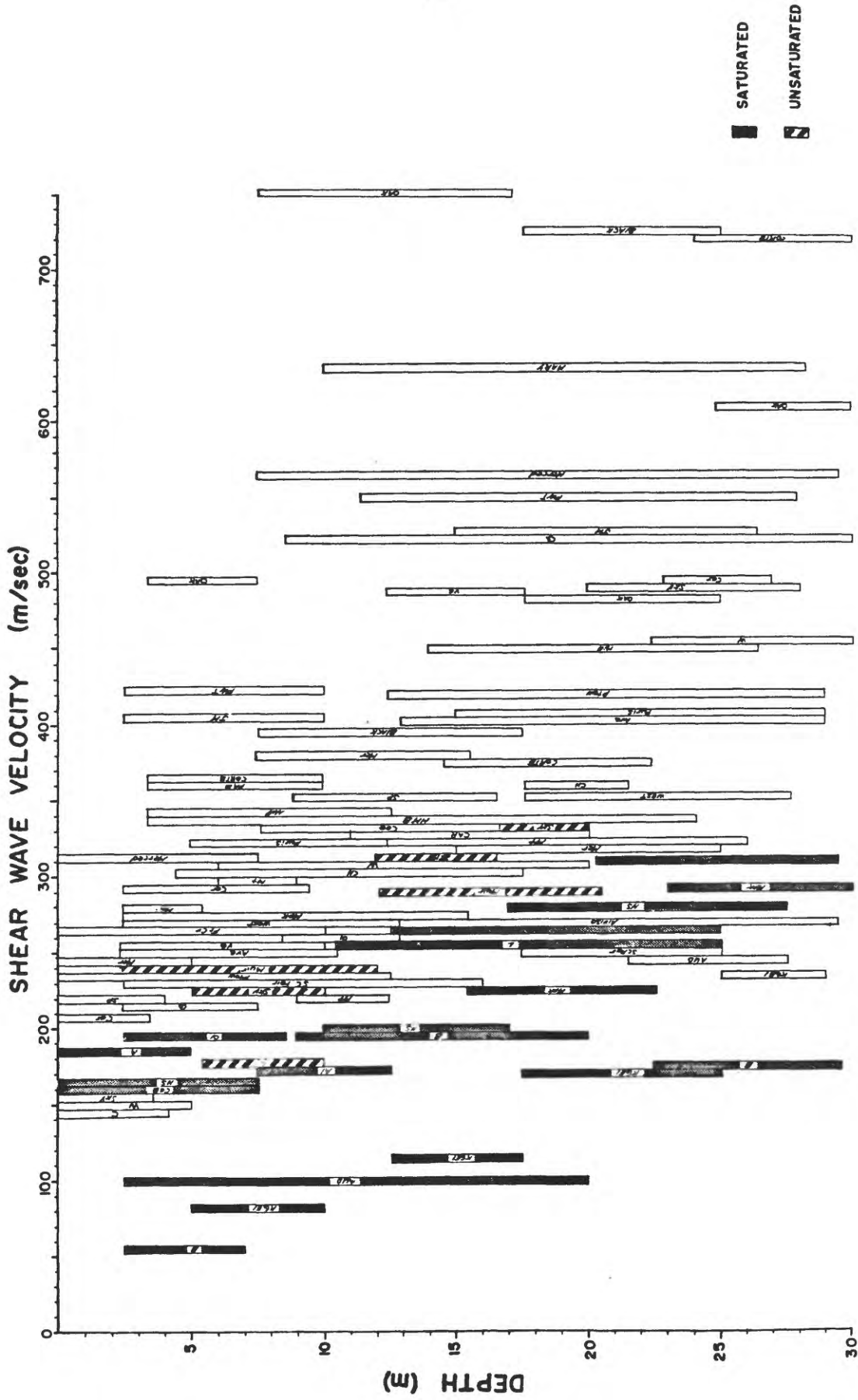


Figure 13. Relative degree of saturation for cohesive sediments as indicated by P-wave velocity measurements.

Figure 14 shows relative degree of saturation for sands as indicated by P-wave velocities. The sediments have been divided into three categories:  $V_p < 1000$  m/sec ("dry"),  $1150 \text{ m/sec} \leq V_p \leq 1300$  m/sec ("near-saturated"), and  $V_p \geq 1500$  m/sec ("saturated"). As was the case for color, no useful subdivision of the sands can be made using degree of saturation. Two weak and opposing trends are evident. In the near-surface, the "dry" sands show lower velocities than the other two groups. However, these lower velocities can be attributed to lower densities, as these sands for the most part have standard penetration blow counts less than 40. At depth, however, the "near-saturated" sands show velocities which are somewhat higher than the saturated sands. The small effect of saturation on S-wave velocity for sands apparent in figure 14 is in agreement with the results of laboratory studies carried out by Hardin and Richart (1963). They found that the shear modulus of saturated Ottawa sand (nearly spherical grains) was less than 5% lower than that for the drained condition (moisture content = 1.4%). No significant effect was observed for crushed quartz.

#### Relative Density

For cohesionless soils, N-value has been related to the relative density and is most meaningful for  $N < 50$ . Since few sands with blow counts lower than 50 were sampled, only one subdivision has been made for cohesionless soils:  $N \leq 40$  (loose to dense) and  $N > 40$  (dense to v. dense). Although relative density is very important in determining the behavior of sands, the factors which control it are not well understood. Grain size and rate of deposition are two parameters which appear to be important (Terzaghi, 1955). Effects of these factors may be evident in



figure 7. The near-surface, v. fine-grained sands deposited on alluvial flood plains fall within the  $N \leq 40$  group while fine- to coarse-grained alluvial sands are in the  $N > 40$  group. In addition to the v. fine-grained sands, the  $N \leq 40$  group includes the loose Holocene dune sands. Lower densities in the dune sands may be the result of different rates of deposition or the wind-laid mode of deposition.

### Depth

The ranges in S-wave velocity measured for the textural groupings in figure 7 generally show an increase with depth. This section will discuss these relationships along with possible explanations for the observed increase in velocity with depth. In order to show their wider applicability, the velocity-depth relationships obtained in the San Francisco Bay region will be compared with velocity gradients formulated by Hamilton (1976) for a compilation of data from a wide geographical distribution of sites. In addition, a comparison will be presented between the S-wave velocities measured in-situ in sands for the present study and those calculated using equations formulated from laboratory studies by Hardin and Richart (1963) to illustrate the possible effects of void ratio, effective stress and time-dependent processes.

Most of the groups of sediments which have been differentiated using texture and standard penetration resistance can be further subdivided on the basis of depth. The v. soft to soft and v. stiff to hard silty clays, dense to v. dense sand, and gravels all show an increase in velocity range with depth and have been divided into near-surface ( $D < 12$  m) and at depth ( $D \geq 12$  m) groupings (Table 1). An increase in S-wave velocity with depth is also shown by the sandy clays and silt loams though the

division was set at 15 m, as there are so few shallow samples in this group. The medium to v. stiff silty clays and the mixed sediments do not show significantly different velocities between the near-surface and at-depth groups. The loose to dense sands were not found at depths greater than 15 m.

Studies of gradients of S-wave velocity with depth have been reported by several authors. Perhaps the most comprehensive is a compilation by Hamilton (1976) of data for water-saturated marine and non-marine sediments. He calculated regression equations relating shear wave velocity with depth for two "end-members" representative of marine sediment types: (1) sands, and (2) silt clays and turbidites (thick layers of silt-clays intercalated with thin layers of silt and sand). For sands at depth of 0.1 to 12 m, the regression equation is:

$$V_s = 128D^{0.28}$$

where D is depth. The equation for silt-clays and turbidites at depths of less than 42 m is:

$$V_s = 116 + 4.65D.$$

Figure 15 shows a comparison between these equations and data of the present study for two groups of sediments equivalent to Hamilton's sediment types: (1) Holocene and late Pleistocene sands, and (2) silty clays and clays and the mixed sediments. Following Hamilton's procedure, the data are plotted using the depth to the midpoint of each depth interval along with the interval velocity. The silt-clay regression equation fits the silty clay-mixed sediment data very well. The sand regression equation does not fit the sand data quite as well, particularly in the near-surface. This apparent discrepancy is due to the fact that Hamilton only

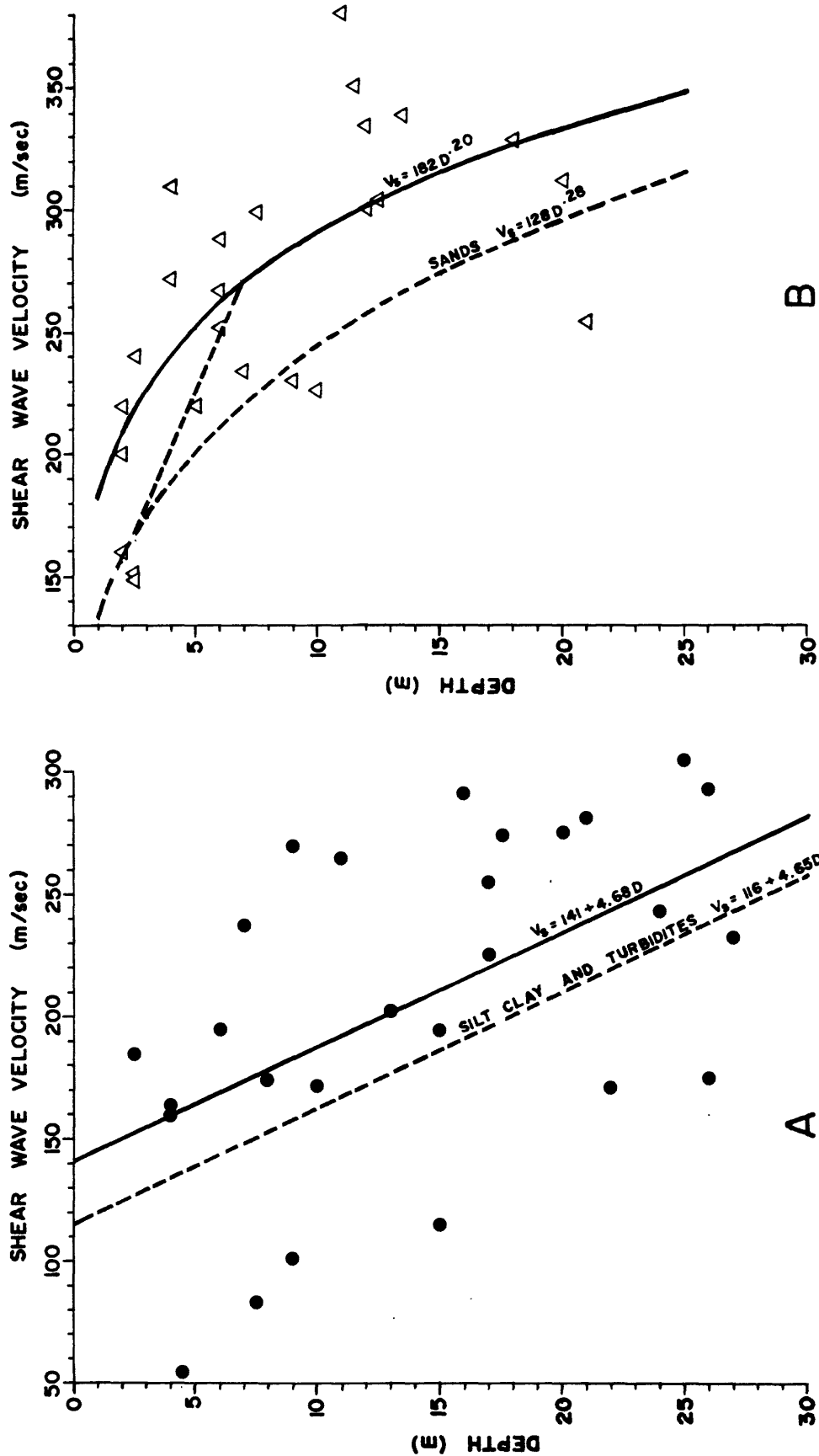


Figure 15. Comparison of data for several groups of sediments from the present study (symbols, solid lines) with regression equations (dashed lines) for data compiled by Hamilton (1976).  
 A, data for fine-grained sediments. B, data for sands.

had 2 measurements below 7 m. A linear trend through his shallow data, plotted as a dashed line in figure 15, shows that the two sets of data are actually quite comparable. Scatter in the two sets of data is nearly the same except that for the present study velocities greater than 300 m/sec were measured in sands at depths less than 7 m.

The reason for this increase in velocity with depth is not clear. Possible explanations are changes in effective stress and/or void ratio due to increasing overburden load which were found to be important factors in laboratory studies. At the KGEI site, decreases in void ratio (from 2.36 to 6.5 m to 1.97 at 15.5 m) may be sufficient to account for velocity increases with depth in a section of soft, normally consolidated silty clay. However, at a nearby site, Audubon School (AUD), no increase in velocity with depth is apparent in similar silty clays from 2.5 to 20 meters. Similarly, at other sites underlain by thick sections of relatively homogeneous materials (Lowry Rd., Parkway Towers, Quintara, etc.), an increase in velocity with depth is not evident.

The effects of time-dependent processes, such as changes in cementation and fabric, can cause the rigidity of the sediment structure to increase beyond values attributable to void ratio and effective stress alone. That time factors can have a significant effect on shear wave velocity in sandy sediments may be seen from a comparison between the in-situ measurements and velocities obtained in laboratory studies. Hardin and Richart (1963) have published equations developed from laboratory experiments using the resonant column technique with samples of round Ottawa sand and crushed quartz. Since these equations relate effective stress for use with the interval velocities, it was necessary

to use only samples for which a reliable bulk density had been obtained. Fifteen such samples from ten sites were used in the analysis. The sands were mostly well-sorted, v. fine- to coarse-grained and subangular to subrounded. Ages of the sands ranged from Holocene to Plio-Pleistocene (Merced Formation) and were deposited in alluvial, eolian and shallow marine environments.

Void ratio ( $e$ ) of each sample was calculated using

$$e = \frac{G\gamma_w - \gamma_t}{\gamma_t - S\gamma_w},$$

where  $\gamma_t$  is the measured bulk density,  $\gamma_w$  is the unit weight of water,  $G$  is the specific gravity of the sand grains (assumed to be 2.65) and  $S$  is the degree of saturation (assumed to be 1). Although P-wave velocity measurements indicate that most of these sands are not saturated, the measured water contents of the samples (16-25%) suggest that most are nearly so. Lower values of  $S$  would give larger void ratios and hence lower values for the calculated shear wave velocity.

Confining pressure was assumed to be equal to the overburden pressure or

$$\sigma = h\gamma_T,$$

where  $h$  is the depth to the midpoint of the velocity interval containing the sample and  $\gamma_T$  is the bulk density of the sample. The actual effective stress is probably substantially lower than the overburden pressure because of the pore pressure of the water. Thus the shear wave velocity calculated using this assumption is again a maximum.

Since the sands used in this analysis are more nearly round than very angular, velocities were calculated using the equation developed for

round Ottawa sand

$$V_s = (170 - 78.2 e) \sigma_o^{0.25} \text{ for } \sigma_o > 2000 \text{ psf}$$

$$V_s = (119 - 56.0 e) \sigma_o^{0.30} \text{ for } \sigma_o \leq 2000 \text{ psf.}$$

Results are summarized in Table 2. Figure 16 shows void ratio, measured  $V_s$  and calculated  $V_s$ . For sands with void ratios greater than 0.6, the computed velocities are very close (within 5%) to those measured in situ, implying that for these sands the important parameters affecting shear wave velocity are effective stress and void ratio as was found to be the case for laboratory samples. The velocity-depth distribution of these sands is shown in figure 17. They correspond generally to the Holocene sands and the v. fine to fine-grained sands of the older formations. For sands with  $e \geq 0.6$ , the computed velocities in most cases are substantially (15-25%) lower than the measured values suggesting that for these sands, additional time-dependent processes such as cementation or fabric changes act to increase the shear wave velocity. This conclusion is supported by the fact that these sands correspond to the fine- to coarse-grained sands of deposits older than Holocene.

A similar analysis for the cohesive sediments was not possible due to the small number of reliable density measurements. However, time-dependent processes seem to have much less effect for the cohesive sediments than for the sands. For example, late Pleistocene medium to v. stiff silty clays do not have significantly different velocities than Holocene silty clays of the same consistency. This finding conflicts with results of laboratory studies of the time-dependent increase of shear wave velocity. For example, Stoke and Richart (1973) found that

TABLE 2

## MEASURED AND CALCULATED PROPERTIES OF SAND SAMPLES

Site	Depth(m)	Bulk Density (gm/cc)	Void Ratio	V <sub>s</sub> Measured	V <sub>s</sub> Calculated
S.C.Fair	6.5	1.90	.83	232	226
Mer	4.5	1.91	.81	225	215
Ava	6.0	1.97	.70	249	244
West	7.5	2.00	.65	268	270
Car	8.0	2.02	.61	288	281
Car	15.5	2.03	.60	330	330
Hill	8.0	2.03	.60	338	285
Sp	12.5	2.05	.57	349	322
West	20.0	2.05	.57	350	364
Mer	11.0	2.05	.57	380	311
Ava	19.5	2.06	.55	404	335
Hill	19.5	2.08	.52	452	376
Sk	24.0	2.12	.47	490	407
Car	25.0	2.12	.47	495	412
Q	21.0	2.13	.46	520	397

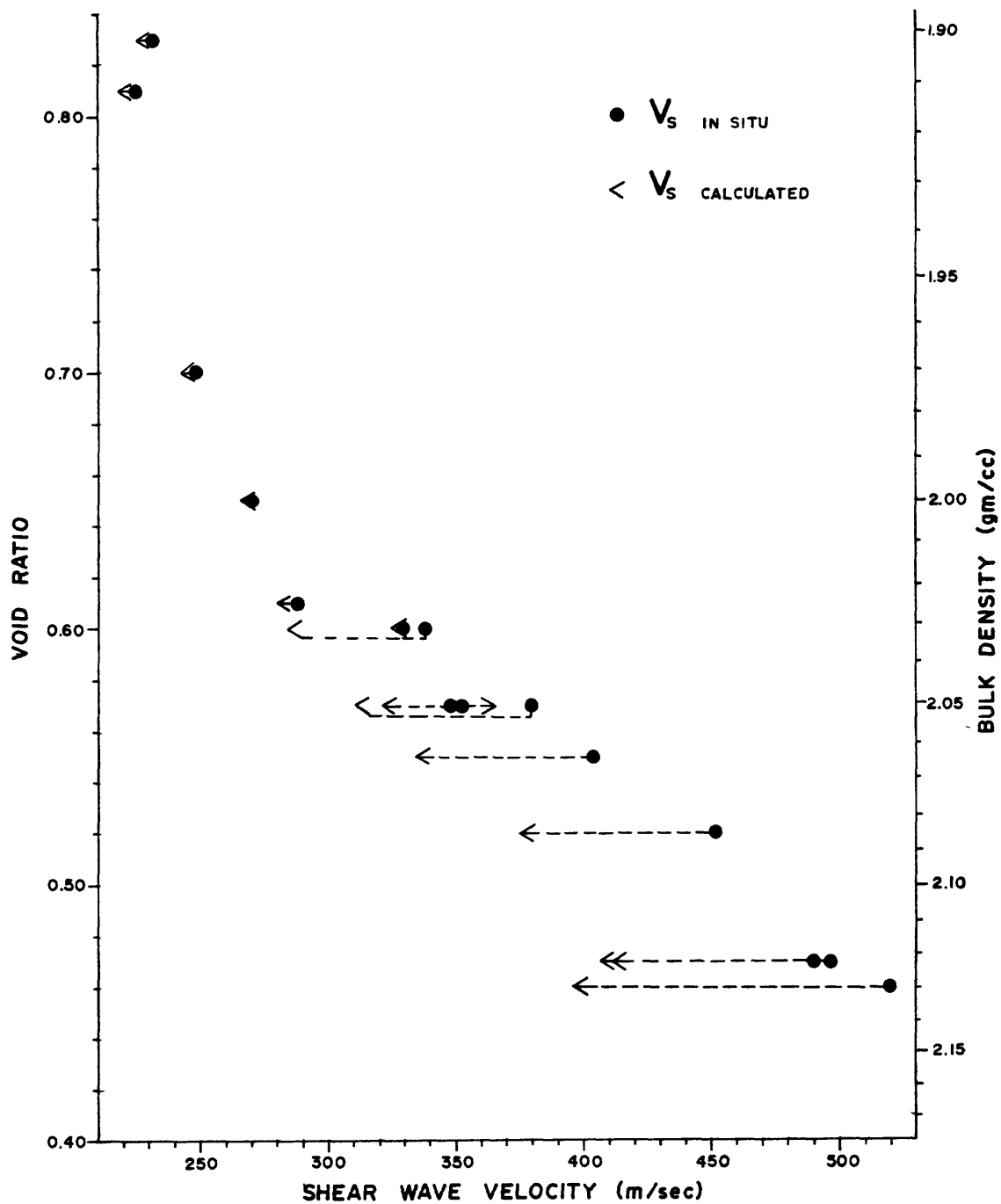


Figure 16. Variation with void ratio of S-wave velocity measured *in situ* in sands and calculated using equations of Hardin and Richart (1963).

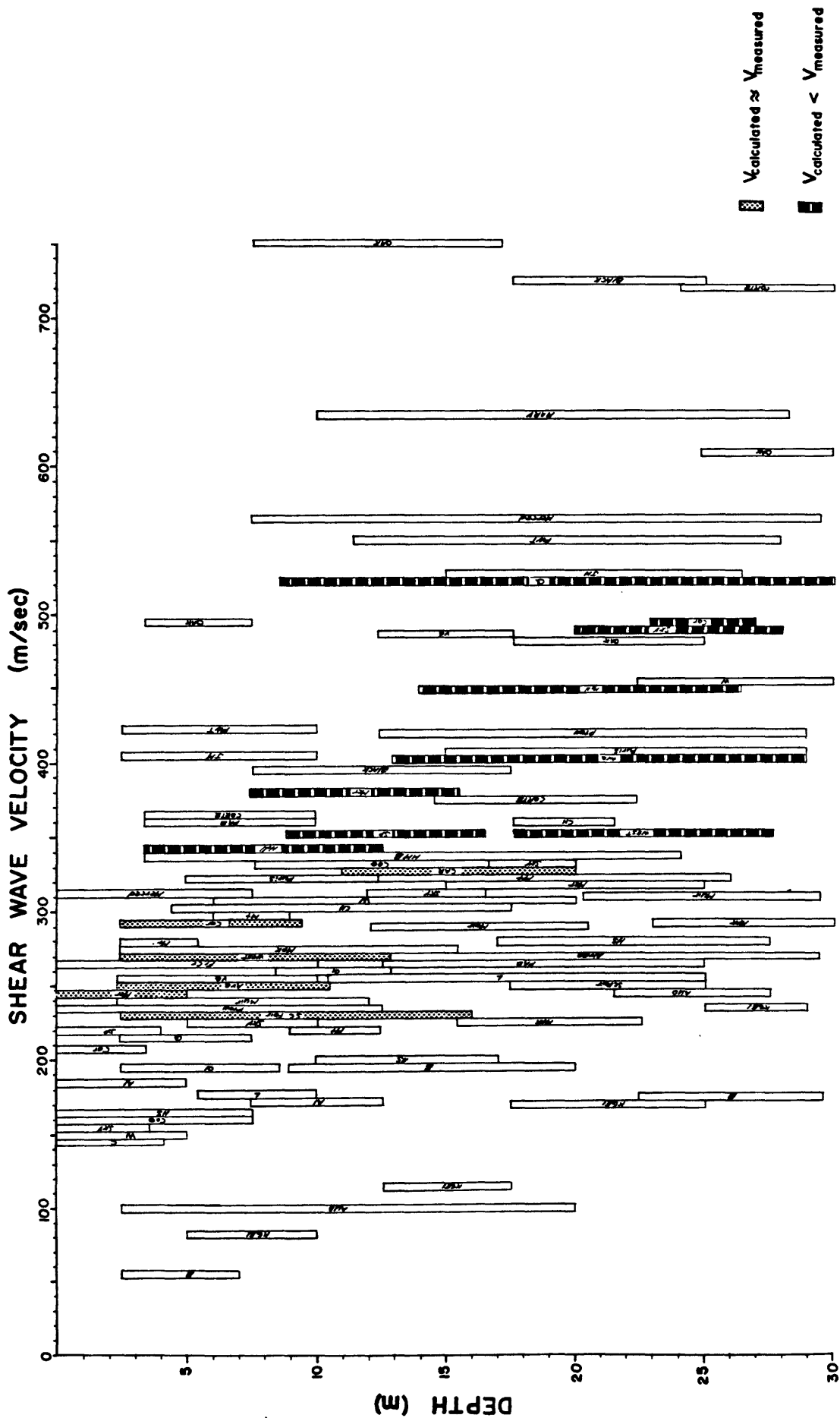


Figure 17. Distribution of sands for which S-wave velocity measured in situ is approximately equal to the calculated velocity versus those for which the in situ velocity is significantly greater than the calculated velocity.

the S-wave velocity of a silty sand increased 1% per log cycle of time, while the increase for a clayey silt was 5.3%. However, even this value for cohesive sediments is insufficient to account for a significant increase in velocity between Holocene (6000-10,000 yrs B.P.) and late Pleistocene (70,000-100,000 yrs B.P.) silty clays. The low value of velocity increase with time for the silty sand suggests that Stoke and Richart did not duplicate in the laboratory all of the time-dependent processes which act in nature.

### Summary

Shear wave velocities measured in unconsolidated to moderately consolidated sedimentary deposits have been compared with several readily determined physical parameters of the materials. Correlations obtained suggest the classification scheme shown in figure 18 for use in differentiating the sediments into seismically distinct groups. Texture (relative grain-size distribution) is the parameter which appears to have the most significant effect on shear-wave velocity in these deposits. Velocity generally increases with increasing average grain size. The sediments have been divided into five textural categories which show distinct velocity characteristics: 1) clay and silty clay, 2) sandy clay and silt loam, 3) sand, 4) gravel, and 5) interbedded fine and coarse-grained sediment.

Several of the textural groups which show relatively wide velocity ranges can be subdivided on the basis of other physical properties as follows:

- 1) Clays and Silty clays have been differentiated into three groups



using standard penetration resistance as a measure of consistency (relative firmness): v. soft to soft ( $N < 4$ ), medium to v. stiff ( $4 \leq N \leq 20$ ) and v. stiff to hard ( $N > 20$ ). Consistency appears to be related to long-term water table effects. Sediments which have been partially or completely desiccated and oxidized are stiffer than those which have remained saturated since deposition. Soil color can be used as an indicator of diagenetic history if penetration resistance data is not available.

- 2) Sands have been subdivided into two groups using standard penetration resistance as an indication of relative density: loose to dense ( $N \leq 40$ ) and dense to v. dense ( $N > 40$ ). The first group includes Holocene sands and v. fine-grained late Pleistocene sands. All other sands through Plio-Pleistocene in age are included in the second group. Shear wave velocity in sands correlates well with density (and hence void ratio). This relationship can be used to make finer velocity estimates (see figure 16, p. 49).

The following five groups show distinctly higher velocities at depth ( $D > 12$  m) than in the near-surface ( $D \leq 12$  m) and have been subdivided accordingly:

- |                     |                            |
|---------------------|----------------------------|
| Clay and silty clay | - Sandy clay and silt loam |
| - v. soft to soft   | - Sand, dense to v. dense  |
| - v. stiff to hard  | - Gravel.                  |

## B. Shear Wave Velocities for Sedimentary Map Units

In the previous section it was shown that the shear wave velocities in near-surface geologic materials can be related to several readily observable physical properties of the materials. Estimation of ground response to earthquakes rests in part on a knowledge of the aerial distribution of these properties. Unfortunately, such information can be obtained only indirectly, if at all, from most geologic maps. Although areas underlain by unconsolidated sedimentary deposits are most susceptible to ground motion amplification hazards, geologic maps ordinarily contain little data about the physical properties of these deposits if they are differentiated at all.

Recent mapping efforts in the San Francisco Bay region have been directed towards providing geologic maps of the sedimentary deposits (Helley and Brabb, 1971; Helley and others, 1972; Lajoie and others, 1974) which are more useful for land-use planning efforts such as seismic zonation. Lajoie and Helley (1975) have described techniques for classifying and mapping alluvial deposits according to age and depositional environment. These two factors control the distribution of the sediments and the primary and secondary physical properties which determine seismic wave velocities. Shear wave velocities measured in the sedimentary units defined using these criteria are shown in figure 19. Mean, range and standard deviation of the velocities for each unit are presented in Table 3. The degree of detail with which the deposits are differentiated allows a corresponding degree of refinement in regrouping into units with significantly different seismic wave velocity characteristics. This section will discuss the distribution of physical properties and S-wave

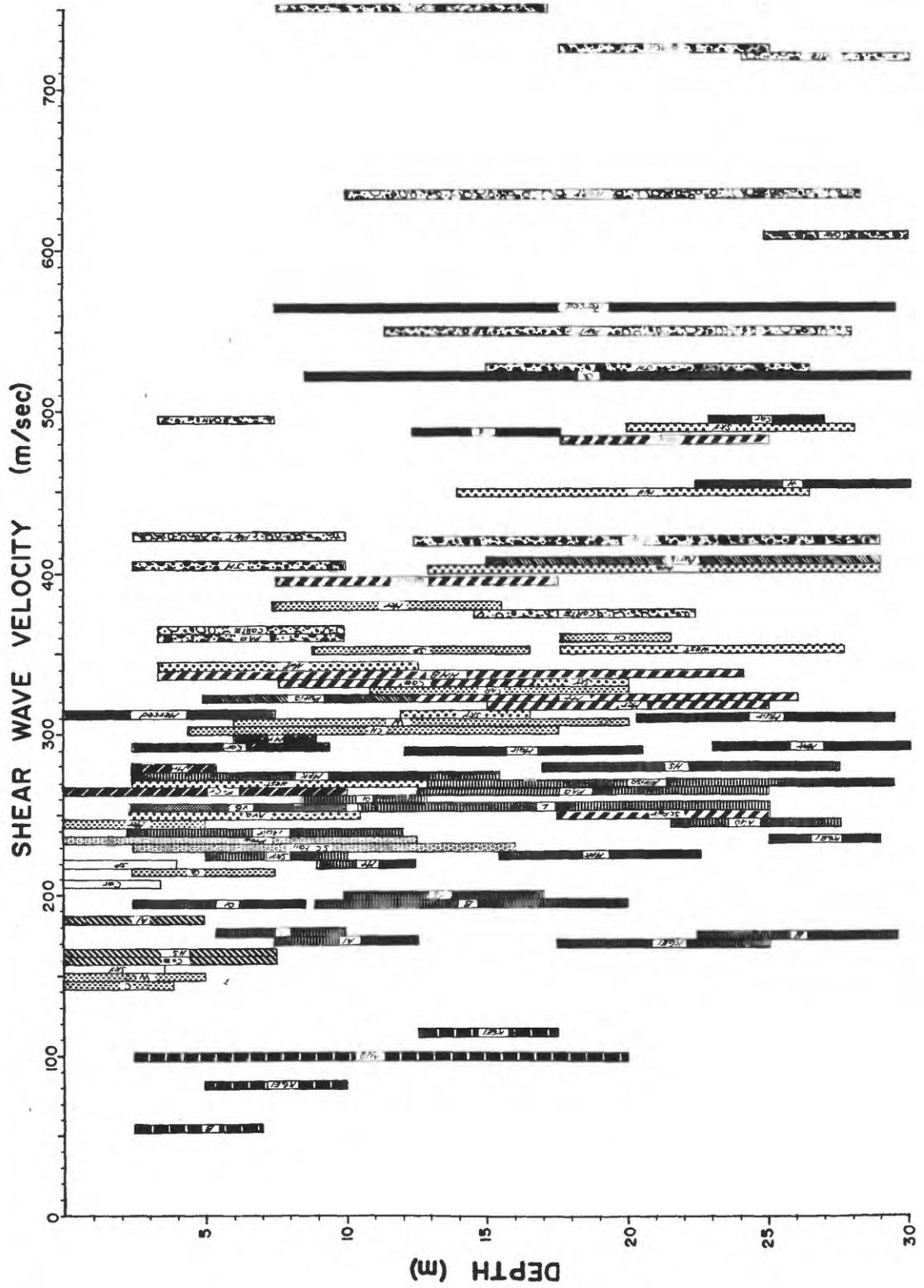


Figure 19. Shear wave velocity-depth intervals for sedimentary deposits grouped according to geologic unit.

TABLE 3

## SHEAR WAVE VELOCITIES IN SEDIMENTARY GEOLOGIC MAP UNITS

Geologic Map Unit	No.	S-Wave Velocity (m/sec)		
		Mean	Standard Deviation	Range
<b>Holocene Deposits</b>				
Artificial fill	3	196	27	159-222
Bay mud				
near surface	3	80	19	54-101
at depth	2	108	7	101-114
Dune sand				
near surface	3	173	32	150-219
at depth	3	311	13	300-330
Fine-grained alluvium	2	162	2	160-164
Medium-grained alluvium	2	233	1	232-234
Coarse-grained alluvium	4	281	12	267-299
<b>Late Pleistocene alluvium</b>				
Fine-grained				
near surface	6	199	27	172-128
at depth	11	243	48	171-307
Medium-grained				
near surface	2	349	11	338-360
at depth	7	367	71	253-485
Coarse-grained				
near surface	2	451	46	405-497
at depth	5	606	123	418-749
Mixed sediment	5	258	15	233-276
<b>Colma Fm.</b>				
near surface	2	280	29	251-310
at depth	5	505	37	457-522
<b>Merced Fm.</b>				
near surface	4	271	41	229-338
at depth	6	390	65	312-490
<b>Santa Clara Fm</b>				
near surface	2	392	30	362-422
at depth	5	675	240	377-1100
Purisima Fm.	2	367	40	327-406

velocity characteristics of the sedimentary mapping units. The velocity-depth relationships obtained in this study will then be compared with the results obtained by Campbell and Duke for several geologic map units in the Los Angeles area.

### Holocene and Late Pleistocene Alluvium

#### Velocity Characteristics

Differences in the velocity characteristics of the Holocene and late Pleistocene alluvium are readily apparent in figure 19. Each of the three Holocene alluvial units shows a distinct and relatively narrow S-wave velocity range (see Table 3). Although the late Pleistocene alluvium has been mapped in the Bay area as a single unit, in this figure it has been divided into several textural groups to facilitate comparison with the Holocene alluvium. These subgroups of late Pleistocene alluvium show wider and overlapping velocity ranges. This difference is partly due to the fact that a wider variety of textures were sampled in the late Pleistocene than in the Holocene alluvium. Specifically, all of the sandy clays, silt loams, and gravelly sediments encountered were late Pleistocene or older. In addition, post-depositional changes have generally resulted in a wider range of physical properties within the late Pleistocene textural groups.

#### Distribution and Physical Properties

The Holocene alluvium deposits, because they have been subject to erosion for a relatively brief time, have the original depositional morphology sufficiently well-preserved to allow for differentiation into depositional sub-environments. In addition, descriptions of the mapped units include textural information obtained from agricultural and engi-

neering soil studies. These data reveal that the sediments deposited in each sub-environment have distinct physical properties. Figure 20 is a schematic longitudinal cross-section through a typical alluvial fan showing the distribution of the geologic map units along with their textural and drainage characteristics. Several geologic logs from sites in different parts of the study area are included in their approximate position on the fan. These logs show typical sedimentary textures and thicknesses encountered. Due to the depositional processes on alluvial fans, texture grades from coarse to fine towards the bay with sand and gravel predominating on the upper parts of the fan and in channels, mixed sand, silt, and clay deposited on alluvial plains at the outer edge of the fan and silty clay and clay deposited in flood basins and in the bay. As a consequence of the water table ceepening away from the bay, the alluvial fan deposits are well-drained while those of the flood basins are poorly drained.

In contrast, it has not been possible to map the areal extent of depositional environments for the late Pleistocene alluvium. The original depositional morphology has been strongly altered by erosion, and except for the upper parts of the fans, the deposits have largely been buried by Holocene sediments. However, it is possible to predict in a general way the distribution of late Pleistocene depositional environments. While the Holocene sediments have been deposited by streams graded to present sea level, the older sediments were deposited by these streams when they were graded to lower stands of sea level during the late Pleistocene. This would mainly have affected sedimentation in the areas now occupied by the bay and flood basins. The bay would have been the site of alluvial deposition, primarily with clay and silty clay in flood basins and well-

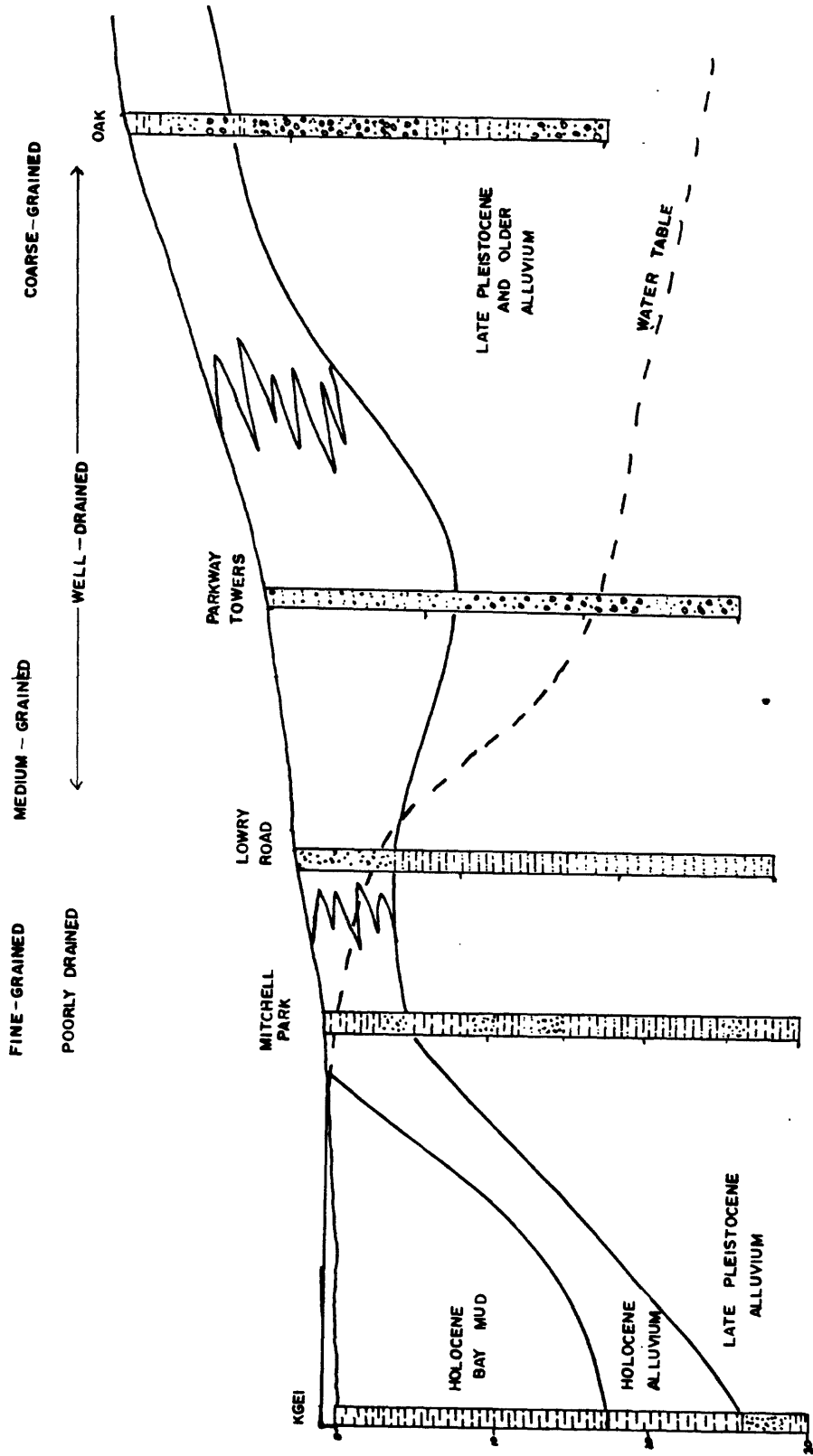


Figure 20. Schematic cross section of alluvial fan-bay complex showing distribution of sediment grain size, age, thickness, and drainage characteristics. Logs of several sites occupied in this study are shown projected to their approximate positions on the fan.

sorted sand and gravel in stream channels. Present flood basin areas would have been the sites of sedimentation similar to that of the outer edges of alluvial fans with mixed clay, silty and sand.

Inspection of geologic logs from sites in this study demonstrate this. These logs are shown in figure 21. Holocene deposits have been delineated on the logs primarily on the basis of sedimentation units and typical thicknesses for each map unit. At sites near the bay the textural sequences show a general coarsening with depth. As expected, the bay mud is underlain by silty clays and well-sorted sands typical of flood basins and stream channels, and the Holocene flood basin sediments are underlain by mixed silty clay, sandy clay, silt and sand. Sand and gravel on the upper parts of the Holocene fans are underlain by similar sediments of late Pleistocene age. In general, fine-grained Holocene alluvium is underlain by fine-grained late Pleistocene alluvium, and coarse-grained Holocene alluvium is underlain by coarse-grained late Pleistocene alluvium.

While textures are similar for both younger and older alluvium at a given site, other physical properties affected by post-depositional changes may be different. Most of the overconsolidation in clays due to dessication seems to take place relatively rapidly, as mottled silty clays of Holocene and late Pleistocene age are indistinguishable on the basis of shear wave velocity. Induration in sands and gravels appears to act at a steadier rate as the older coarse-grained sediments show significantly higher velocities than the younger coarse-grained alluvium.

Figure 22 shows the alluvial cross section shown in figure 20, along with location of depositional environments, textural groupings and



Figure 21. Geologic logs of sites on Holocene and Late Pleistocene sedimentary deposits. Depth intervals over which S-wave velocity was calculated are colored according to texture. Probable thickness of Holocene sediments is indicated.

measured range of velocity.

#### Bay Mud

Estuarine sediments have accumulated in San Francisco Bay for the last 9,000 years. These deposits are predominantly soft, normally consolidated clay and silty clay with minor sand, shell and peat layers. Velocities measured in the bay mud (55-115 m/sec) are distinctly lower than those for any other map unit.

#### Dune Sand

Sands underlying the three sites on the ocean side of San Francisco mapped as dune sand show three distinct velocity layers. At each site, there is a surficial layer 5 to 8.5 meters thick having a velocity of 150 to 210 m/sec. This sand has probably formed active dunes in the recent past (Schlocker, 1974). Although predominantly medium- to fine-grained, this sand shows velocities similar to alluvial very fine to fine sand and silty clay. At two sites, Windmill and Chain of Lakes, this layer is underlain by a thicker layer with a velocity of 300 m/sec. These two layers may represent dune sands deposited during Episodes I and II of the Flandrian Transgression as delineated by Cooper (1967). At two sites, Quintara and Windmill, another layer with a velocity of 450 to 520 m/sec was found. This layer is capped by a well-developed soil and is probably the Colma formation.

Probable dune sands were also found at the two sites on the bay side of San Francisco. At each site yellowish brown, fine- to medium-grained sand underlies estuarine sand and silty clay. Velocities measured in this sand are very similar to those in the second layer at the ocean side dune sites. This sand is underlain by a 2-meter-thick layer of greyish

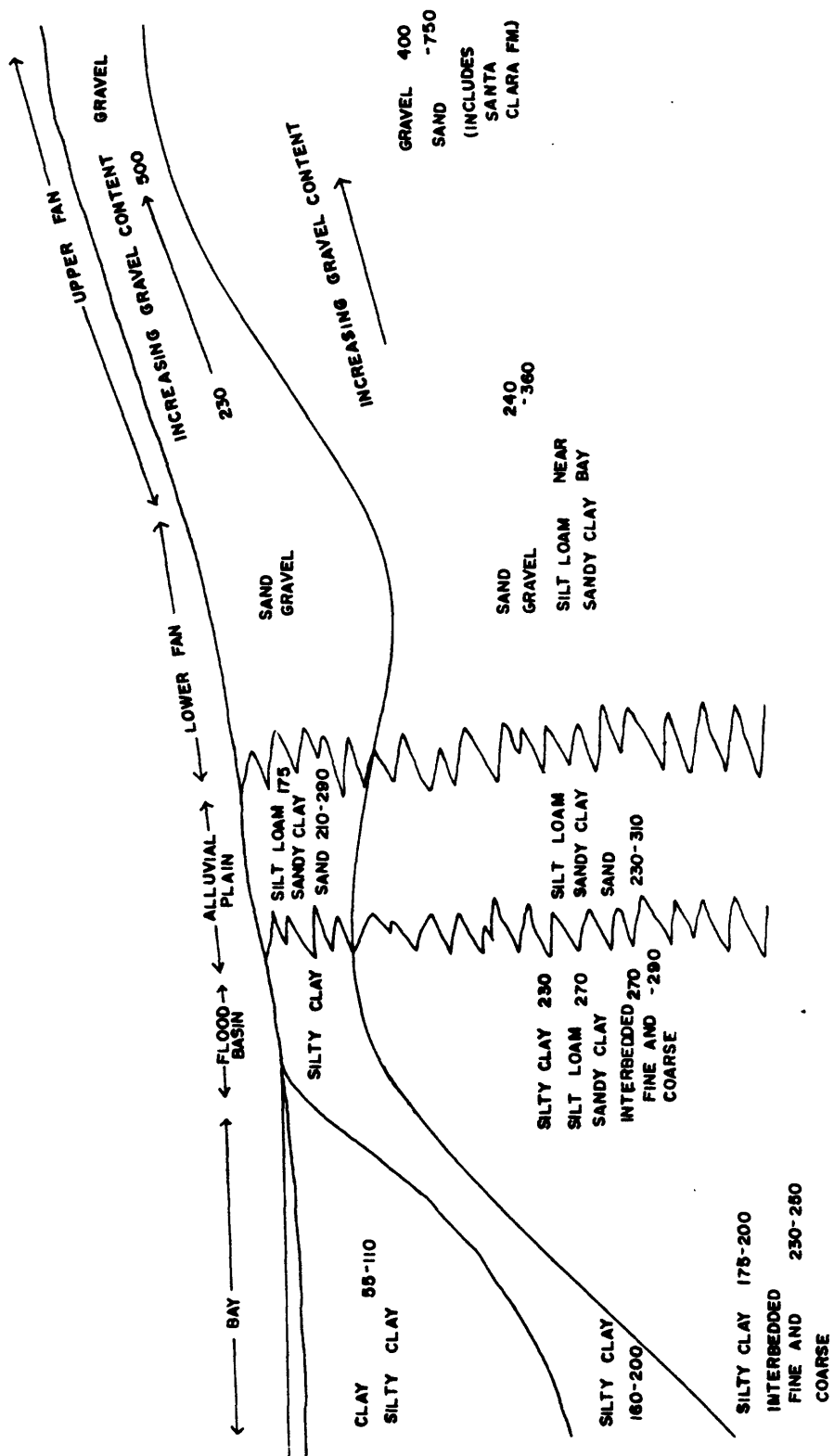


Figure 22. Schematic cross section showing distribution of depositional environments, textural groupings (from Fig. 7) and S-wave velocity ranges.

green silty clay which may represent the late Pleistocene estuarine deposit of Atwater et al. (1977). This layer is in turn underlain by yellowish brown, fine- to medium-grained sand showing the higher velocities measured in the third layer at the ocean side dune sites and is included in the Colma Formation.

Atwater et al. (1977) grouped the sandy sediments of the Merritt Sand in the Oakland area with the eolian deposits of San Francisco. Although the Merritt Sand sampled in this study had a somewhat higher silt and clay content and higher velocities (by 30 m/sec) than the dune sands in San Francisco, the Merritt Sand is here included in the dune sand category.

#### Artificial Fill

Although artificial fill underlies at least six sites, layers of sufficient thickness for obtaining velocities were found at only three sites. These fill materials were predominantly fine to medium sand derived from dune deposits or the Merced Formation. Velocities are comparable to those for in-situ dune sands.

#### Merced Formation

The Merced Formation, of Pliocene-Pleistocene age, while composed predominantly of fine to medium sand, contains thick beds of silty clay, silt, and very fine sand. It is not possible, however, to differentiate the formation for mapping purposes on this basis. The sands, although substantially older, show near-surface velocities similar to those for the late Pleistocene sands. Velocities at depth are significantly higher than those measured in the near-surface materials.

#### Colma Formation

The Colma Formation, of Pleistocene age, consists chiefly of fine to

medium sand. At depths less than 12 m shear wave velocities are similar to those in sand of other ages having the same texture. At depth, however, velocities are somewhat higher than similar sands of the Merced Formation, even though the Colma is substantially younger. A possible explanation for this result is that the Colma has been exposed to more intense weathering than the Merced at some time since deposition. Colors (see figure 12) of the Colma are generally yellowish brown and strong brown, while those of the Merced sands are usually olive brown. Also, strongly oxidized soil horizons at the top of the Colma were found at several sites. A greater degree of cementation might be the result of such weathering.

#### Santa Clara Formation

The Santa Clara Formation, of Pliocene-Pleistocene age, consists of poorly indurated sandstone and clayey to sandy gravels and moderately indurated sandy gravels. Velocities in the sandstones and poorly indurated sandy gravels are not significantly different from those in sediments with similar textures of different ages. Sediments similar in texture to the poorly-sorted gravelly clays and sands at Maryknoll were not found at younger sites. However, velocities in this material appear to be high in view of the large amount of fine-grained material included and may be due to weak induration. Velocities in the conglomerates at the Stevens Creek site are twice (550 vs. 1100) those measured in the poorly indurated gravels at other sites.

#### Purisima Formation

The Purisima Formation, of Pliocene age, was sampled at one site where it consisted entirely of poorly indurated fine sandstone. The velocities obtained were similar to those for fine sands of the Merced

Formation.

Comparison with Results for the Los Angeles Area

In order to evaluate the applicability of the relationships established in the San Francisco Bay region, it is of interest to compare the results of the present study with those conducted in other geographic areas. At present, the only study of comparable scope is that of Campbell and Duke (1976) for the Los Angeles area.

Campbell and Duke employed the surface refraction method to measure velocities in a variety of geologic deposits. In horizontally or sub-horizontally stratified deposits, this technique frequently results in higher velocities than for the downhole method used in the present study (Schwarz and Musser, 1972). This is due to anisotropic seismic characteristics of the materials, primarily preferred orientation of the grains parallel to bedding planes. Hence propagation velocities are higher in the horizontal direction than in the vertical. Using a simplified model for ellipsoidal grains, Kitsunezaki (1971) calculated the ratio of  $V_s$  in the horizontal direction to  $V_s$  in the vertical to be 1.55.

Campbell and Duke present relationships between shear wave velocity and depth for several units of Holocene and Pleistocene soils in the Los Angeles area. Data for depths greater than 1 m are reported for three groups:

- 1) Unconsolidated Soils - loose or soft natural or artificially placed soils; low gravel content.
- 2) Recent Alluvium - Holocene age alluvial deposits - slightly older and more consolidated than unconsolidated soils.
- 3) Old Alluvium - Pleistocene age alluvial and terrace deposits;

partially consolidated.

Regression equations for these three groups are plotted in figure 23, along with data for several map units used in the present study. Comparison between the two sets of data can only be tentative as the textural compositions of the Los Angeles units are uncertain. The Unconsolidated Soils may be texturally comparable to the recent estuarine mud of this report as Recent Alluvium and compacted fill are excluded from it. As Campbell and Duke distinguish a separate category for gravelly soils, the Recent and Old Alluvium categories presumably are comprised of fine-grained sediment and sand. Bearing these uncertainties in mind, it appears from figure 23 that the velocities reported for Recent Alluvium are comparable, while those reported for Unconsolidated Soils and Old Alluvium are substantially higher than those measured in the present study.

In view of the problems encountered in applying Campbell and Duke's results, the need for data from other geographic areas remains. For this reason the work of the present study is being extended to the Los Angeles area in conjunction with a program of detailed mapping of the sedimentary deposits.

### Summary

Shear wave velocities have been measured in each of the map units defined for sedimentary deposits in the southern San Francisco Bay region. The range of velocities for a given map unit is dependent on the variety of materials which have been included in the unit. The Holocene sediments have been differentiated into depositional environments on the basis of relatively well-preserved original geomorphic expression. Deposits in each of these environments show characteristic physical properties such as

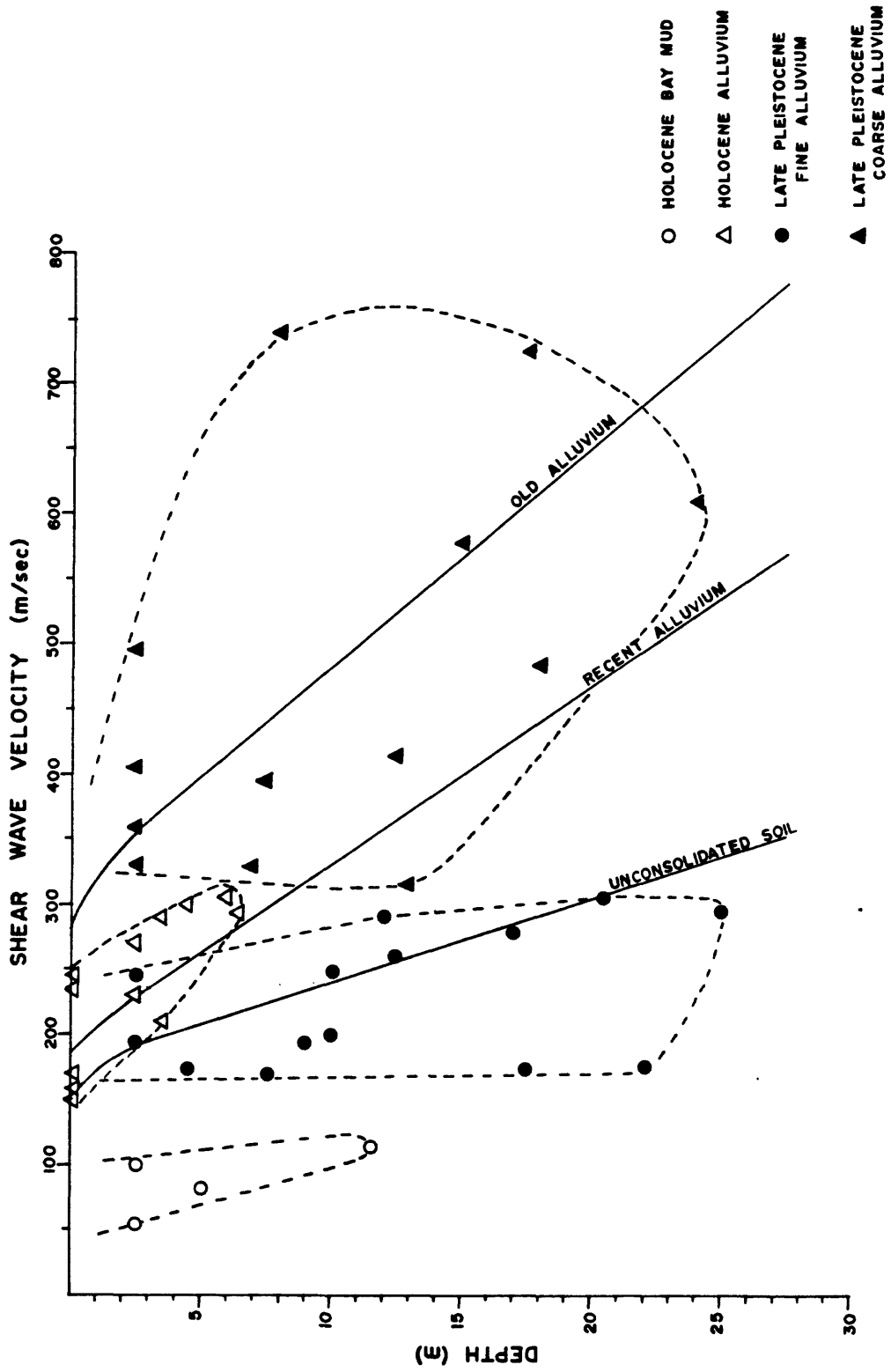


Figure 23. Comparison of data from the present study for several groups of sediments (symbols) with regression equations for in situ refraction measurements reported by Campbell and Duke (1976) for the Los Angeles Basin.

texture, density and drainage. Accordingly, each of the Holocene alluvial, estuarine, and eolian map units has a distinct and relatively narrow range of S-wave velocity.

The late Pleistocene and older map units, on the other hand, show relatively wide and overlapping velocity ranges. These sediments have not been differentiated and mapped in as great a detail as has been possible for the Holocene deposits. The original depositional morphology has been strongly altered by erosion and tectonism and the deposits have been extensively covered by younger sediments. These older sediments also encompass a wider range of textures, such as sandy clay and gravel, than are found in the Holocene deposits. And post-depositional conditions have been more variable within the older deposits, resulting in a wider range of physical properties within the textural groups. For the late Pleistocene deposits, however, the fine-grained materials can be differentiated on maps from the coarse-grained sediments at least in a general way. As the velocity ranges for the fine- and coarse-grained sediments are quite different, their seismic responses should also vary. Thus this distinction should be made on geologic maps where possible.

In addition to physical and genetic criteria, the age of the deposits has been used as an important factor in defining geologic map units. Differences in age, however, frequently do not correlate with significant variation in the physical properties which affect seismic velocities. A number of the geologic units thus defined have very similar velocity ranges and can be combined into seismically distinct groups. These groups are shown in figure 24 and listed in Table 4.

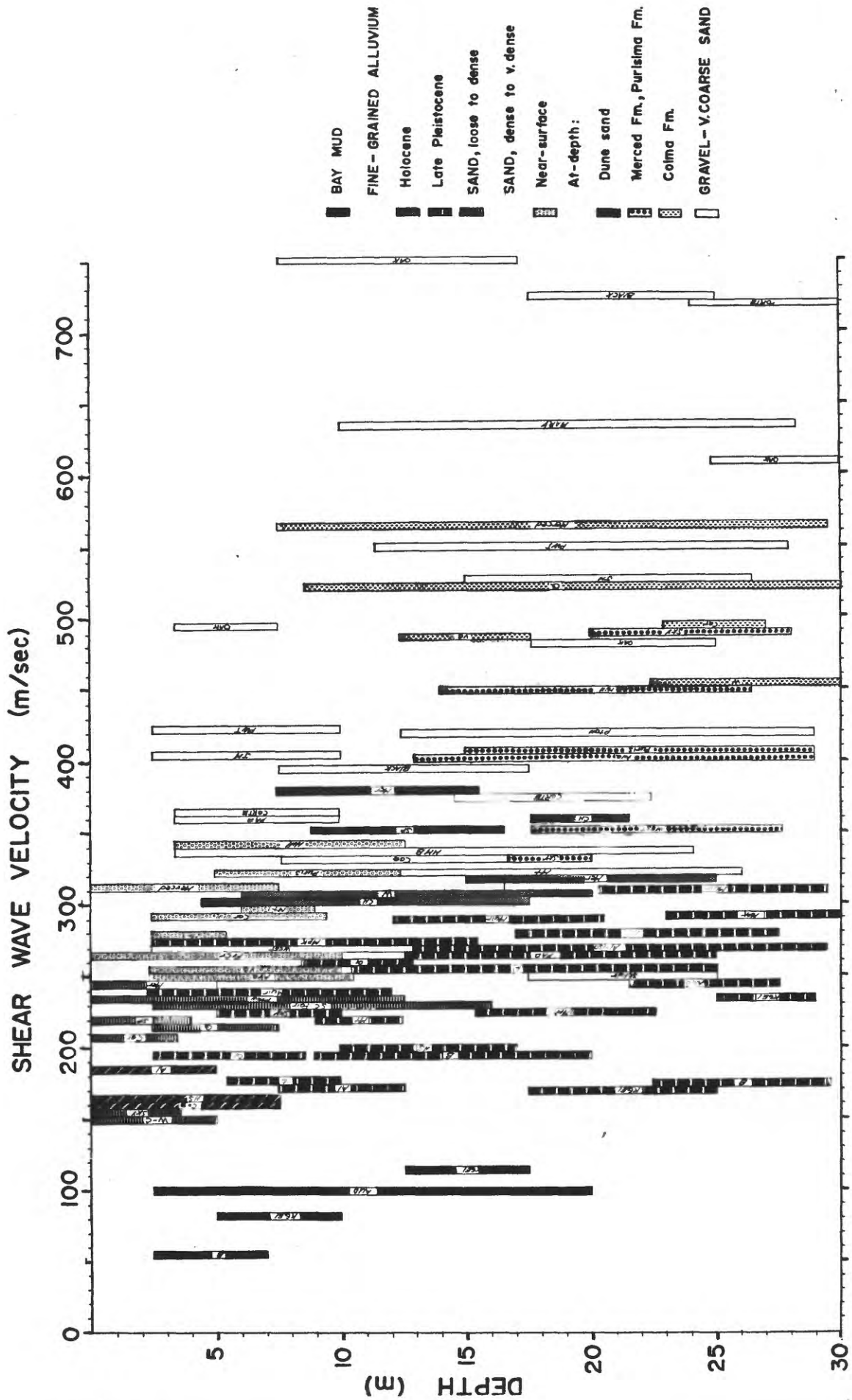


Figure 24. Seismically distinct geotechnical units for sedimentary deposits.

TABLE 4

SHEAR WAVE VELOCITIES IN SEISMICALLY DISTINCT GEOTECHNICAL  
UNITS OF SEDIMENTARY DEPOSITS

Geotechnical Unit	Geologic and Physical Property Units Included	Depth (m)	$V_s$ (m/sec)
Bay mud	clay-silty clay	0-10	55-100
	v. soft-soft	10-20	100-115
Holocene fine-grained alluvium	clay-silty clay med.-stiff	0-7.5	160-175
Late Pleistocene fine-grained alluvium	Clay-silty clay sandy clay silt loam	0-12	165-275
	Interbedded fine and coarse sediment	12-30	165-300
Sand	Dune sand ( $D < 7.5m$ ) Artificial fill	0-15	150-245
	Holocene v. fine-fine sand Merritt sand		
	Merced Fm		
Sand dense-v. dense near surface	Colma Fm. Holocene coarse Purisima Fm	0-12	250-340
	Dune Sand Merritt Sand	5-20	300-380
Gravel and v. coarse Sand	Late Pleistocene medium and coarse Santa Clara Fm.	2.5-20 10-30	340-500 320-740
	Merced Fm. at depth Purisima Fm.	12-30	310-490
Colma Fm. at depth	Colma Fm.	7.5-30	450-520

### C. Shear Wave Velocities in Bedrock Materials

#### Correlations between S-wave Velocity and Physical Properties

Bedrock materials underlie twenty-three sites at the surface. In addition, boreholes at four other sites penetrated bedrock below unconsolidated sedimentary deposits at depths of 10.5 to 21 meters. Fourteen sites were located on rocks of the Franciscan assemblage, including sandstone and shale, greenstone, chert, serpentine and sheared rocks, while granitic rocks were sampled at four sites and Tertiary sandstone, shale, conglomerate and volcanic rocks at nine localities. The effects of weathering, hardness, and fracture spacing on the velocities measured in these materials will be discussed first. Next, the velocity characteristics of the geologic map units will be discussed. A classification of the map units into seismically distinct groups will then be presented.

#### Weathering

The physical properties of the bedrock materials at each of these sites were found to vary with depth depending on the degree of weathering. The depth to which the bedrock has been significantly altered by weathering processes varies considerably from site to site due to differences in lithology and permeability. In general, though, three zones are developed: a surficial layer of unconsolidated residual material formed in-situ by deep weathering of bedrock and usually less than 2.5 meters thick; a zone of moderately to deeply weathered rock generally 10 to 12.5 meters thick; and fresh to slightly weathered bedrock.

Figure 25 shows the results of S-wave velocity measurements in the bedrock materials, along with degree of weathering. In most cases, the velocity-depth intervals obtained from travel-time curves correspond

closely to weathering zones delineated on the geologic logs. As most sites are located on ridge tops or artificially cut areas, the unconsolidated surficial layer is generally too thin to allow accurate measurement of velocity. At six localities, however, this zone is 5 to 10 meters thick. The velocities and other physical properties of these surficial materials were found to be similar to those of unconsolidated sedimentary deposits of the same texture and so will not be considered further.

The variation in depth of weathering evident in figure 25 is partly a result of differences in lithology. Several rock types, particularly chert, porcelaneous shale and serpentine (sites: PBK, MO, SM, CREST) are little affected by weathering even at relatively shallow depths while granitic rock (sites: DIG, FRC, PEAK) and greenstone (site: FOOT) may be significantly weakened to depths greater than 30 meters. The great depths to which granitic rock may be affected are a result of the manner in which it weathers (Wahrhaftig, 1965). Biotite in the rock is more unstable than either feldspar or quartz. Its alteration to clay minerals is accompanied by a volume change large enough (up to 40%) to shatter the other minerals. Thus the rock is greatly weakened even though it has undergone only slight chemical weathering. The micro-fracturing increases the permeability of the rock and facilitates additional weathering.

The effect on S-wave velocity of changes in physical properties accompanying moderate weathering is shown in figure 26. In this figure, the velocity in fresh rock is plotted versus the difference between the velocity in the fresh rock and the velocity in moderately to deeply weathered rock of the same lithology at the same site. The velocity difference increases with increasing strength of the fresh rock: 80-250 m/sec

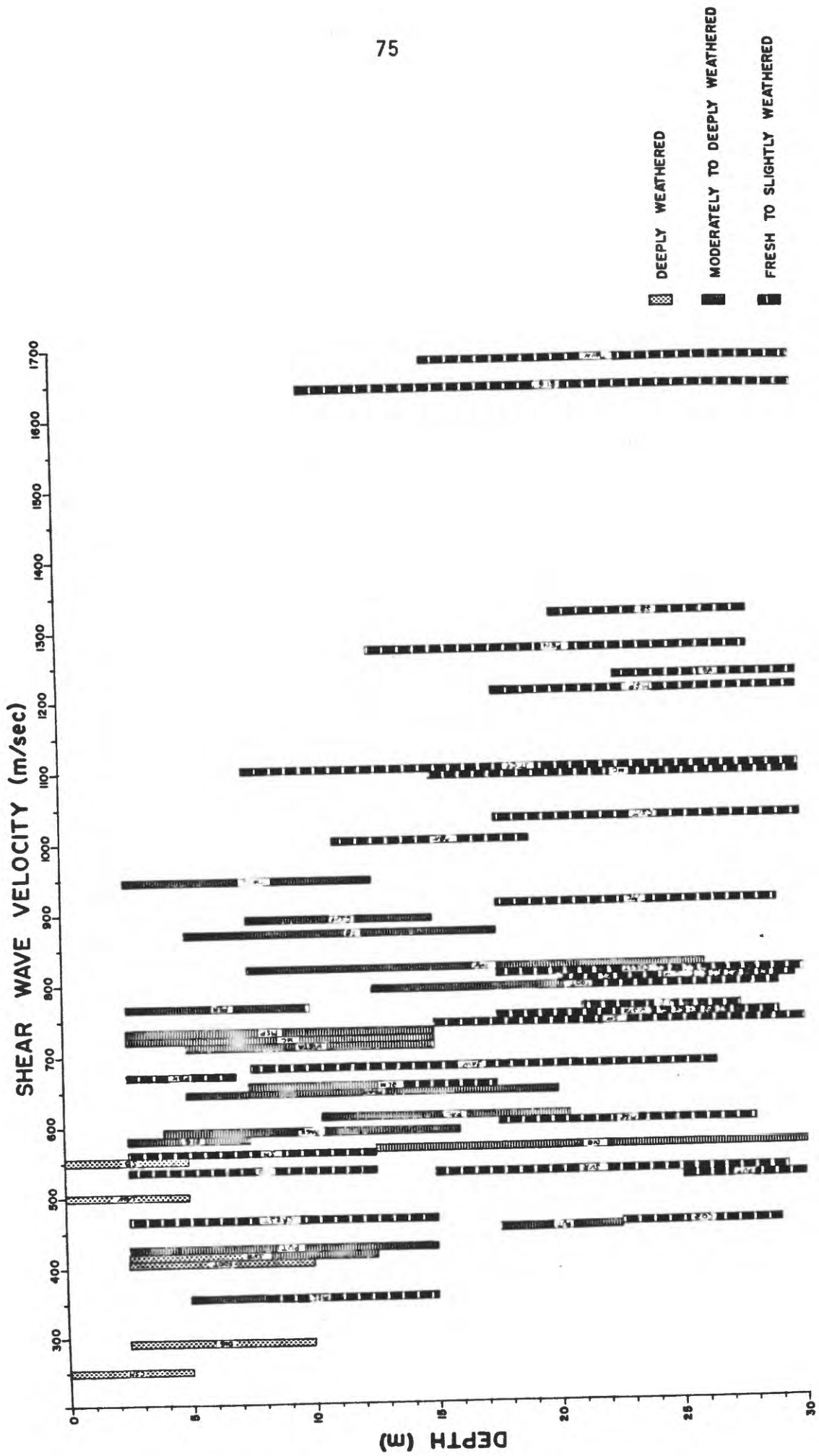


Figure 25. Relative degree of weathering in bedrock materials.

for low to medium strength sedimentary rocks and 750-1050 m/sec for high strength igneous rocks.

Weathering effects the progressive disintegration of rock through both mechanical and chemical processes. Mechanical weathering primarily involves the opening of existing fractures accompanied by the formation of new fractures. Chemical weathering decreases the hardness of the intact rock through dissolution of cement and decomposition of minerals. The properties, rock hardness and spacing of fractures, have been found to significantly affect the engineering characteristics of rock (Deere, 1963) and are readily observable in the field. Figure 27 shows the velocity-depth intervals in bedrock materials grouped according to rock hardness and fracture spacing. Lithologies having each combination of these properties are listed for each group. Mean, range and standard deviation of velocities for each group are shown in Table 5.

#### Hardness

Hardness is a measure of the strength and toughness of the intact rock. It is related to lithology and the characteristic fabric shown by each rock type. Igneous rocks have crystalline fabrics consisting of interlocking crystals. When fresh, these rocks are hard, or, as in the case of agglomerate or serpentine, may be composed of hard masses in a soft matrix of ash or sheared serpentine. Sandstones, on the other hand, have a cemented fabric in which the interstitial void space of a granular material is partially or completely filled with a cementing agent. These rocks display a wide variation in hardness depending on the degree of induration.

While a hardness distinction was not made between well-indurated

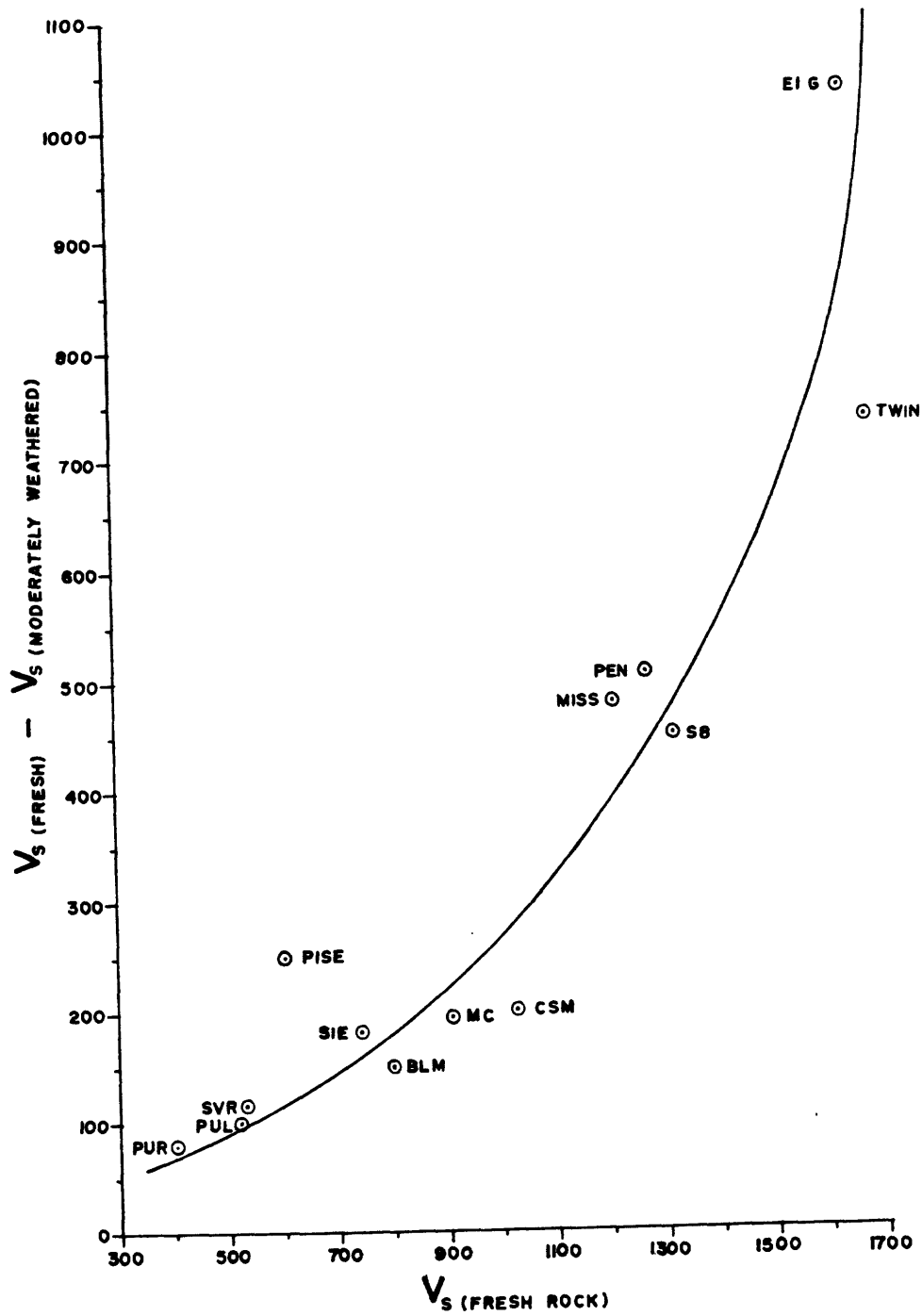


Figure 26. Variation of the difference between shear wave velocity in moderately weathered and fresh rock with velocity in fresh rock.

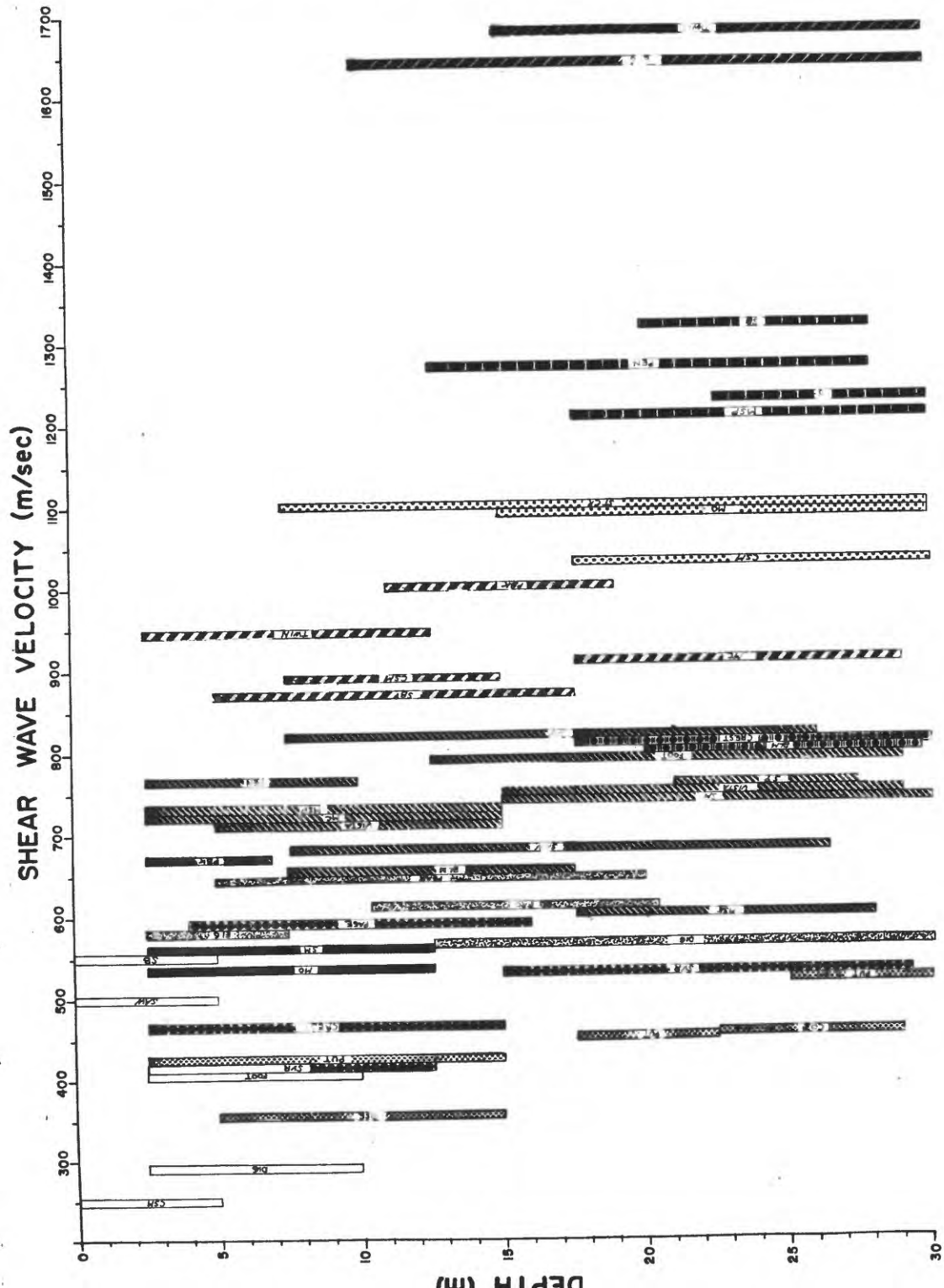


Figure 27. Bedrock materials differentiated according to physical properties. Deeply weathered materials not included as they have velocities similar to sediments of the same texture.

TABLE 5

## SHEAR WAVE VELOCITIES IN BEDROCK MATERIALS

Physical Property Unit	Shear Wave Velocity (m/sec)			
	No.	Mean	Standard Deviation	Range
A. Igneous Granite Greenstone	2	1660	20	1640-1680
B. Sandstone	4	1257	42	1210-1320
C. Sandstone Conglomerate	3	1073	31	1030-1100
D. Igneous Greenstone Rhyolite Sandstone Shale	5	923	48	871-1000
E. Igneous Greenstone Rhyolite Sandstone Shale	14	728	58	655- 823
F. Grus	4	600	30	564- 644
G. Shale	4	510	56	415- 560
H. Sandstone	4	470	48	425- 552
I. Igneous Serpentine Agglomerate Basalt Sedimentary	2	806	3	802- 809
J. Igneous Serpentine Agglomerate Basalt Sedimentary	2	528	63	465- 592

sandstone and granite or basalt, the greater rigidity of the interlocking fabric is shown by the shear-wave velocities in figure 27. Although the sandstones of group B generally have more widely spaced fractures, the crystalline rocks of group A have substantially higher velocities. At closer fracture spacings, however, this difference in fabric does not appear to result in a significant difference in shear wave velocity: rocks of different lithologies but having similar hardnesses and fracture spacings also have similar velocities.

Figure 28 shows the grouping of velocity-depth intervals based on hardness alone. In general, each hardness grouping shows a wide range in shear wave velocity. The crude method used to test hardness in this study does not allow for detailed classifications which might correlate with velocity. It may also be that small differences in hardness do not result in significant differences in S-wave velocity. Deere (1963) points out that for rock engineering purposes, it is not the slight differences in hardness from one rock to another that are important, but rather the large variations.

#### Fracture Spacing

Figure 29 shows the velocity-depth intervals grouped according to fracture spacing alone. The influence of fracture spacing on shear wave velocity appears to be greater than that of either lithology or hardness. Relatively small differences in the range of fracture spacing correlate well with significant changes in the velocities measured. This result accords with conclusions from theoretical studies of the elasticity of rock by Walsh and Brace (1966). They investigated the effects of two types of rock porosity, pores (which affect rock hardness) and cracks on

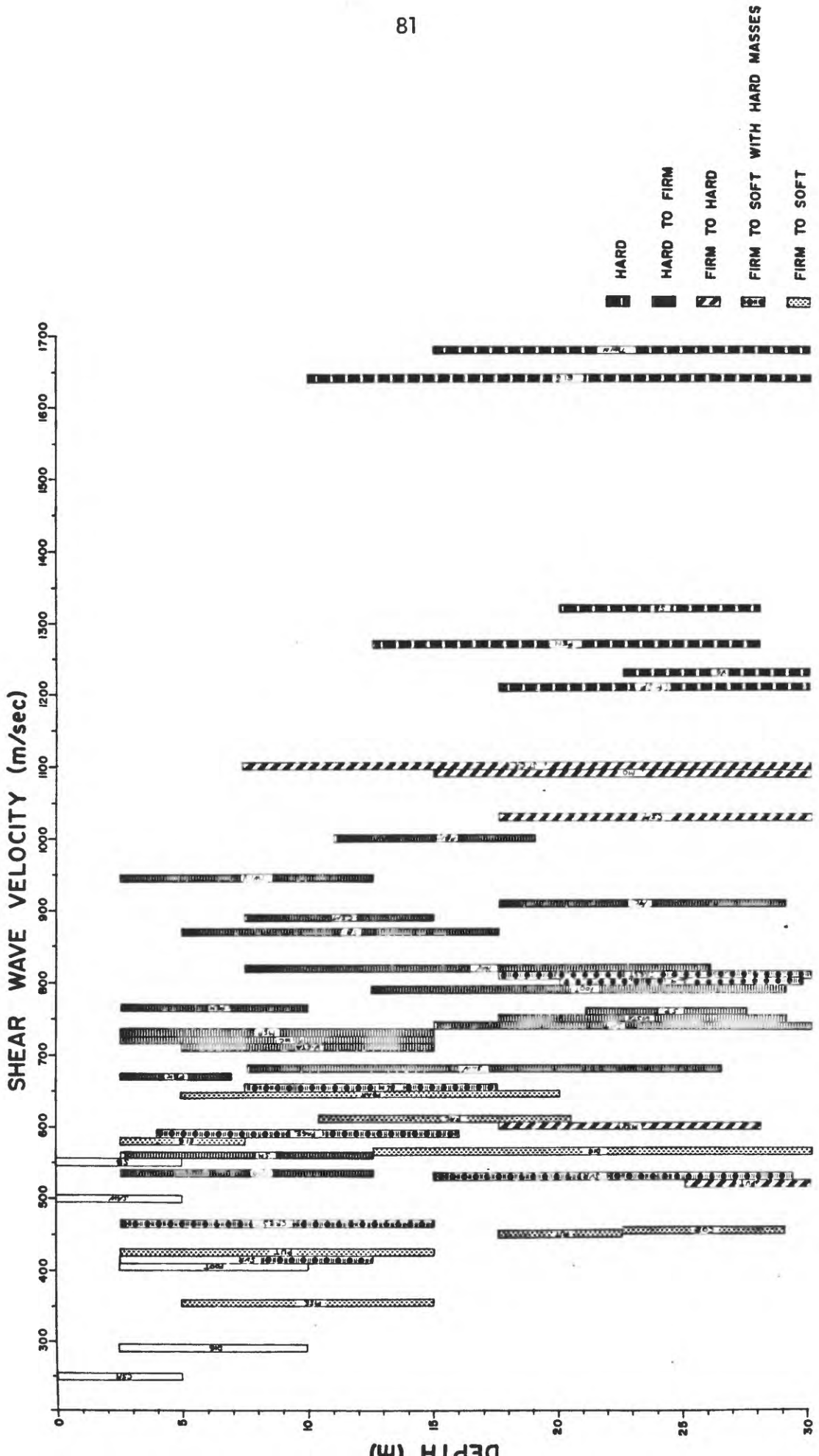


Figure 28. Bedrock materials categorized according to hardness.

the elastic moduli of rock. They found that the effect of cracks on the elastic moduli is nearly the same as that of an equal volume density of pores even though the porosity in the case of pores is much greater. Thus, formation of cracks in a rock could significantly lower the elastic modulus without changing the porosity appreciably. Furthermore, it is the longest cracks, such as joints, or bedding plane partings which have the greatest effect.

Fracture spacing thus provides the basis for a classification scheme with respect to shear wave velocity for the bedrock materials. Over most of the range of velocity measured in bedrock materials in this study, S-wave velocity increases with increasing distance between fractures. The main exceptions are: (1) the sandstones in group H (figure 27) which have low velocities due to weak cementation; (2) the granitic gneiss in which, although the rock is shattered, fragments remain interlocking and thus have higher velocities than rocks which have been tectonically sheared; and (3) the igneous rocks in group A (figure 27) which have been discussed previously.

#### Shear Wave Velocity for Bedrock Map Units

Figure 30 shows the velocity-depth intervals for bedrock materials grouped according to standard geologic map units. Tertiary rocks have been divided into two groupings, clastics and volcanics, although each of the nine Tertiary sites was located in a different geologic map unit. Mean range, and standard deviation of the velocities in each geologic map unit are shown in Table 6. Figure 30 shows that a classification based on standard geologic map units alone is not very satisfactory. In some units, such as the Franciscan clastics, materials of widely varying

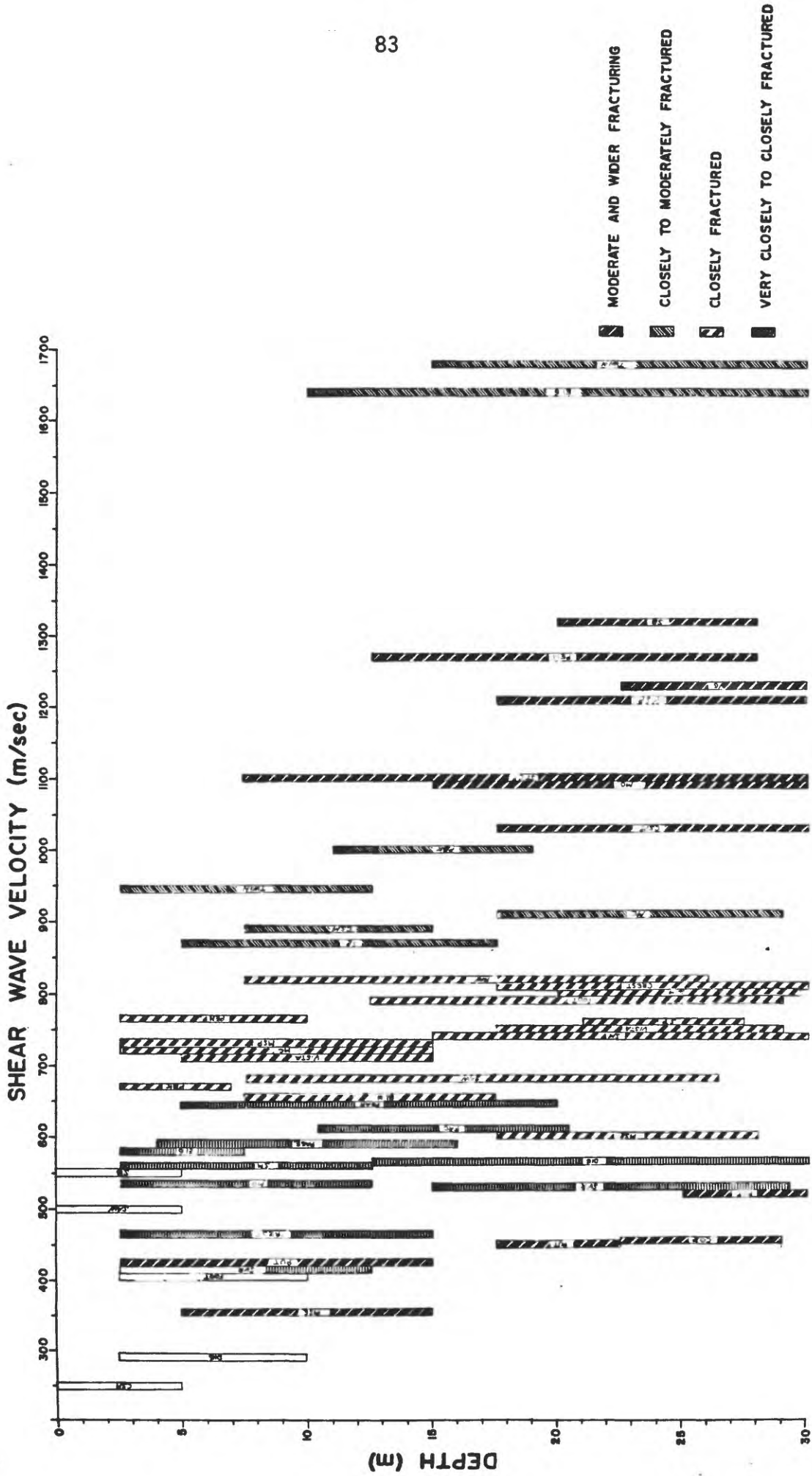


Figure 29. Bedrock materials categorized according to fracture spacing.

physical properties are included and velocities span the complete range measured in bedrock materials, and some rocks with very similar physical properties, such as the sandstones of group B in figure 27, are assigned to three separate map units.

A map classification based on the physical properties of the geologic map units has been prepared for the study area (Wentworth and Ellen, in press). This classification is particularly useful in identifying geologic units which are relatively homogeneous and for grouping those units which have similar physical properties. The many Tertiary map units, for example, can be grouped into several categories which have similar properties and relatively narrow velocity ranges. However, the problem of units which are very heterogeneous in physical properties, such as the Franciscan assemblage and the granitic rocks, remains. For this reason only a relatively broad classification of the rock units is proposed. Table 7 presents this scheme with velocities for both the moderately weathered and fresh material listed.

### Summary

Shear wave velocities have been measured in a variety of rock types in the uplands around San Francisco Bay. Units sampled include a range of Tertiary sedimentary and volcanic rocks, most lithologies of the Franciscan assemblage and the granitic rocks.

Velocities were found to correlate well with the hardness and fracture spacing of the materials. These properties are strongly affected by the degree of weathering. Weathering affects the progressive disintegration of rock through the opening of existing fractures, the formation of new fractures, and decreasing the hardness of the intact rock through disso-

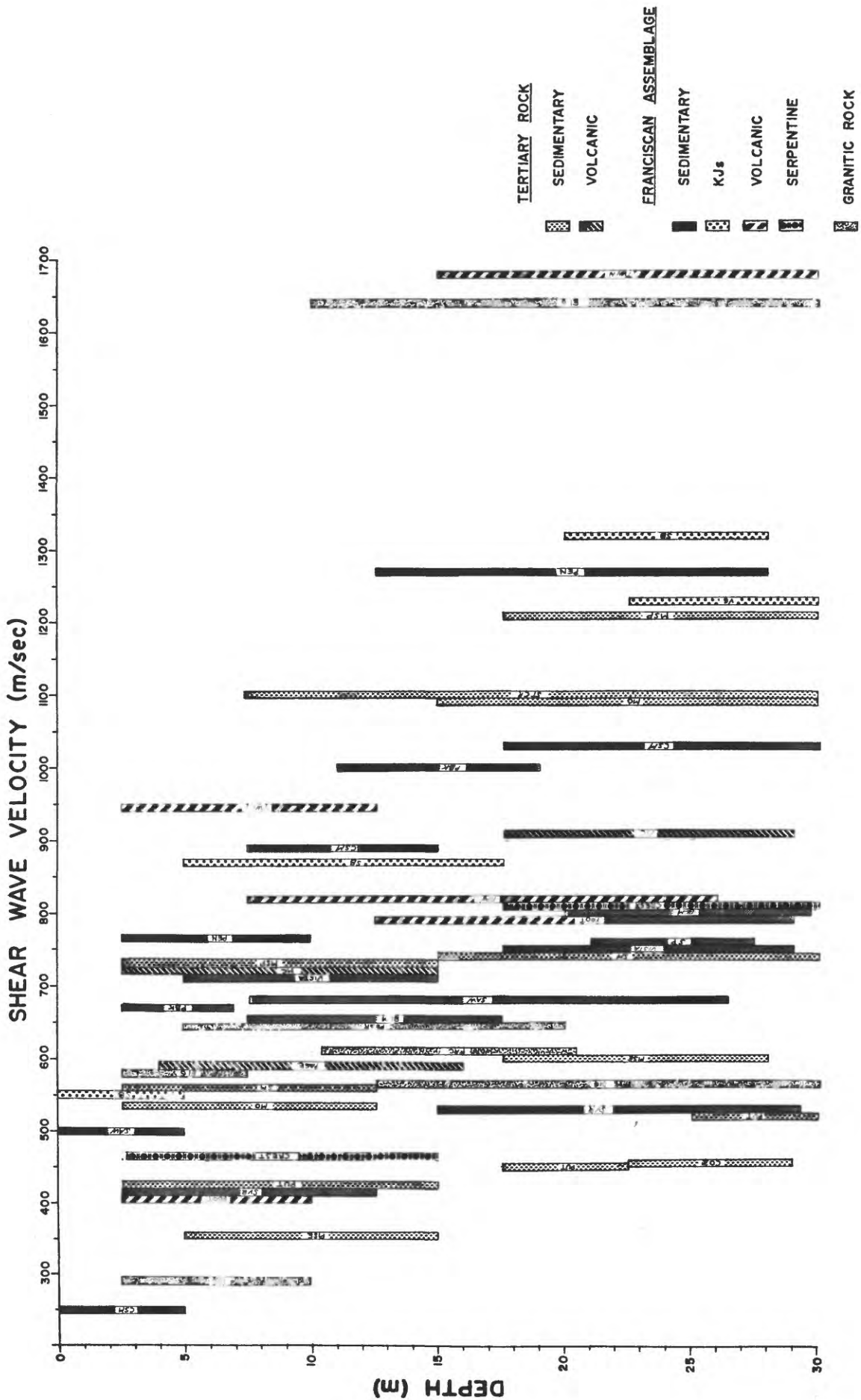


Figure 30. Bedrock materials grouped according to geologic unit.

TABLE 6  
SHEAR WAVE VELOCITIES IN BEDROCK GEOLOGIC UNITS

Geologic Map Unit	No.	Shear Wave Velocity (m/sec)		
		Mean	Standard Deviation	Range
Tertiary				
Clastics	13	677	271	356-1210
Volcanics	3	742	130	592-911
Franciscan Fm.				
Clastics	18	737	227	249-1270
Volcanics	5	929	416	406-1680
KJS*	3	1140	194	871-1320
Serpentine	2	637	172	465-809
Granitic	6	721	427	288-1640

\*Sandstone at San Bruno Mountain

TABLE 7  
SHEAR WAVE VELOCITIES IN BEDROCK GEOTECHNICAL UNITS

Geotechnical Unit	Weathering	Physical Property Groups (from Fig.27)	No. of Measurements	S-Wave Velocity (m/sec)		
				Mean	Standard Deviation	Range
<b>Tertiary (Miocene-Paleocene)</b>						
Sandstone	Moderate	H,G	4	470	85	356-560
Shale	Fresh	H,E	5	560	105	451-739
Sandstone Conglomerate	Moderate	E,J	3	680	60	592-728
Rhyolite Agglomeration	Fresh	B,C,D	4	1080	107	911-1210
<b>Franciscan</b>						
Sandstone	Moderate	D,E,J	6	718	158	415-892
Shale	Fresh	B,C,D,E,I,J	12	903	250	530-1320
Chert	Moderate	D.E.I	4	841	120	791-943
Volcanic rocks	Fresh	A	1	1680		
<b>Serpentine</b>						
Granitic	Moderate (Grus)	F	4	600	30	564-644
	Fresh	A	1	1640		

lution of cement and alteration of minerals. Fracture spacing was found to be the most important factor affecting S-wave velocity. Velocity increases with increasing fracture spacing. Hardness was most important for the soft sandstones which have low velocities in spite of moderate and wider fracture spacings.

Most of the standard geologic map units do not show distinct velocity ranges due to the wide variation in physical properties of materials included in them. The classification of Wentworth and Ellen (in press), based on hardness and fracture spacing of the bedrock materials, is very useful for grouping the Tertiary units into classes with similar physical properties. These groups show relatively narrow velocity ranges. The distribution of physical properties for Franciscan lithologies and the granitic rocks cannot be mapped in detail, however, Only very wide velocity ranges can be indicated for these rocks.

#### D. P-Wave Velocities for Sedimentary Deposits and Bedrock Materials

Compressional wave velocities for the unconsolidated to moderately consolidated sedimentary deposits and the bedrock materials are presented in figures 31 and 32, respectively. To facilitate comparison with the S-wave data, the physical properties classifications delineated for the sediments in figure 7 and the bedrock materials in figure 27 are used in figures 31 and 32. Mean range and standard deviation of the velocities are presented in tables 8 and 9. Except for the higher velocity rock units, the physical property groups do not show distinct compressional wave velocities. The sedimentary groups show overlapping P-wave velocity ranges of 300 to 1500 m/sec while most of the bedrock groups have ranges of 500 to 1700 m/sec. The dissimilar P- and S-wave characteristics of the physical property groupings reflect differences in the parameters which control the velocities of the two types of waves.

##### Factors Affecting P-wave Velocity

##### Effective Stress and Void Ratio

Many studies, both theoretical and experimental, have been conducted to investigate the parameters which affect compressional wave velocities in porous media such as soils and rocks. Of particular interest are those laboratory measurements of P-wave velocities which have been made in conjunction with studies of S-wave velocities in dry and water-saturated sands (Hardin and Richart, 1963), sand-clay mixtures (Rao, 1966) and sandstones (King, 1968). These studies demonstrate that compressional wave velocities vary with changes in effective stress and void ratio in a manner similar to that of shear waves.

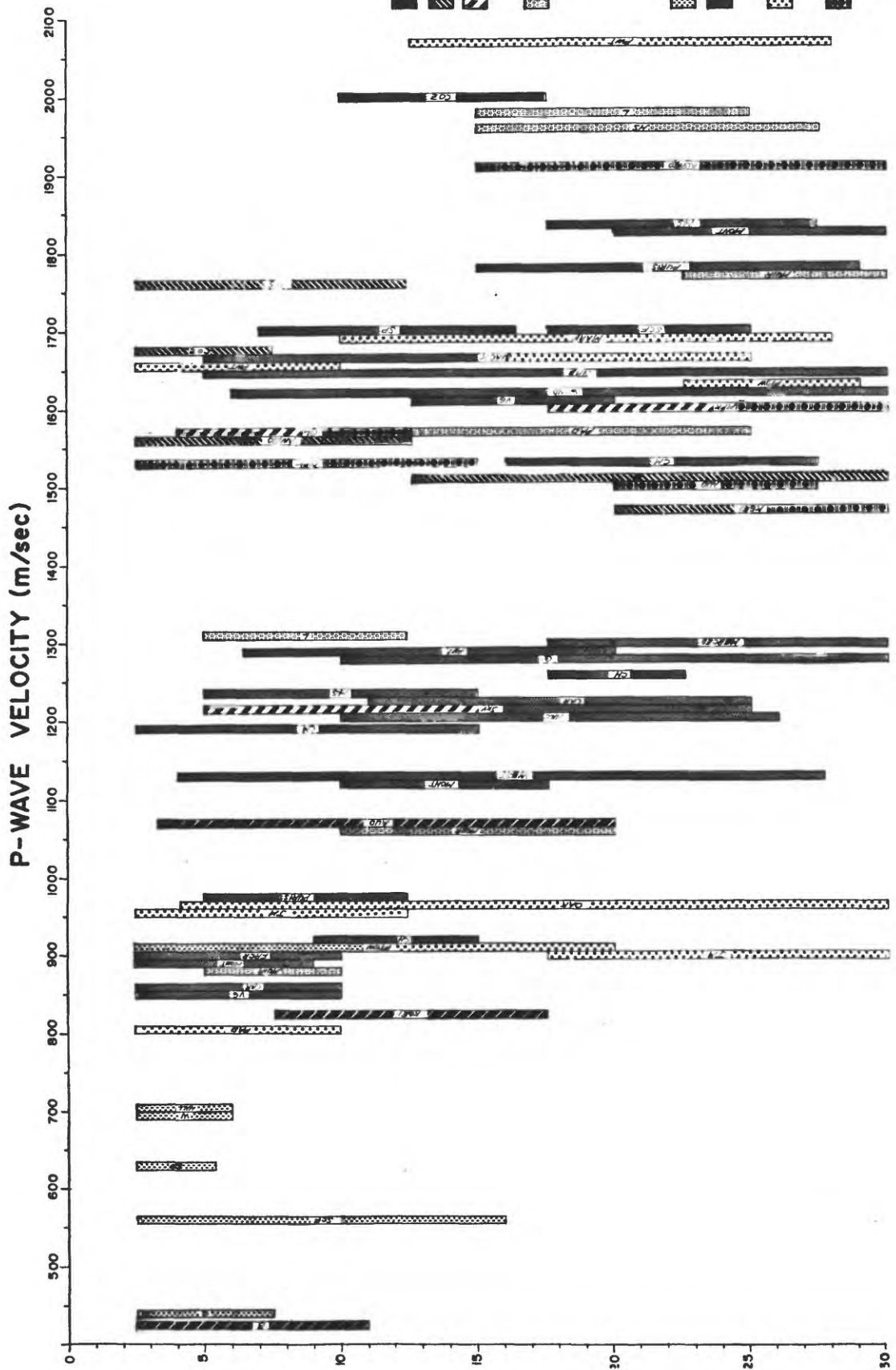


Figure 31. Compressional wave velocities in sedimentary deposits grouped according to physical properties.

TABLE 8

## P-WAVE VELOCITIES IN SEDIMENTARY PHYSICAL PROPERTY UNITS

Physical Property Unit	No.	Mean	Standard Deviation	Range
Silty Clay and Clay				
V. soft to soft	4	680	282	395-1070
Med. to v. stiff	6	1583	100	1470-1760
V. stiff to hard	3	1363	151	1210-1570
Sand Clay and Silt Loam	6	1537	416	880-1960
Sand				
N $\leq$ 40	8	579	157	497-2000
N $>$ 40	32	1263	383	497-2000
Gravel	9	1383	420	906-2070
Mixed Sediment	5	1596	160	1470-1910

# P-WAVE VELOCITY (m/sec)

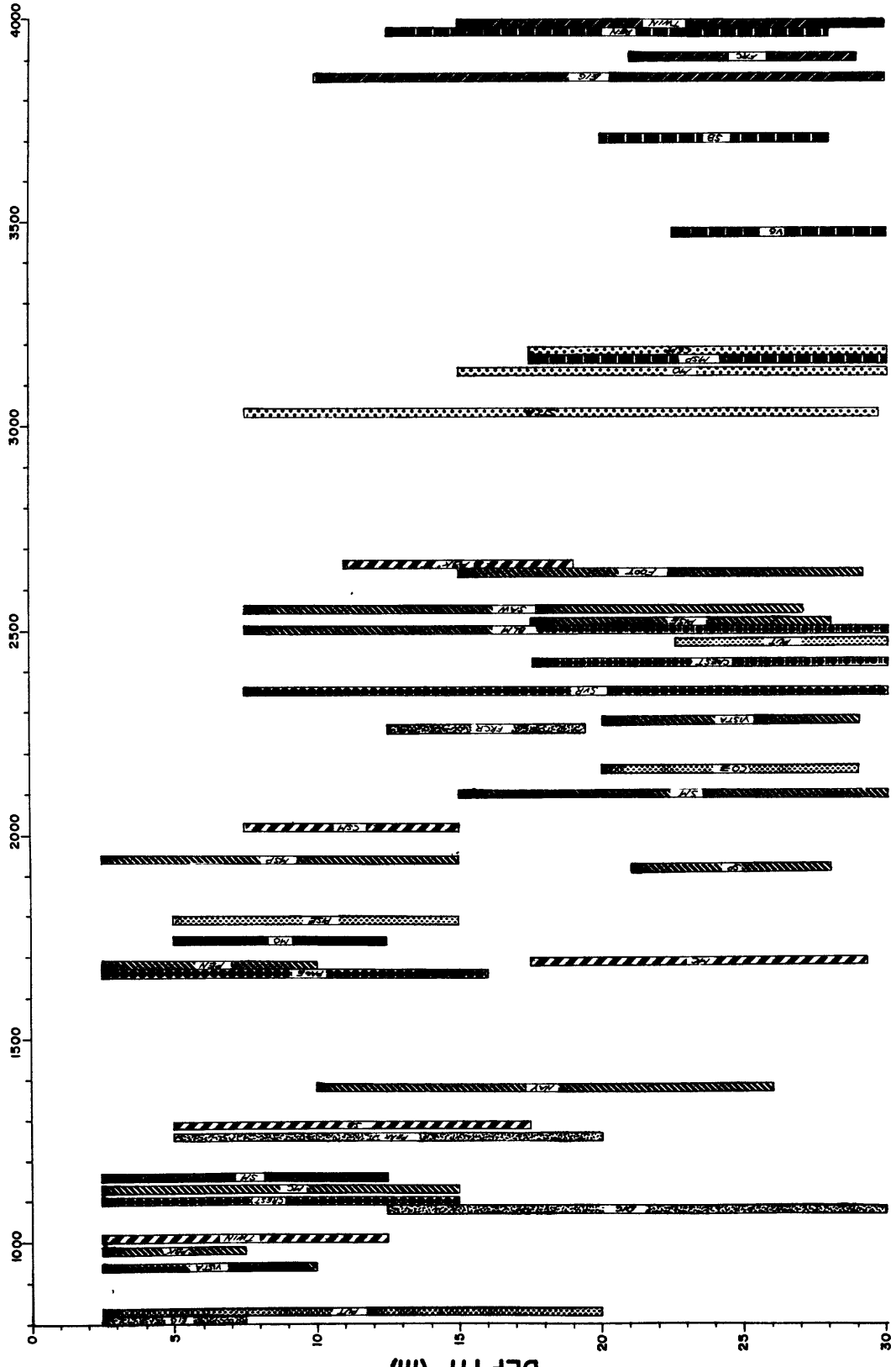


Figure 32. Compressional wave velocity in bedrock materials grouped according to physical properties.

TABLE 9

## P-WAVE VELOCITIES IN BEDROCK PHYSICAL PROPERTY UNITS

Physical Property Unit	No.	P-wave velocity (m/sec)		
		Mean	Standard Deviation	Range
A Igneous	3	3910	53	3850-3980
B Sandstone	4	3572	295	3160-3960
C Sandstone Conglomerate	3	3106	55	3030-3160
D Igneous Sandstone Shale	5	1734	570	1020-2650
E Igneous Sandstone Shale	14	1790	616	800-2640
F Grus	5	1233	545	738-2260
G Shale	3	1750	485	1160-2350
H Sandstone	4	1817	630	810-2470
I Igneous Sedimentary	2	2460	40	2420-2500
J Igneous	2	1380	290	1090-1670

### Interstitial Fluids

The most significant difference between the behavior of P- and S-waves lies with the effect of interstitial fluids. The shear wave generally shows only slight changes with degree of saturation primarily due to the effect on bulk density. In cohesive soils, however, degree of saturation strongly effects soil structure and pore pressure and thus the shear wave velocity. Hardin and Drenevich (1972) report a 5% decrease in shear modulus for a silty clay with an increase in degree of saturation from 70% to 100%.

On the other hand, interstitial fluids strongly influence P-wave velocities in soils and rock through effects on the bulk modulus. Hamilton (1969) has pointed out that the "system" bulk modulus is a function of the aggregate bulk modulus of the mineral grains, the bulk modulus of the pore fluid, the bulk modulus of sediment or rock structure and the porosity. The bulk modulus of a gas-water mixture at low pressure is nearly equal to the bulk modulus of the gas alone. Thus, as Brandt (1960) has shown theoretically, the introduction of any amount of gas into a water-saturated sediment results in a large initial reduction in P-wave velocity, followed by a leveling off at this decreased velocity level. He calculated a P-wave velocity of 1720 m/sec for a water-saturated quartz sand with a porosity of 40% and at a water depth of 30 m. At a gas saturation of 1%, the P-wave velocity decreases to 333 m/sec and increases with depth. This theoretical result is dependent on a homogeneous gas distribution. This is probably not the case with actual sediments. Brandt's experimental data show an initial rapid decrease of several hundred meters per second at low gas saturations, followed by a

less steep decline to about 60% water-saturation, followed by a leveling off at about 333 m/sec. Similar results have been obtained in the laboratory for sand-clay mixtures (Rao, 1966) and sandstones (Wyllie, Gregory, and Gardner, 1956).

Natural solid-water-gas mixtures occur above the water table in soil and rock materials. Thus, sharp increases in P-wave velocity occur at the water table. For sedimentary deposits, the bulk modulus of the sediment structure is much lower than that of water (Hamilton, 1969); the water table is marked by an increase in P-wave velocity to approximately 1500 m/sec. In figure 31, sediments with P-wave velocities below 1300 m/sec are unsaturated, while those with velocities above 1450 m/sec may be taken as fully water-saturated. This velocity gap may reflect the experimental behavior in sediments observed by Brandt.

For rocks, however, the structure bulk modulus is greater than that of water. While there is an increase in P-wave velocity at the water table in rocks, it is not indicated by a rise to any particular value. Wyllie et al. (1956) observed P-wave velocity increases of 250-650 m/sec with full saturation in cores of sandstone ranging in porosity from 16% to 30%. Measured water levels (Roth, 1978) show that bedrock materials in figure 32 with velocities less than 1700 m/sec are above the water table, while those with velocities greater than 2100 m/sec are probably below it; between these two values, both saturated and unsaturated bedrock materials occur.

Solid-water-gas mixtures may also occur below the apparent water table in unconsolidated sediments, due to the presence of small amounts of gas derived from the decay of organic matter deposited with the sediment.

This is a likely cause of low P-wave velocities observed in the bay muds. Significant concentrations of methane have been widely recognized in similar estuarine and deltaic sediments which have sufficiently high concentrations of organic matter and high rates of deposition. For example, in Chesapeake Bay sediments, Reeburgh (1969) reports methane concentrations of 85-150 ml/liter at a depth of 1 m under conditions appropriate for bubble formation.

### Summary

Compressional wave velocities measured in the sedimentary deposits and bedrock materials do not show the strong correlation with other physical properties found for shear wave velocities. Most of the physical property classifications show wide (300-1700 m/sec) and overlapping velocity ranges. For materials above the water table, the wide variation can be attributed to differences in degree of saturation which strongly affects compressibility. The variation for saturated materials, however, is not as readily explained.

Using P-wave velocities, seismically distinct units cannot be delineated with the degree of refinement possible for shear waves. P-wave velocities are useful, however, in predicting some aspects of the seismic response of geologic materials. For this reason, the P-wave velocities of the geotechnical units found to have distinct shear wave velocity characteristics are presented in figure 33 and table 10 for the sediments and figure 34 and table 11 for the bedrock materials. Velocities for both saturated and unsaturated materials are listed. Even when this division is made, the sedimentary units do not show distinct

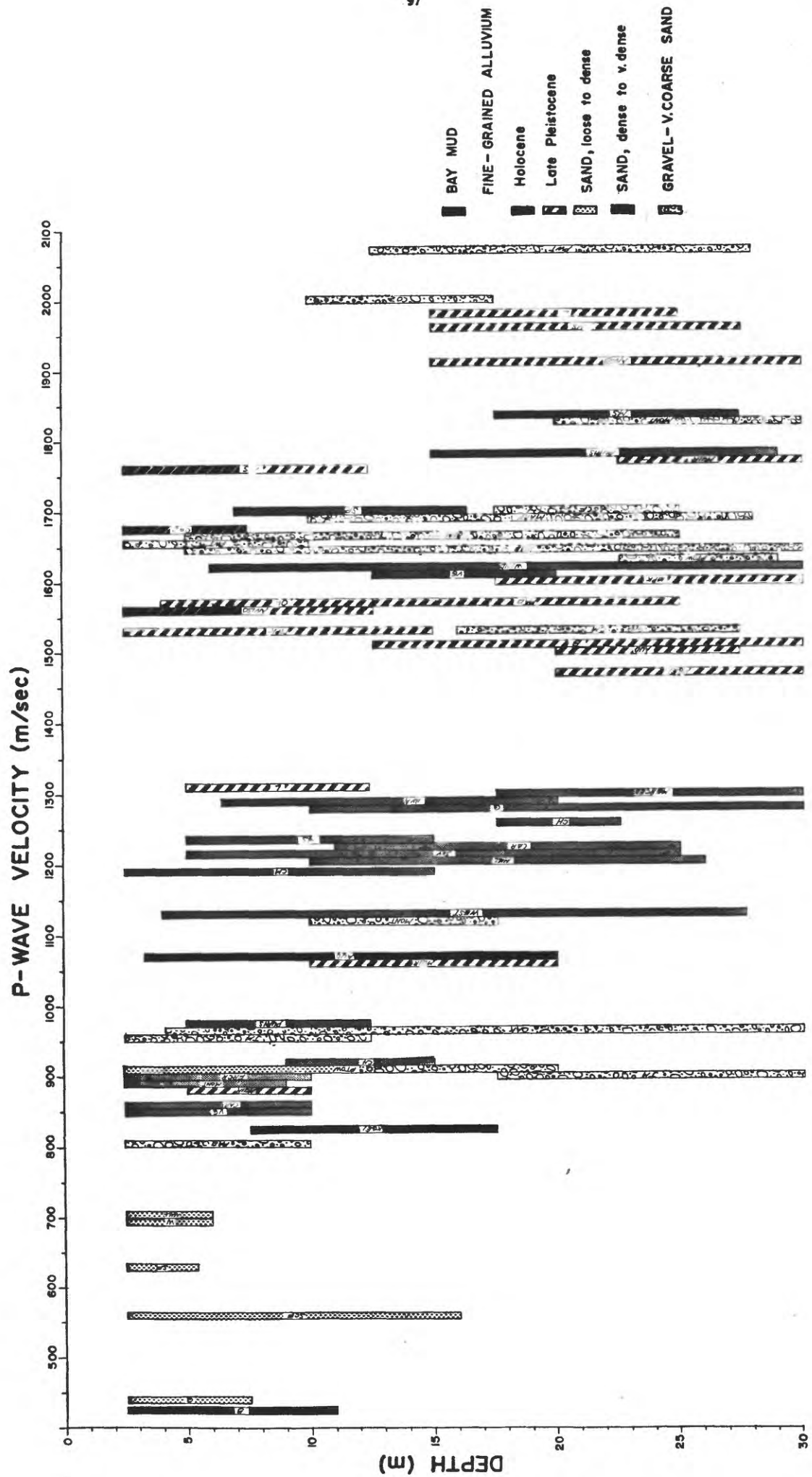


Figure 33. Compression 1 wave velocities in seismically distinct geotechnical units for sedimentary deposits.

TABLE 10

Geotechnical Unit	Relative Water Content	No. of Measurements	Mean	Range of P-Wave Velocity
Bay Mud	Saturated	3	775	427-1070
Holocene fine-grained	Saturated	3	1660	1560-1760
Late Pleistocene fine-grained	Unsaturated	3	1080	880-1310
	Saturated	13	1670	1470-1980
Sand, Loose-dense	Unsaturated	5	650	442-910
Sand, dense-v. dense	Unsaturated	17	1080	703-1300
	Saturated	5	1700	1610-1830
Gravel-V. Coarse Sand	Unsaturated	6	940	806-1120
	Saturated	10	1740	1530-2070

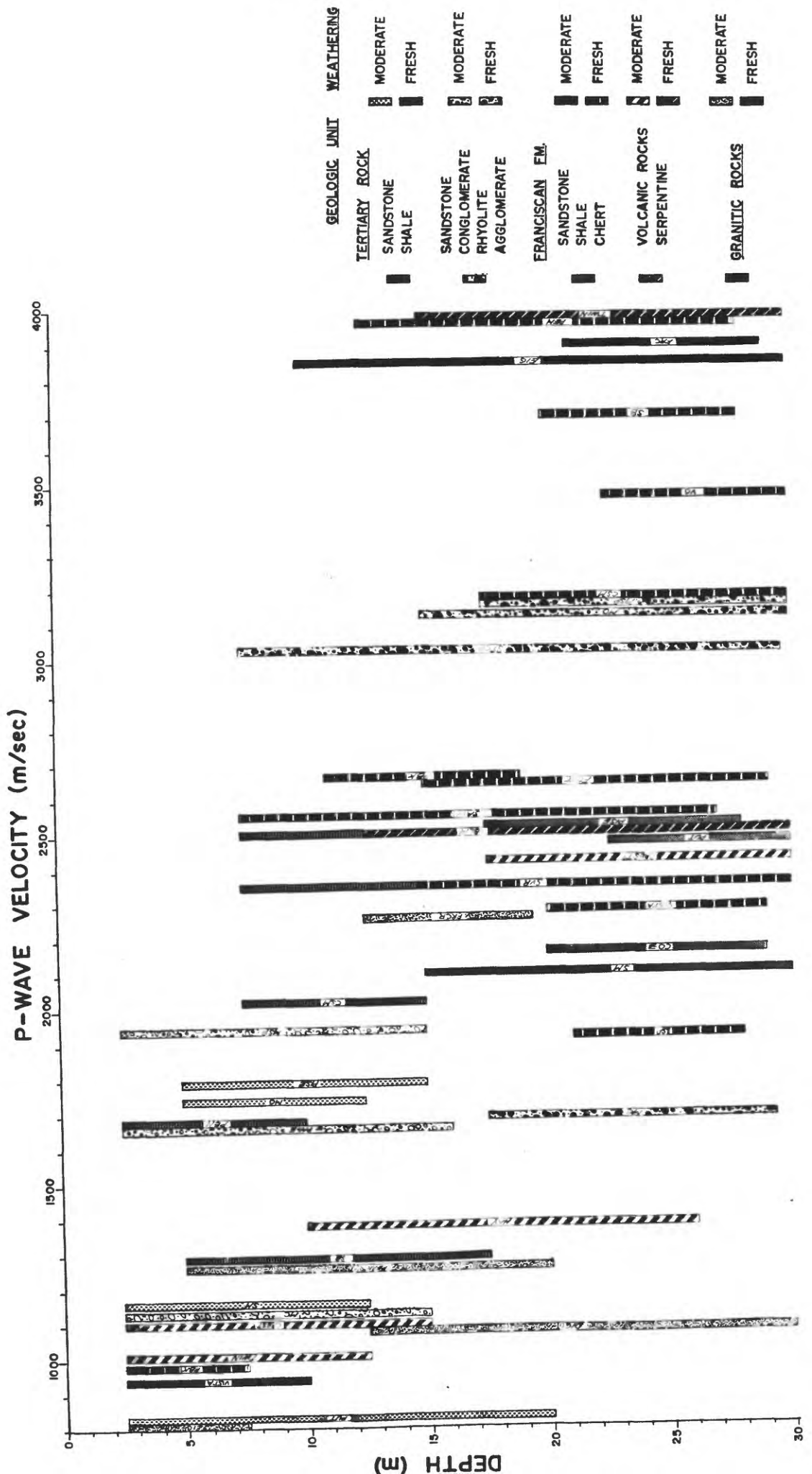


Figure 34. Compressional wave velocities in seismically distinct bedrock geologic units.

TABLE 11  
P-WAVE VELOCITIES IN BEDROCK GEOLOGIC UNITS

Geologic Unit	Weathering	Relative Water Content	No. of Measurements	P-Wave Velocity Range
Tertiary (Miocene-Paleocene)				
Sandstone	Moderate	Unsaturated	2	840-1160
Shale		Saturated	2	1740-1790
	Fresh	Saturated	2	2100-2520
Sandstone	Moderate	Unsaturated	1	1080
Conglomerate		Saturated	2	1670-1940
Rhyolite	Fresh	Unsaturated	1	1690
Agglomerate		Saturated	3	3030-3160
Franciscan				
Sandstone	Moderate	Unsaturated	4	930-2020
Shale		Saturated	2	2350-2500
Chert	Fresh	Unsaturated	1	980
		Saturated	11	1920-3960
Volcanic Rocks	Moderate	Unsaturated	3	1020-1380
Serpentine		Saturated	2	2420-2640
	Fresh	Saturated	1	3980
Granitic	Moderate (Grus)	Unsaturated	3	830-1260
		Saturated	1	2260
	Fresh	Saturated	2	3850-3900

P-wave velocity ranges. The bedrock units, on the other hand, show a similar pattern for shear and P-wave velocities. Velocities in the Tertiary rocks show several distinct ranges while velocities in the Franciscan sedimentary rocks span the entire range of P-wave velocities measured in bedrock materials.

#### E. Elastic Moduli

##### Shear and Bulk Moduli

Calculated values of shear modulus and bulk modulus are presented in figure 35. The geologic materials have been divided into three groups: fine-grained soils (silty clays, sandy clays and silt loams); coarse-grained soils (sands and gravels), and bedrock. Values of shear modulus are plotted versus shear wave velocity and values of bulk modulus are plotted versus P-wave velocity.

##### Poisson's Ratio

Values of Poisson's ratio calculated from measured P- and S-wave velocities are presented in figure 36. The materials have again been divided into fine-grained soils, coarse-grained soils, and bedrock. A dashed line separates the values for saturated and unsaturated materials. For saturated materials, Poisson's ratio varies within relatively narrow limits for a given shear wave velocity. The fine-grained soils have a distinct, narrow range of Poisson's ratio (0.485 - 0.5). Although the coarse-grained soils and bedrock have very different shear-wave velocity ranges, they show very similar ranges of Poisson's ratio: 0.43 - 0.49 for coarse-grained soils, 0.41 - 0.48 for rocks. In contrast, unsaturated materials have a very wide range of values for a given shear wave velocity. This illustrates the necessity of specifying whether materials are

saturated or unsaturated in reporting or estimating values of Poisson's ratio.

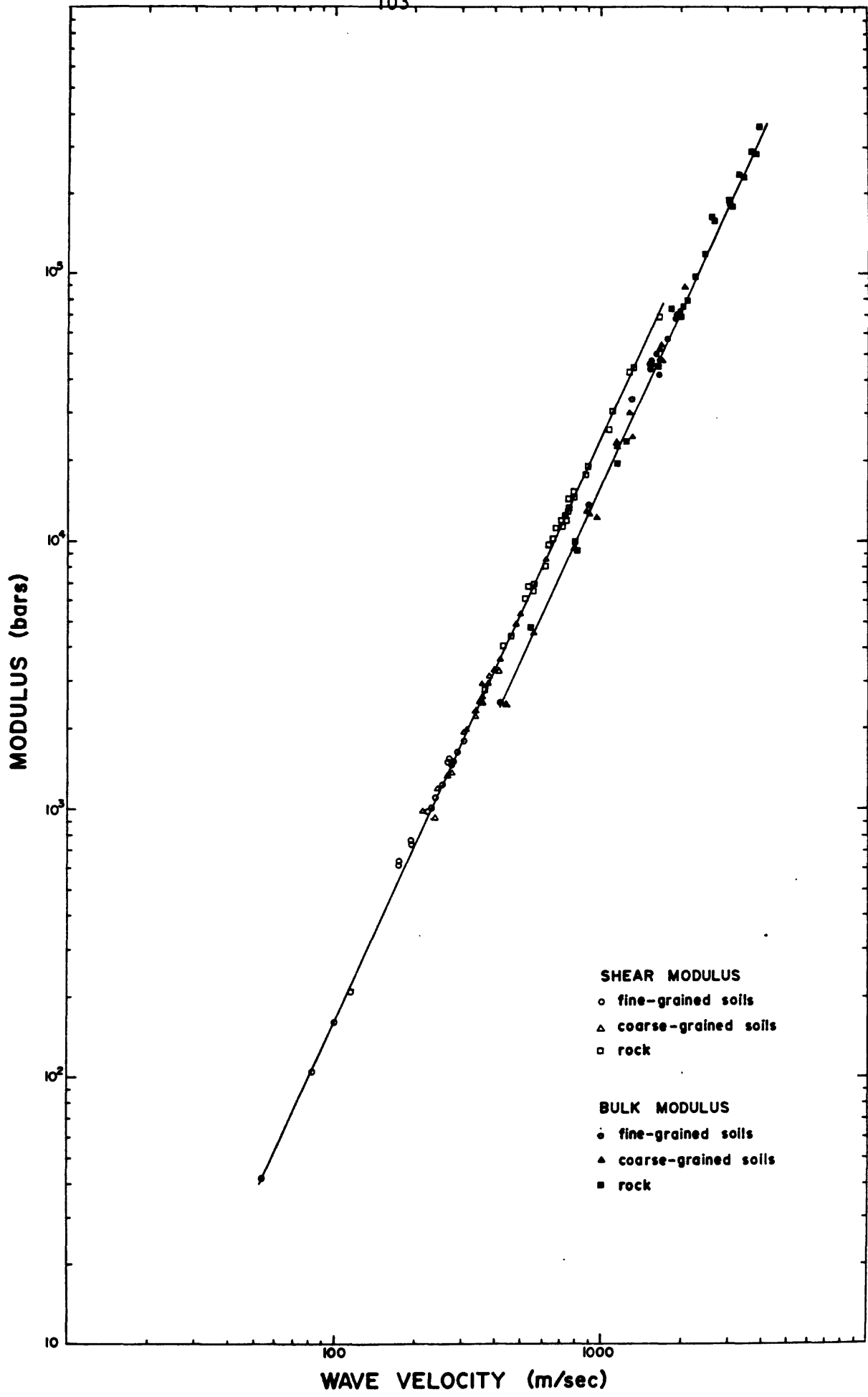


Figure 35. Variation of shear modulus with shear wave velocity and bulk modulus with P-wave velocity.

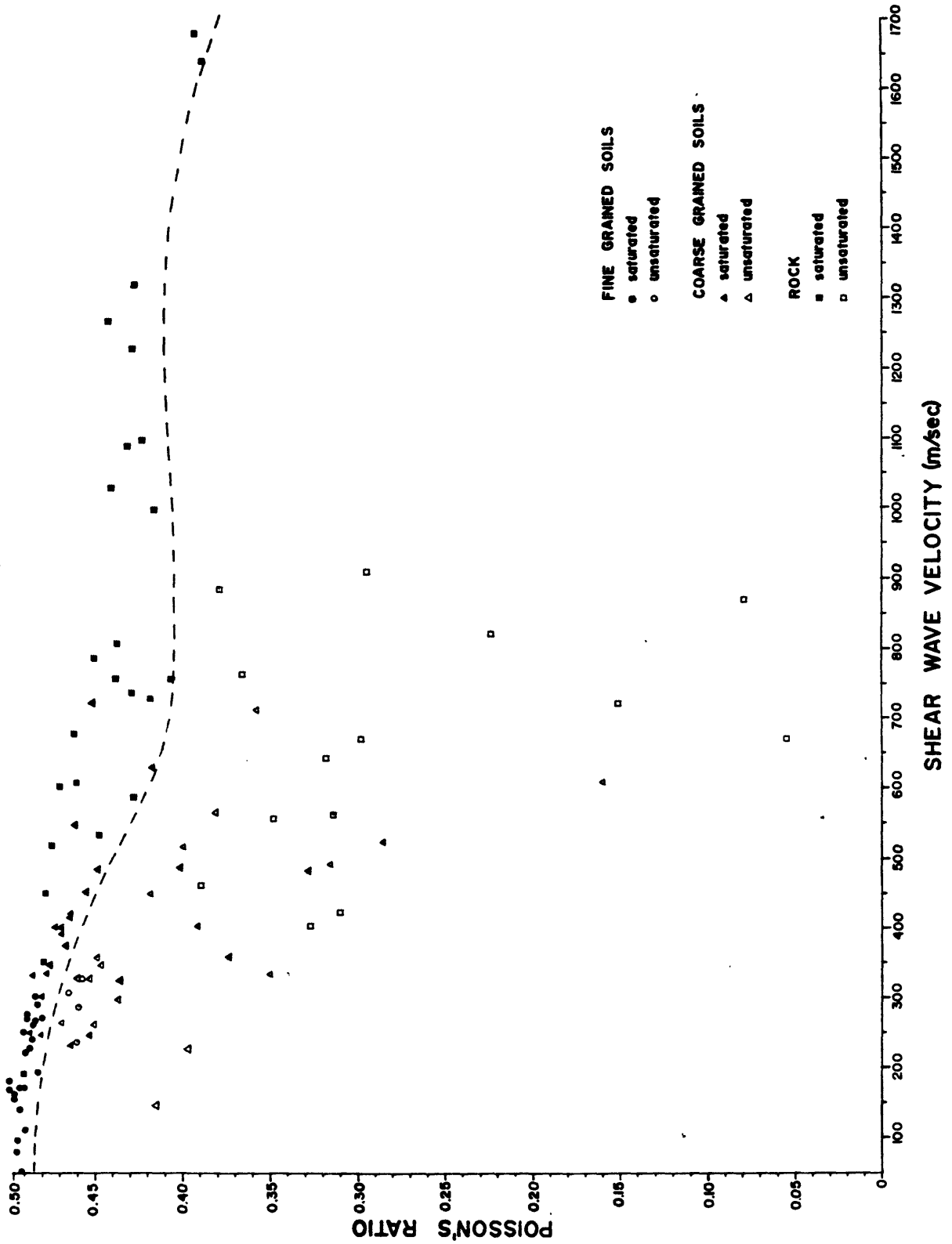


Figure 36. Variation of Poisson's ratio with S-wave velocity in soils and bedrock materials. Dashed line separates saturated and unsaturated materials.

## SUMMARY

Seismic wave velocities have been measured at 59 sites in the southern San Francisco Bay region in a wide range of near-surface (0-30m) geologic materials. These velocities have been compared with several physical properties of the materials which can be readily determined in the field. Shear wave velocity was found to correlate with these properties much more strongly than P-wave velocity. Correlations obtained suggest a classification scheme useful in defining seismically distinct geotechnical units.

For unconsolidated to semi-consolidated sediments the following conclusions can be drawn:

(1) Texture (relative grain size distribution) has the most significant effect on shear wave velocity. At a given depth, velocity increases as average grain size increases. Five textural groupings were defined: (1) clay and silty clay, (2) sandy clay and silt loam, (3) interbedded fine and coarse sediment, (4) sand, and (5) gravel.

(2) Standard penetration resistance can be used to subdivide several of the textural groupings which show relatively wide velocity ranges. For the clays and silty clays, SPR can be used as a measure of consistency (relative firmness) to delineate three groups: v. soft to soft ( $N < 4$ ), medium to v. stiff ( $4 \leq N \leq 20$ ) and v. stiff to hard ( $N > 20$ ). Sands can be divided into two groups using SPR as a measure of relative density: loose to dense ( $N \leq 40$ ) and dense to v. dense ( $N > 40$ ). The first group is comprised of Holocene and v. fine-grained late Pleistocene sands. All other sands through Plio-Pleistocene in age are included in the second group. Density (and void ratio) correlates well with shear wave velocity in sands and can be used to make more detailed velocity estimates.

(3) Long-term water table effects strongly influence consistency and hence shear wave velocity in clays and silty clays. Sediments which have been desiccated and weathered are stiffer than those which have remained saturated since deposition. Soil color can be used to divide the fine-grained sediments into three groups: saturated, poorly-drained and well-drained. These groups coincide with those defined on the basis of standard penetration resistance. A similar correlation between soil color and velocity is not apparent in sands.

(4) Short-term water levels, as indicated by P-wave velocities, do not effect shear-wave velocities in sands. Evidence for fine-grained sediments is inconclusive as the few samples of these sediments which were not saturated were also slightly coarser-grained (sandy clays) and may have had higher velocities for this reason.

(5) Five groups shows distinctly higher velocities at depth ( $D \leq 12m$ ) than in the near-surface ( $0 > 12m$ ) and can be subdivided on this basis:

clay and silty clay	sandy clay and silt loam
--v. soft to soft	sand, dense to v. dense
--v. stiff to hard	gravel

For the bedrock materials the following conclusions can be drawn:

(1) Fracture spacing has the most significant effect on shear wave velocity. Velocity generally increases as fractures become more widely spaced. Four categories of fracture spacing were used: (1) moderate and wider, (2) close to moderate, (3) close, and (4) close to v. close.

(2) Hardness does not effect S-wave velocity as strongly as does fracture spacing. Five categories of hardness were defined: (1) hard, (2) hard to firm, (3) firm to hard, (4) firm to soft with hard masses, and (5) firm to soft. Each of these groups shows relatively wide velocity ranges.

(3) Lithology is important in differentiating strong sedimentary from strong igneous rocks.

(4) Although velocity increases with depth at each bedrock site, the velocity variations can be attributed to weathering or tectonic fracturing. Weathering affects the progressive break-down of the rock through the opening of existing fractures, the formation of new fractures and decreasing hardness of the intact rock through dissolution of cement and alteration of minerals.

The classification schemes based on physical properties can be used to regroup the map units defined for the San Francisco Bay region into seismically distinct groups. The range of seismic velocities for a given map unit is dependent on the variety of materials which have been included in the unit, which is largely a function of the age of the deposit. Each of the Holocene map units shows a distinct and relatively narrow range of shear wave velocity. Older sedimentary deposits and bedrock materials, which have been strongly affected by diagenetic changes and tectonism, show relatively wide and overlapping velocity ranges. The oldest materials--the Franciscan Fm. and the granitic rocks--have velocities which span nearly the entire range of recorded S-wave velocity.

For the unconsolidated to semi-consolidated sedimentary deposits, nine seismically distinct geotechnical units have been defined:

- |     |  |                                   |
|-----|--|-----------------------------------|
| i   | Bay mud                                  | Sand, dense to v. dense at depth: |
| ii  | Holocene fine-grained alluvium           | vi Dune sand                      |
| iii | Late Pleistocene fine-grained            | vii Merced Fm., Pruisima Fm.      |
| iv  | Sand, loose to dense                     | viii Colma Fm.                    |
| v   | Sand, dense to v. dense near-<br>surface | ix Gravel and v. coarse sand      |

For the bedrock materials five seismically distinct geotechnical groups have been differentiated:

	Tertiary Rocks		Franciscan Fm.
	Sandstone (firm-soft)		Sandstone
i	Shale	iii	Shale
			Chert
	Sandstone (firm to hard)		
	Conglomerate	iv	Volcanic Rocks
ii	Rhyolite		Serpentine
	Agglomerate	v	Granitic Rocks

Compressional wave velocities measured in the sedimentary deposits and bedrock materials do not show the strong correlation with other physical properties found for shear wave velocities. For materials above the water table, the wide velocity variations found for each geotechnical group can be attributed to differences in degree of saturation which strongly affects compressibility. For this reason, P-wave velocity was not used to define seismically distinct geotechnical groups.

Values of Poisson's ratio for saturated materials were found to vary within relatively narrow limits. While fine-grained soils could be differentiated from other materials, Poisson's ratio could not be used to distinguish between coarse-grained soils and bedrock materials. Unsaturated materials were found to have a very wide range of Poisson's ratio for a given shear wave velocity. For these reasons, Poisson's ratio was not used to define seismically distinct geotechnical groups.

## REFERENCES

- Aetron-Blume-Atkinson, 1965, Geologic site investigation for Stanford Linear Accelerator Center: Report No. ABA-88.
- Borcherdt, R. D., 1970, Effects of local geology on ground motion near San Francisco Bay: Bull. Seism. Soc. Am., 60, 29-61.
- Borcherdt, R. D., and Healy, J. H., 1968, A method for estimating the uncertainty of seismic velocities measured by refraction techniques: Bull. Seism. Soc. Am., 58, p. 1769-1790.
- Brandt, H., 1960, Factors affecting compressional wave velocity in unconsolidated marine sand sediments: Acoustical Society of America Journal, v. 32, p. 171-179.
- Campbell, K. W., and Duke, C. M., 1976, Correlations among seismic velocity, depth and geology in the Los Angeles area: School of Engineering and Applied Science, UCLS, UCLA-ENG-7662.
- Cooper, W. S., 1967, Coastal dunes of California: Geol. Soc. America Mem. 104, 131 p.
- Deere, D. U., 1963, Technical description of rock cores for engineering purposes: Felsmechanik und Ingenieurgeologie, v. 1, no. 1, p. 16-22.
- Ellen, S. D., Wentworth, C. M., Brabb, E. E., and Pampeyan, E. H., 1972, Description of geologic units, San Mateo County, California: Accompanying U.S. Geol. Survey Miscellaneous Field Studies Map, MF-328.
- Gibbs, James F., and Borcherdt, Roger D., 1974, Effects of local geology on ground motion in the San Francisco Bay region, California, a continued study: U.S. Geol. Survey Open-file Rept. 74-222.

Gibbs, James F., Fumal, Thomas E., and Borchardt, Roger D., 1975, In-situ measurements of seismic velocities at twelve locations in the San Francisco Bay region: U.S. Geol. Survey Open-file Rept. 75-564.

\_\_\_\_\_ 1976, In-situ measurements of seismic velocities in the San Francisco Bay region...Part II: U.S. Geol. Survey Open-file Rept. 76-731.

Gibbs, James F., Fumal, Thomas E., Borchardt, Roger D., and Roth, Edward F., 1977, In-situ measurements of seismic velocities in the San Francisco Bay region...Part III: U.S. Geol. Survey Open-file Rept. 77-850.

Hamilton, E. L., 1969, Sound velocity, elasticity and related properties of marine sediments, North Pacific. II. Elasticity and elastic constants: Naval Undersea Research and Development Center Technical Publication 144, 66 p.

\_\_\_\_\_ 1976, Shear-wave velocity versus depth in marine sediments: a review: Geophysics, v. 41, p. 985-996.

Hardin, B. O., and Drenevich, V. P., 1972a, Shear modulus and damping in soils: Measurement and parameter effects: Proc. Am. Soc. Civil Eng., J. Soil Mech. Found. Div., v. 98, p. 603-624.

\_\_\_\_\_ 1972b, Shear modulus and damping in soils: Design equations and curves: Proc. Am. Soc. Civil Eng., J. Soil Mech. Found. Div., v. 98, p. 667-692.

Hardin, B. O., and Richart, F. E., 1963, Elastic wave velocities in granular soils: Proc. Am. Soc. Civil Eng., J. Soil Mech. Found. Div., v. 89, p. 33-65.

- Helley, E. J., and Brabb, E. E., 1971, Geologic map of late Cenozoic deposits, Santa Clara County, California: U.S. Geol. Survey Misc. Field Studies Map MF-335.
- Helley, E. J., Lajoie, K. R., and Burke, D. B., 1972, Geologic map of late Cenozoic deposits, Alameda County, California: U.S. Geol. Survey Misc. Field Studies Map MF-429.
- Joyner, William B., and Chen, Albert T. F., 1975, Calculation of non-linear ground response in earthquakes: Bull. Seism. Soc., v. 65, p. 1315-1336.
- King, M. S., 1968, Ultrasonic compressional and shear-wave velocities of confined rock samples: Proc. 5th Canadian Rock Mechanics Symposium, p. 127-156.
- Kitsunezaki, C., 1965, In-situ determination of variation of Poisson's ratio in granite accompanied by weathering effect and its significance in engineering projects: Bull. Disaster Prevention Res. Inst., v. 15, p. 19-41.
- \_\_\_\_\_, 1971, Field-experimental study of shear waves and the related problems: Contributions, Geophysical Institute, Kyoto University, No. 11, p. 103-177.
- Kobayashi, N., 1959, A method of determining the underground structure by means of SH waves: Zisin, ser. 2, v. 12, p. 19-24.
- Komornik, A., Rohrllich, V., and Wiseman, G., 1970, Overconsolidation by dessication of coastal late-Quaternary clays in Israel: Sedimentology, v. 14, p. 125-140.
- Lajoie, K. R., and Helley, E. J., 1974, Differentiation of sedimentary deposits for seismic-zonation purposes. Chap. III, in A prelimi-

- nary analysis of seismic zonation in the San Francisco Bay region: U.S. Geol. Survey Prof. Paper 941-A, p. A39-A51.
- Lajoie, K. R., Helley, E. J., Nichols, D. R., and Burke, D. B., 1974, Geologic map of unconsolidated and moderately consolidated deposits of San Mateo County, California: U.S. Geol. Survey Misc. Field Studies Map MF-575.
- Lambe, T. W., and Whitman, R. V., 1969, Soil Mechanics: John Wiley and Sons, Inc., New York.
- Meade, R. H., 1968, Compaction of sediments underlying areas of land subsidence in central California: U.S. Geol. Survey Prof. Paper 497-D, 39 p.
- Ohsaki, Y., and Iwasaki, R., 1973, On dynamic shear moduli and Poisson's ratios of soil deposits: Soils and Foundations, v. 13, p. 61-73.
- Rao, H. A. Balakrishna, 1966, Wave velocities through partially saturated sand-clay mixtures: The response of soils to dynamic loadings: Report 24, Dept. of Civil Eng., Mass Inst. Tech.
- Reeburgh, W. S., 1969, Observations of gases in Chesapeake Bay sediments: Limnology and Oceanography, v. 14, p. 368-375.
- Rosenquist, I. T., 1960, Physico-chemical properties of soils: Soil water systems: Norwegian Geotechnical Institute Pub. 37, p. 1-14.
- Roth, E., 1978, Water level measurements in 59 shallow boreholes in the San Francisco Bay region: U.S. Geol. Survey Open-file Rept. (in press).
- Schlocker, Julius, 1974, Geology of the San Francisco North Quadrangle, Calif.: U.S. Geol. Survey Prof. Paper 782, 109 p.
- Schwarz, S. D., and Musser, J. M., 1972, Various techniques for making

- in-situ shear wave velocity measurements - a description and evaluation: Proc. Inter. Conf. Microzonation, Seattle, Wash., v. II, p. 593-608.
- Seed, H. B., and Idriss, I. M., 1969, Influence of local soil conditions on building damage potential during earthquakes: Report No. EERC 69-15, Univ. of Calif., Earthquake Eng. Research Center, Berkeley, Calif., 26 p.
- Soil Survey Staff, 1951, Soil Survey Manual: U.S. Department of Agriculture Handbook 18.
- Stoke, K. H., and Richart, F. E., 1973, In-situ and laboratory shear wave velocities: Proc. 8th Int. Conf. Soil Mech. Found. Eng., v. 1, pt. 2, p. 403-409.
- Terzaghi, K., 1955, Influence of geological factors on the engineering properties of sediments: Economic Geology, 50th Anniversary Vol., pt. II, p. 557-618.
- U.S. Army Corps of Engineers, 1960, The unified soil classification system: Tech. Memorandum No. 3-357, Waterway Experiment Station, Vicksburg, Mississippi.
- Vergnaud, J. P., 1974, Effects of small changes in a soil deposit on its seismic response characteristics: Int. Inst. of Seismology and Earthquake Eng. Individual Studies, v. 10, p. 175-192.
- Wahrhaftig, C., 1965, Stepped topography of the southern Sierra Nevada, California: Geol. Soc. Amer. Bull., v. 76, p. 1165-1190.
- Walsh, J. B., and Brace, W. F., 1966, Elasticity of rock: A review of some recent theoretical studies: Felsmechanik and Ingenieur-geologie, v. IV, p. 283-297.

- Warrick, R. E., 1974, Seismic investigation of a San Francisco Bay mud site: Seismol. Soc. America Bull., v. 64, p. 375-385.
- Wentworth, C. M., and Ellen, S., 1977, Hillside materials and their significance for land-use planning, San Francisco Bay region: U.S. Geol. Survey Open-file Rept. (in press).
- Wood, H. O., 1908, Distribution of apparent intensity in San Francisco: in The California earthquake of April 18, 1906, Report of the State Earthquake Investigation Commission: Carnegie Inst. Washington, Publ. 87, p. 220-245.
- Wyllie, M. R. J., Gregory, A. R., and Gardner, L. W., 1956, Elastic wave velocities in heterogeneous and porous media: Geophysics, v. 21, p. 41-70.